消化管運動調節に与るカハールの介在細胞の細胞組織学的研究

課題番号　１３６７０５７２

平成１３年度～１５年度　科学研究費補助金（基盤研究Ｃ２）
研究成果報告書

平成１６年５月

研究代表者

小室輝昌

（早稲田大学人間科学部　教授）

目次

平成１５年度科学研究費補助金（基盤研究Ｃ２）研究成果報告書

１、課題番号　：１３６７０５７２

２、研究課題　：消化管運動調節に与るカハールの介在細胞の細胞組織学的研究

３、研究代表者：小室輝昌　（早稲田大学人間科学部　教授）

４、研究協力者：関　馨介　（早稲田大学人間科学部助手）
三井　烈　（早稲田大学人間科学研究科）

５、研究経費　：

平成１３年度：１０００　千円
平成１４年度：１３００　千円
平成１５年度：１０００　千円
計：３３００　千円

6、研究発表

（ア）学会誌等

Seki K. and Komuro T. Distribution of interstitial cells of Cajal and gap junction protein, Cx 43 in the stomach of wild-type and W/W^{v} mutant mice. Anat. Embryol. 206:75-65,2002

Mitsui R. and Komuro T. Direct and indirect innervation of smooth muscle cells of rat stomach, with special reference to interstitial cells of Cajal. Cell Tissue Res. 309: 219-227,2002

Mitsui R. and Komuro T. Distribution and ultrastructure of interstitial cells of Cajal in the gastric antrum of wild-type and Ws/Ws rats. Anat. Embryol.206,2003, 453-460

Komuro, T. Morphological features of interstitial cells of Cajal. Gann Monograph on Cancer Research, No52, Gatrointestinal stromal tumor (GIST): from pathology to molecular target therapy. 2004, In press.

（イ）口頭発表

三井烈、小室輝昌（2001）ラット幽門部におけるカハールの介在細胞と神経支配。　第１０６回日本解剖学会全国学術集会（於、高知）

関馨介、小室輝昌（2001）カハールの介在細胞の機能的異型性。
第 57 回日本電子顕微鏡学会全国学術集会

関馨介、小室輝昌（2001）食道- 胃領域における *c-kit* 陽性細胞の細胞組織化学的研究。　第 17 回臨床食道噴門研究会　（於、札幌）

小室輝昌（２００２）　Introduction – 細胞間コミュニケーション
第５９会日本顕微鏡学会学術講演会シンポジウム　（於、札幌）

小室　輝昌、関　馨介、三井　烈、池田　愛美（２００２）カハールの介在細胞の分布と細胞学的異型性
生理学研究所研究会「消化管機能」　（於、岡崎）

Terumasa Komuro (2003). A quantitative estimation of ICC networks in the guinea-pig small intestine. International Symposium for the Smooth Muscle Rhythmicity.: The Second Meeting of Pacific Rim Discussion Group on ICC. (Singapore)

7、研究成果

（ア）研究の背景および目的

急激な研究の進展を見せるカハールの介在細胞（ICC）ついては、注目されて来たペースメーカー機能が証明される一方、ICC が内包していた重要な課題が新たな標的となりつつある。ICC が神経支配を受け gap junction によって筋と連絡することが示されたことは、もともと Cajal（1911）によって示唆された ICC の興奮伝達介在説を意味するもので、自律神経系末梢部における支配様式の見直しと ICC の機能的細胞分化の可能性を示唆するものである。

前者は、骨格筋神経筋接合部との比較のうえで、分化した伝達装置を持たないと考えられてきた平滑筋組織における常識を覆すもので、消化管各部位は勿論、他の臓器における神経支配に関する詳細な再吟味を提起している。

後者は、これまで研究の中心をなしてきたマウスやラットでの成果が示すごとく、ペースメーカー機能を持つ ICC（小腸筋層間神経叢部に代表される）と興奮伝達を専らとする ICC（小腸深部筋神経叢部に代表される）が、細胞分化における c-Kit への依存度、微細構造上の特徴等に相違を示す事実に由来しており、ICC の subtype としての特性の問題と、それらを規定する要因の解析を迫っている。

このような背景の中、本研究では、機能的役割の上で（ペースメーカーと）二分する ICC の興奮伝達能に焦点を当て、先ず消化管各部位における神経興奮伝達様式について、ICC の介在を念頭に免疫組織化学的、微細構造的に詳細に検索し、既知の観察事実と併せて消化管運動調節機構を総合的に理解するよう努めた。

（イ）研究実施計画と結果

平成１３年度

独立した細胞型として漸く認められて来たカハールの介在細胞（ICC）については、現時点の課題として、臓器や組織層の相違による細胞学的、機能的多様性の検証が挙げられるが、胃に関する微細構造学的報告は少なく、中でも縦走筋内の ICC については、全く知られていない。また、一般に消化管縦走筋では神経支配が乏しく、筋一筋間の gap junction も無いか非常に少ないと報告

されており、これまで、筋運動の制御機構についても、充分に説明されていない。そこで、本年度の研究では、ICC による間接支配の可能性を検討するため、ラット胃を材料として、幽門部筋層における ICC の分布、密度については c-KIT 抗体により免疫組織化学的に観察すると共に、神経支配、筋との連絡の有無、微細構造上の特徴等については電子顕微鏡的手法により検索した。

その結果、ラット胃幽門部の筋層では、筋層間神経叢の周辺部に多くの c-KIT 陽性細胞（ICC）が見られ、輪走筋内、縦走筋内にも散在性に観察された。また、輪走筋最内層と粘膜下結合組織層との境界部にも ICC が認められたことは、胃の他の部位には無い特徴として注目に値する。

縦走筋内の ICC は豊富なミトコンドリア、中間径フィラメント、カヴェオラを含み、同種細胞間、平滑筋と gap junctions を形成する点で、これまで報告されてきた輪走筋内の ICC と共通する特徴もつことが示された。また、シナップス小胞を多量に含む神経終末と密接して観察された。他方、神経終末は両筋層の平滑筋とも直接密接する像が観察された。このことより、ラット胃幽門部の平滑筋は、ICC を介する間接支配と神経による直接支配との平行支配を受けるものと結論された。そして、これは、従来、定説とされてきた自律神経系末梢部における支配様式に新しい視点を付加するものである。

平成１４年度

ペースメーカー機能と興奮伝達能をもつカハールの介在細胞（ICC）は、消化管の部位に固有な収縮、弛緩運動を反映するものと推定されるが、ラットやマウスの胃では、同一器官内の部位によって変異を示すことが、我々の予備的実験から判明しており、ICC の subtypes の機能的、形態学的特性を相関させながら考察する上で良い試料である。そこで、本年度の研究では、胃の各領域、組織層における ICC の分布を明らかにすると共に、ICC 各亜型の細胞学的特性を知るため、正常および c-kit に 突然変異のある W/Wv マウスの胃を材料に用い、ICC の 分布については c-kit 免疫組織化学により、また筋束の電気的結合度を知る目安としては gap junction 蛋白(Cx43) の分布密度について、免疫組織学的に検索した。

その結果、正常マウス胃の噴門、胃底、胃体（重層扁平上皮部）の良く発

達した輪走(CM)および縦走(LM)筋層には多くの ICC が観察されたが、筋層間神経叢(AP)には認められなかった。筋層間神経叢の ICC は胃体（腺上皮部）への移行部近傍より出現し始め、幽門部には非常に密度高く観察された。一方、gap junction 蛋白 Cx43 は、噴門、胃底、胃体（重層扁平上皮部）、幽門部を通じて、輪層筋層に散在性に弱く観察されたが、胃体（腺上皮部）の ICC-CM の少ない部位では、高い密度で観察された。

これらの観察より、マウス胃では、ペースメーカー機能をもつ ICC-AP の出現する胃体（腺上皮部）が自律的蠕動運動の起始部にあたると推定された。また、噴門、胃底、胃体（重層扁平上皮部）、幽門部の輪走筋層の細胞間の電気的結合度は弱く、豊富な ICC が神経信号の伝達に介在するものと推定された。他方、W／Wv マウスでは、胃の全領域を通じて ICC-CM, ICC-LM は欠損する傍ら、幽門部の ICC-AP は少数観察された。このことは、ICC の亜型によって c-kit/SCF 系に対する依存性に相違のあることを示すものであり、今後の重要な課題と考えられた。

平成１５年度

消化管運動調節機構の解析を企図した多年に渡る腸管神経系の研究成果は、各種運動ニューロン、知覚ニューロン、介在ニューロン等を含む回路図を書き上げているが、カハールの介在細胞（ICC）が消化管蠕動運動のペースメーカーおよび平滑筋への興奮伝達機能を有することが明らかとなって来た現在、これに組み込むべき ICC に関する詳細なデータが必要である。本研究では、このような観点からモルモットの小腸を材料として、ICC の形態計測学的検索を行った。試料は全載伸展標本として c-Kit および PGP9.5 免疫組織化学染色を施し、共焦点レーザー顕微鏡により観察した。

体重約３００g、腸管の円周（平均 20mm）の動物の空腸では、ICC-AP は平面上で多方向に突起を伸ばす多極性の細胞で、突起の先端間の距離はしばしば２００μm を越えるが、円周に沿った長さは平均約１５０μm で、円周あたりの数は約１３０個であった。このことは、蠕動運動が腸管の長軸上の一点を通る腸壁の円周から起ると考えるとき、少なくとも約１３０個の筋層間神経叢の ICC（ICC-AP）が同時に発火するものと推定された。

深部筋神経叢の ICC（ICC-DMP）は同じく多極性の細胞であるが、突起は輪走筋に沿って走行するため、円周方向の突起の長さは約２００～３００μm、円周あたりの数は約 80 個、腸管長軸方向の細胞列の間隙は平均 50μm であった。また、ICC-CM は輪走方向に位置する長さ約２５０～３５０μm の双極性の細胞で、非常にまばらに散在するため、細胞列の間隙は測定から除外した。従来の著者らの研究から、小腸の輪走筋は豊富な gap junctions によって結合している事が判明しているが、ICC-CM は筋束内の興奮伝達には補助的な役割をもつものと推定された。一方、興奮伝達の主役をなす ICC-DMP を介した神経信号により腸壁の円周上の筋束が収縮弛緩する際には、恐らく、腸管長軸方向に５０μm ほどの幅にある平滑筋束が最小の単位として連動するものと推定された。尚、これらの成果については、現在、論文発表準備中である。

8、発表論文

Cell Tissue Res (2002) 309:219–227
DOI 10.1007/s00441-002-0592-1

REGULAR ARTICLE

Retsu Mitsui · Terumasa Komuro

Direct and indirect innervation of smooth muscle cells of rat stomach, with special reference to the interstitial cells of Cajal

Received: 9 November 2001 / Accepted: 30 April 2002 / Published online: 3 July 2002

Abstract Interstitial cells of Cajal in the circular (ICC-CM) and longitudinal (ICC-LM) muscle layer of the rat gastric antrum and their innervation were studied ultrastructurally. Both ICC-CM and ICC-LM are characterized by many mitochondria, rough and smooth endoplasmic reticulum, caveolae, and formation of gap junctions with each other and with muscle cells, though ICC-LM tend to show more variable cytoplasmic features depending on section profiles. Close contacts between nerve terminals and both ICC-CM and ICC-LM are observed. These possible synaptic structures are characterized by: (1) accumulation of synaptic vesicles in nerve varicosities, (2) a narrow gap (about 20 nm) between pre- and postjunctional membranes, (3) lack of a basal lamina between pre- and postjunctional membranes, and (4) the presence of an electron-dense lining on the inner aspect of prejunctional membranes. Almost the same characteristics are observed between the nerve terminals and the muscle cells of both circular and longitudinal muscle layers of the same specimens. Therefore, we conclude that the smooth muscle cells of both circular and longitudinal layers of the rat antrum are directly and indirectly innervated via ICC. Their functional significance is discussed.

Keywords Interstitial cells of Cajal (ICC) · Neuromuscular junction · Stomach · Ultrastructure · Rat (Wistar)

This study was supported by a grant from the Ministry of Education and Science of Japan (13670572) and by a Waseda University Grant for a Special Research Project (2001A-601)

R. Mitsui · T. Komuro (✉)
Department of Basic Human Sciences, School of Human Sciences, Waseda University, Tokorozawa, Saitama 359-1192, Japan
e-mail: komuro@human.waseda.ac.jp
Fax: +81-429-48-4314

Introduction

A widely accepted notion is that smooth muscle cells do not form clear neuromuscular synaptic structures comparable to those of the skeletal muscles and that the varicose terminal portions of nerve fibers release transmitter "en passage" to the nearest muscle cells located at distances of 15–2,000 nm (Burnstock 1977), in spite of the close innervation of the gut longitudinal muscles which has been suggested (Richardson 1958; Llewellyn-Smith et al. 1993). However, later ultrastructural studies using serial sections demonstrated the existence of well-organized neuromuscular junctions in the rat urinary bladder (Gabella 1995) and in the guinea pig ileum (Klemm 1995).

On the other hand, a number of morphological studies of interstitial cells of Cajal (ICC) in the last decade have revealed that certain types of ICC are closely apposed to nerve terminals and form numerous gap junctions with neighboring smooth muscle cells at different levels of the gastrointestinal tract in many species (see reviews by Komuro 1999; Komuro et al. 1999). These studies suggested that ICC are mediators between the nerves and muscles. In fact, recent physiological studies demonstrated functional significance of ICC in both inhibitory (Burns et al. 1996; Ward et al. 1998) and excitatory (Ward et al. 2000) neurotransmission in the mouse stomach. Thus, these ICC are considered to be primary targets of enteric motor innervation and play an important role in enteric neurotransmission (Ward and Sanders 2001).

Regarding subtypes of ICC, immunohistochemical studies reported their presence in the longitudinal muscle layer (LM) of the digestive tract (Burns et al. 1997; Toma et al. 1999; Torihashi et al. 1999), but no descriptions have elucidated the ultrastructural features of ICC-LM in any part of the digestive tract.

Therefore, the present study was primarily designed to elucidate the ultrastructural features of ICC-LM including their innervation and intercellular connections in the rat stomach, and their characteristics are compared to

Fig. 1 A longitudinal section of the rat gastric antrum stained with toluidine blue. The inner circular muscle layer (*CM*) is composed of about 40–60 layers of smooth muscle cells and subdivided by well-developed connective tissue septa which give passage to blood vessels and nerve bundles. The outer longitudinal muscle layer is relatively thin and is composed of about 10–15 layers of the muscle cells. The myenteric ganglion can be seen between two muscle layers (*asterisk*). A large blood vessel is seen in the submucosal layer (*V*). ×190

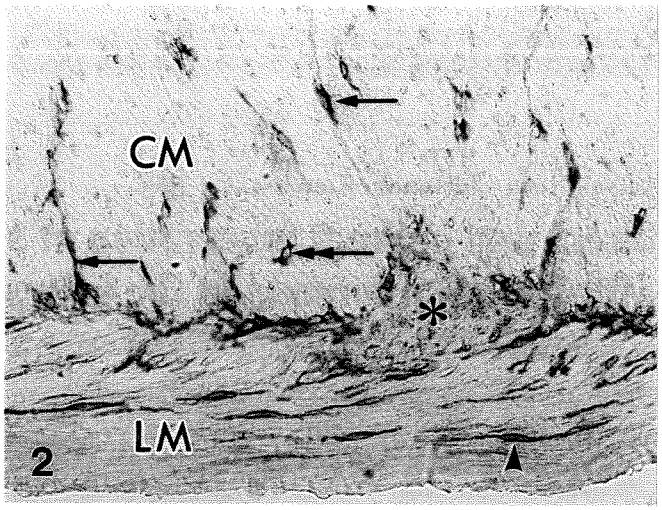

Fig. 2 A longitudinal section of the rat antrum stained for c-Kit immunohistochemistry. c-Kit-positive cells were found within longitudinal muscle layer (*LM*), circular muscle layer (*CM*), and the myenteric plexus region. ICC-LM (*arrowhead*) are bipolar in shape and run parallel to the longer axis of longitudinal muscle cells. ICC-CM are predominantly observed in the connective septa (*arrows*) as well as within the muscle bundles (*double-headed arrow*) (*asterisk* myenteric ganglion). ×110

those of the circular musculature. We also examined whether the smooth muscle cells of the circular and longitudinal layer receive direct or indirect innervation via ICC.

Materials and methods

Adult Wistar rats of both sexes (aged 4–10 weeks) were used in the present study. The rats were deeply anesthetized by ether inhalation. All procedures were performed in accordance with the guidelines for the care and use of laboratory animals in the School of Human Sciences of Waseda University.

Immunohistochemistry

Whole stomachs were removed from the anesthetized rats. After rinsing out the luminal contents of the stomachs with phosphate-buffered saline (PBS), parts of the antrum were cut and immersed in OCT compound and then frozen with liquid nitrogen. Longitudinal sections (10 μm thick) of the antrum were cut with a cryostat, mounted on glass slides, and fixed with acetone for 10 min at room temperature. The specimens were incubated with 4% Block Ace solution (Dainippon Seiyaku) for 20 min at room temperature to reduce non-specific immunoreactivity and then incubated with a rabbit polyclonal antibody against human c-Kit (Santa Cruz Biotechnology) at a dilution of 1:50 for 1 h at room temperature. After washing in PBS, the specimens were incubated with a peroxidase-conjugated secondary antibody against rabbit Ig (DAKO; K4002) for 30 min at room temperature. The peroxidase reaction was developed in 50 ml 0.1 M TRIS-HCl buffer containing 6 mg 4-chloro-1-naphthol (Sigma) and 8 μl 30% H_2O_2.

Electron microscopy

Stomachs were moderately inflated by PBS and then animals were perfused through the left ventricle of the heart with PBS for a prewash and with a fixative (containing 3% glutaraldehyde and 4% paraformaldehyde in 0.1 M phosphate buffer, pH 7.4). The antrum was removed, cut into small pieces and placed in the same fixative for 4 h at 4°C. The specimens were then rinsed in the same buffer, postfixed in 1% osmium tetroxide in the same buffer for 2 h at 4°C, rinsed in distilled water, block stained overnight in a saturated solution of aqueous uranyl acetate, dehydrated in a graded series of ethyl alcohols and embedded in Epon epoxy resin. After examination of semithin sections stained with toluidine blue, ultrathin sections were cut using a Reichert ultramicrotome and double stained with uranyl acetate and lead citrate for observation with a JEOL JEM 1200EXII electron microscope.

Fig. 3 A low-power electron micrograph of the circular muscle layer of the rat antrum. Elongated ICC-CM (*asterisks*) are located in septal spaces between muscle bundles, in which muscle cells are oriented almost perpendicular to the longer axis of the ICC-CM and show angular profiles of their cross sections (*CM*). Small nerve bundles (*arrow*) are located close to the process of ICC-CM. ×3200. *Inset*: The gap junction indicated by an *arrow* in Fig. 4. ×70,000 ▶

Fig. 4 Higher magnification of the perinuclear cytoplasm of the ICC-CM (*IC-CM*) in the upper part of Fig. 3 on a neighboring section. Many mitochondria, RER, Golgi apparatus, and caveolae (*arrowheads*) are observed. This ICC-CM forms a gap junction (*arrow*) with a thin process of the same type of cell. ×10,000

Fig. 5 The further distal portion of the same ICC-CM in Fig. 4, which shows abundant intermediate filaments (*arrows*) and caveolae. ×19,000

Fig. 6 ICC-CM (*IC-CM*) and a fibroblast-like cell (*FL*) located around a nerve bundle in the circular muscle layer. FL shows an electron-lucent cytoplasm and is characterized by dilated cisternae of the RER. ICC-CM is in contact with nerve varicosity containing many synaptic vesicles (*arrow*). ×19,000. *Inset*: Higher magnification of the varicosity in Fig. 6. Gap between two membranes measures about 20 nm. Presynaptic electron-dense lining is observed at both edges of the contact area. ×44,000

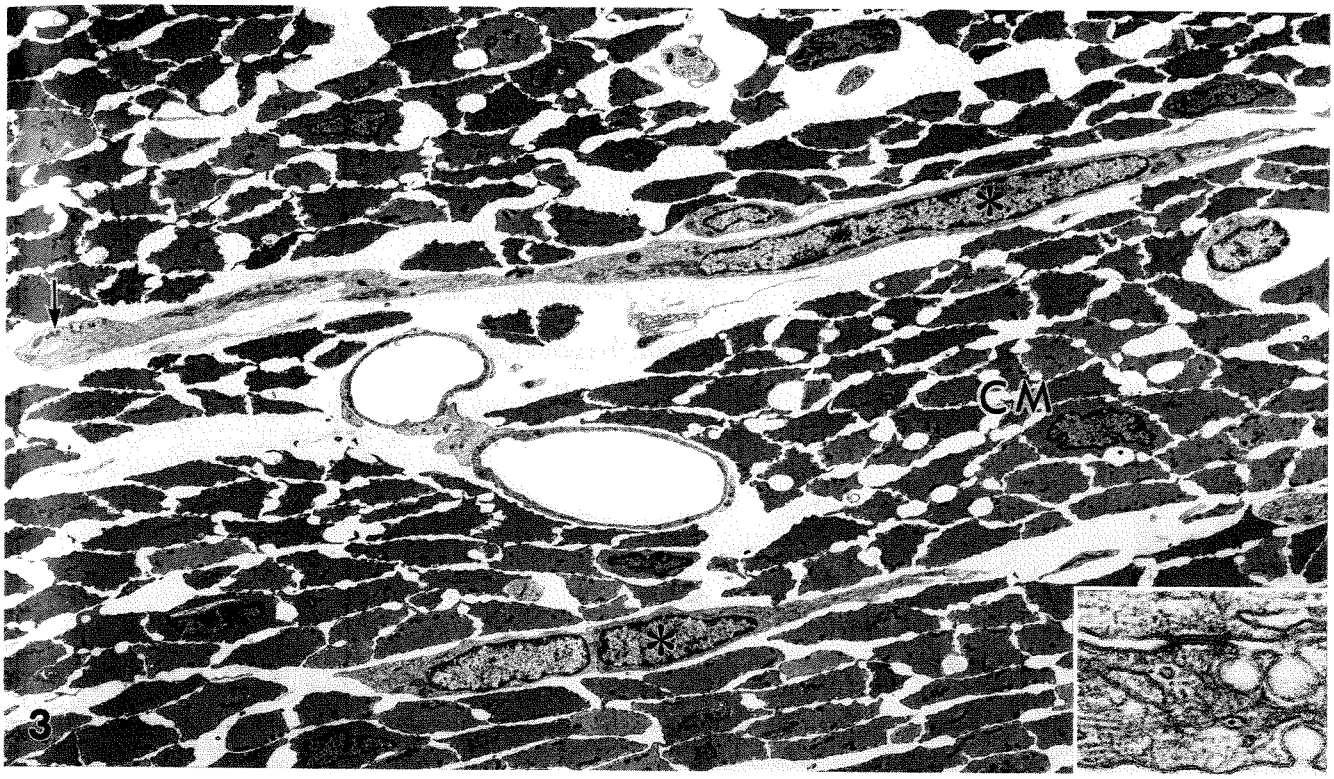
C-M
3

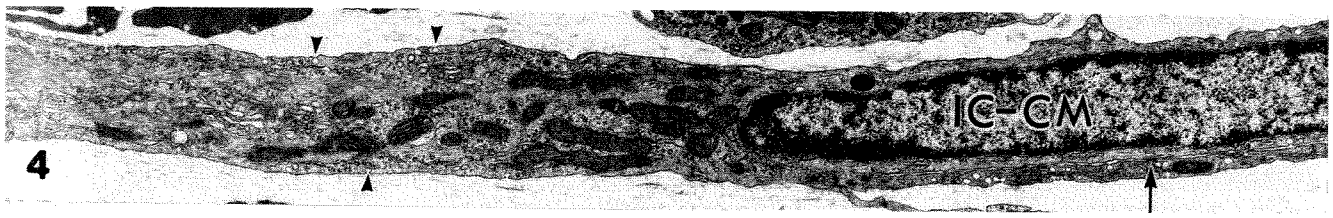
IC-CM
4

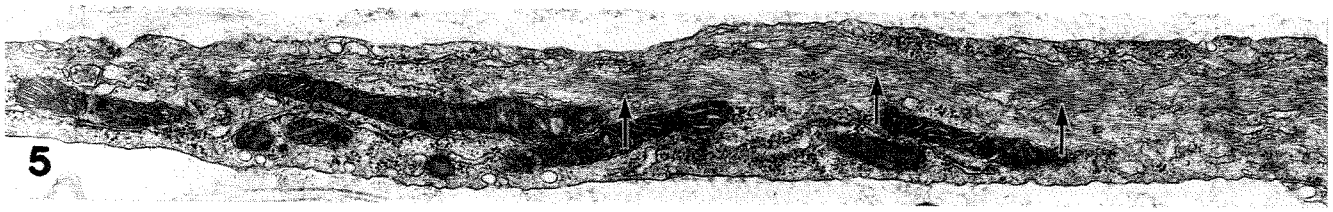
5

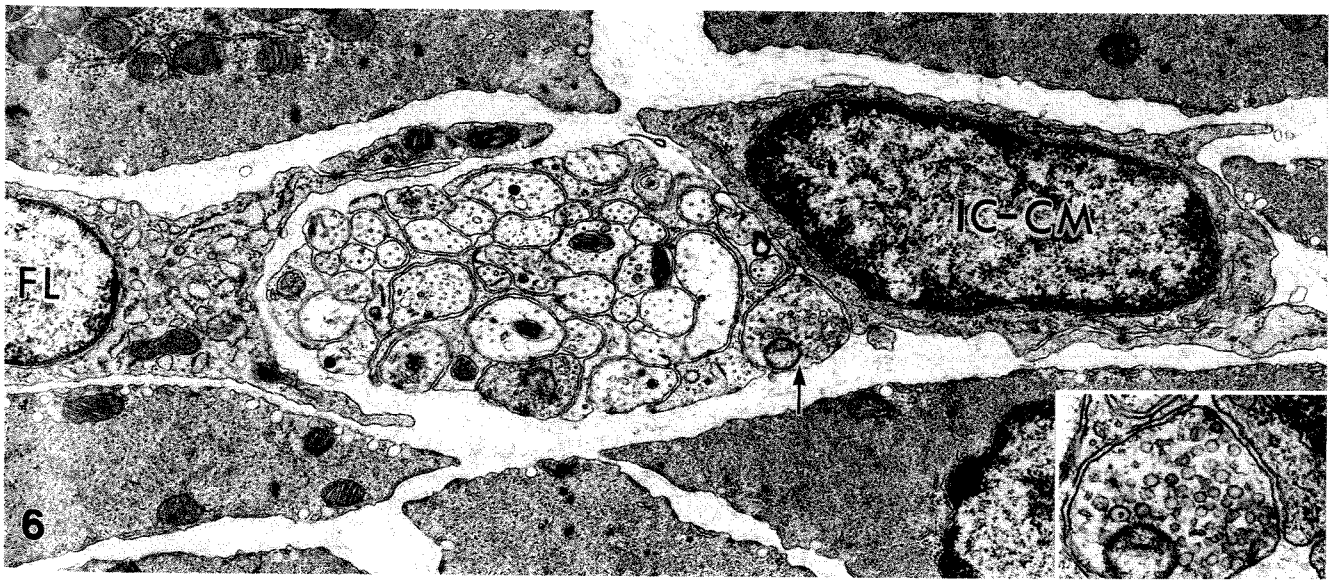
IC-CM
F.L
6

Results

The tunica muscularis of the rat antrum was composed of the inner circular and the outer longitudinal layers separated by the myenteric plexus (Fig. 1). The circular muscle layer was composed of about 40–60 layers of smooth muscle cells and was subdivided by connective tissue septa that contained blood vessels and thick nerve bundles. The longitudinal layer was composed of about 10–15 layers of muscle cells which partially contained muscle bundles running obliquely.

Immunohistochemistry

Immunoreactive cells for c-Kit staining were observed within both circular and longitudinal muscle layers, and between the two muscle layers, i.e., in the region of the myenteric plexus (Fig. 2). In the circular muscle layer, c-Kit-positive cells were predominantly located in the connective tissue spaces (septa) separating muscle bundles while they were sparsely distributed within the muscle bundles. c-Kit-positive cells were numerous and were regularly distributed in the longitudinal muscle layer. They were bipolar in shape and were oriented parallel to the longer axis of the surrounding smooth muscle cells.

Electron microscopy

ICC-CM of the rat antrum were mainly observed in septa between muscle bundles of the circular muscle layer (Fig. 3). ICC-CM were often oriented perpendicularly to the longer axis of the circular muscle cells. Their perinuclear cytoplasm contained many mitochondria, Golgi apparatus and rough (RER) and smooth (SER) endoplasmic reticulum (Fig. 4). Intermediate filaments were particularly rich in their cytoplasmic processes (Fig. 5). Caveolae were observed, but there was no basal lamina around the cell membranes. Gap junctions of ICC-CM with each other (Figs. 3, inset, 4) and between ICC-CM and circular muscle cells were often found as previously described (Ishikawa et al. 1997). Close contacts between the ICC-CM and nerve varicosities were often observed (Fig. 6). A basal lamina did not intervene between the two membranes and their gap distance measured less than 20 nm. Electron-dense linings, similar in appearance to the active zone in synapses in the central nervous system, were observed on the membranes of these varicosities.

ICC-LM of the rat antrum were characterized by the presence of numerous mitochondria, well-developed RER and SER, Golgi apparatus and caveolae, and lack of a continuous basal lamina around the cell membranes (Figs. 7, 8, 9, 10). Many mitochondria were found mainly in the perinuclear cytoplasm (Fig. 7), but they were not uniformly distributed in the cytoplasmic processes (Figs. 8, 9, 10). This feature was clearly seen in a series of serial sections of the same cell (Figs. 7, 8).

RER was also unevenly distributed in the cytoplasm of ICC-LM. In any particular part of its cell process the ICC-LM might appear similar to a fibroblast (Fig. 9). However, cisternae of RER in ICC-LM were usually flattened and distinguishable from those of the fibroblasts, which were usually dilated and filled with flocculent materials. In contrast, SER was often observed as subsurface cisternae located immediately beneath the cell membranes closely facing other cells of the same type (Fig. 10).

In short, they showed a wide range of cytoplasmic appearances depending on section profiles and in this respect they seemed to be different from the ICC described in other tissue regions (see Komuro 1999).

Another important feature of ICC-LM was the formation of gap junctions with the same type of cells and with neighboring smooth muscle cells (Figs. 9, 10, left inset). Gap junctions between ICC-LM were frequently found in the regions in which the subsurface cisternae-like structures were located, as described above (Fig. 10). These gap junctions were particularly large and measured up to 2 μm in length along the two cell membranes in single ultrathin sections. Gap junctions between longitudinal muscle cells have not been observed so far.

Close appositions between ICC-LM and axon varicosities containing many synaptic vesicles were occasionally observed (Fig. 10, right inset). The closest distance between the two membranes measured about 20 nm. The cell membranes of those varicosities were naked and not covered by either glial processes or a basal lamina. Electron-dense lining was occasionally observed in the cytoplasmic aspect of the axonal membranes. One type of varicosity containing a mixture of small flattened vesicles with a shorter diameter of about 35 nm and large granular vesicles with a diameter of about 110 nm has been observed.

Close neuromuscular contacts were frequently observed within the muscle bundles of the circular musculature (Fig. 11). Distances between the axonal mem-

Fig. 7 An electron micrograph showing the perinuclear cytoplasm of ICC-LM in the longitudinal muscle layer of the rat antrum (*IC-LM*). Many mitochondria, Golgi apparatus and caveolae (*arrows*) are seen. ×20,000 ▶

Fig. 8 Another section profile of ICC-LM of the same cell in Fig. 7 (*IC-LM*), which shows a similar appearance to the fibroblast except for the presence of caveolae (*arrows*). ×11,000

Fig. 9 The cytoplasmic process of ICC-LM, which contains well-developed RER and many mitochondria. This cytoplasmic process is identified as ICC-LM by the formation of a big gap junction with the muscle process (*arrow*) and by the presence of caveolae on the cell membrane (*arrowheads*). ×39,000

Fig. 10 Two processes of ICC-LM connecting with each other's gap junctions (*arrow*). Subsurface cisternae (*arrowheads*) are observed along the cell membrane of one ICC-LM process. A nerve varicosity (*N*) containing synaptic vesicles is closely associated with another ICC-LM. ×24,000. *Left inset*: Higher magnification of the gap junction indicated by an *arrow*. ×68,000. *Right inset*: Nerve varicosity (*N*) in contact with ICC-LM with a gap of about 20 nm. ×36,000

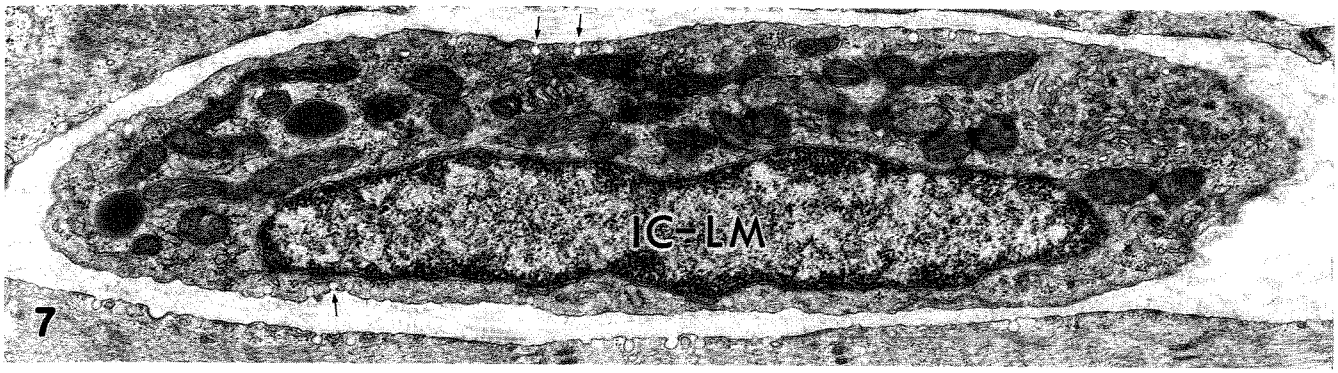

7

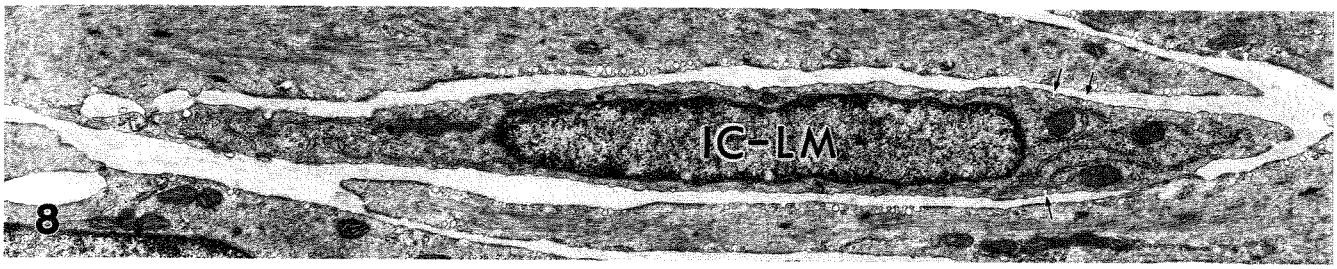

8

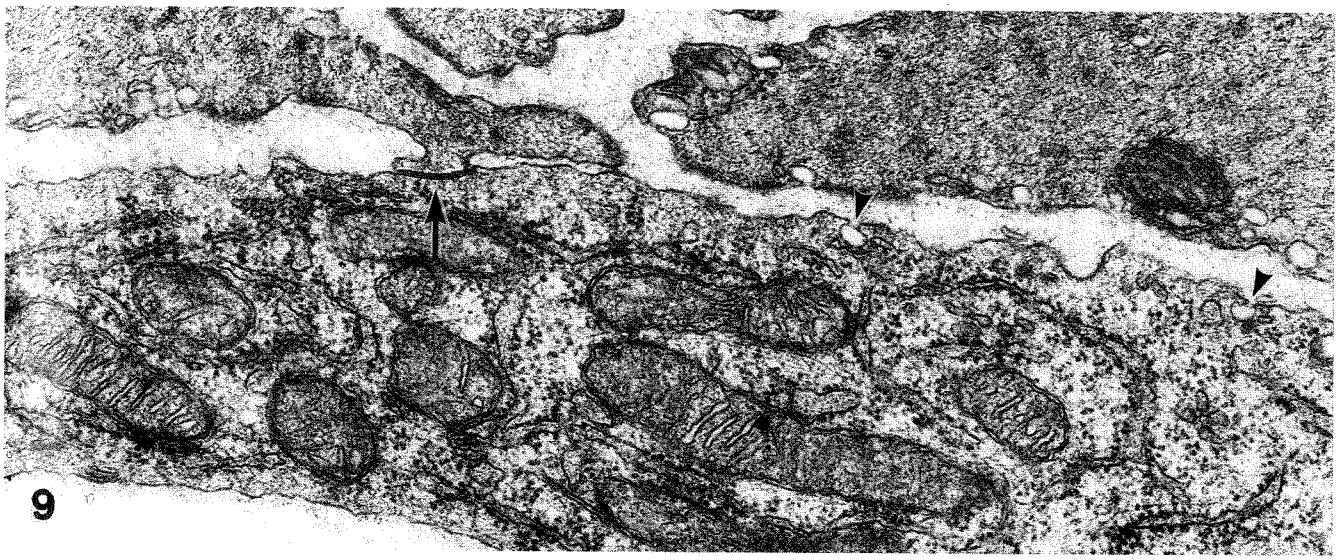

9

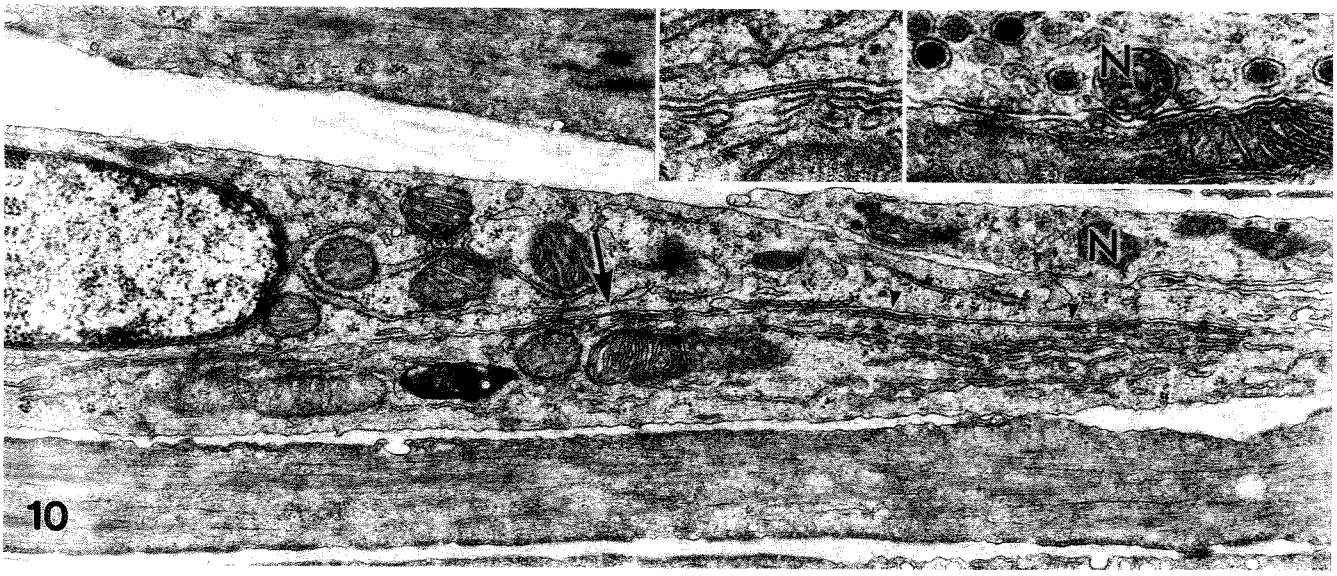

10

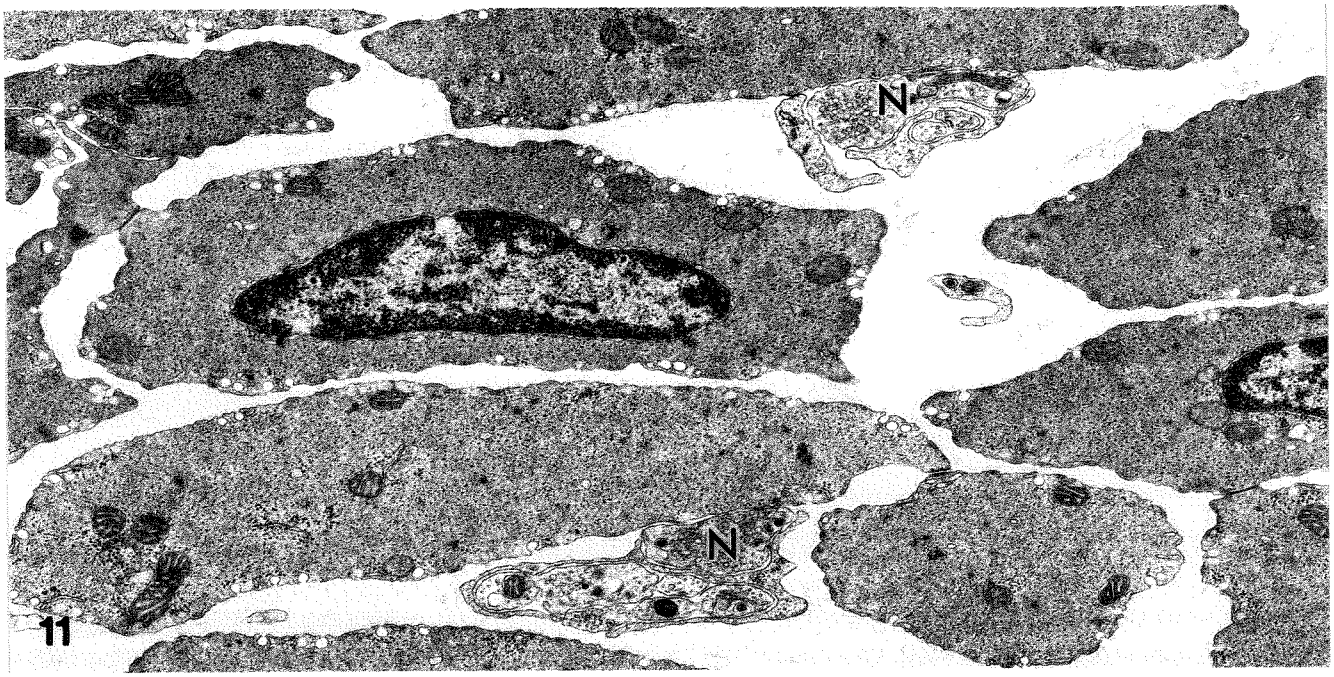
N
N
11

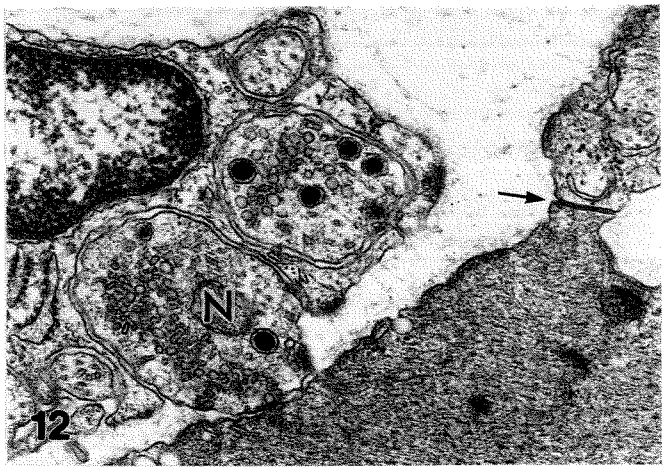
N
12

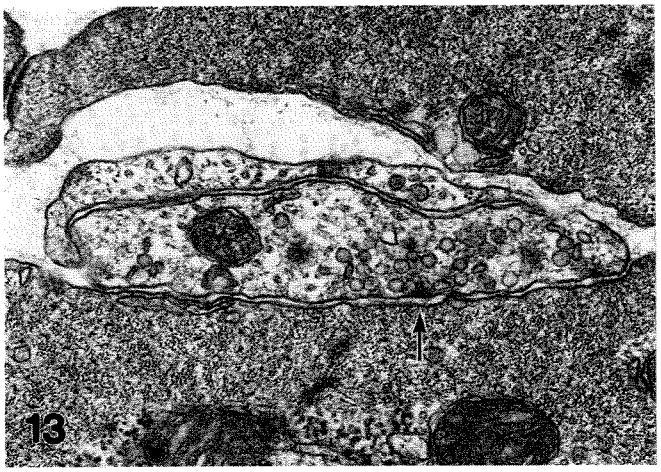
13

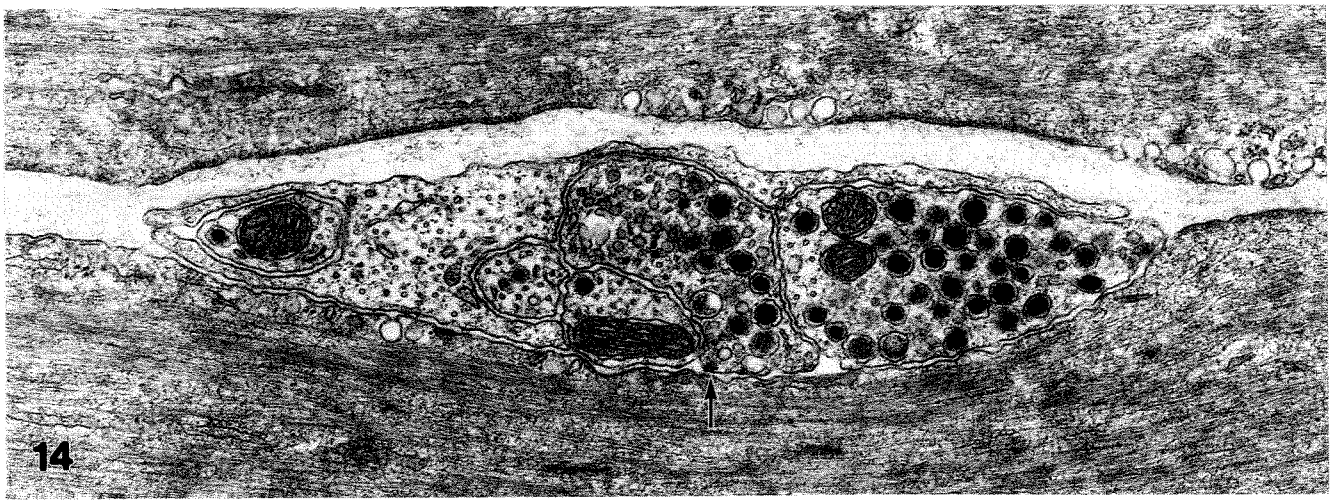
14

branes and muscle membranes were in the range of about 10–20 nm (Figs. 12, 13). Electron-dense linings were observed on the cytoplasmic aspect of the axon varicosities (Fig. 13). Here, two types of varicosities were observed, one containing many small flattened vesicles with a shorter diameter of about 35 nm (Fig. 12) and the other containing mainly small round agranular vesicles (Fig. 13) with a diameter of about 50 nm mixed with a few large granular vesicles.

Axon varicosities containing many synaptic vesicles also made close contact with the longitudinal muscle cells, with gaps of 10–20 nm (Fig. 14). Two types of varicosities, one containing a mixture of small round agranular vesicles and large granular vesicles, and the other containing only large granular vesicles, were seen (Fig. 14). The muscle cell membranes facing these varicosities did not have any specialized structures, but they showed a slightly concave surface.

Discussion

The present observations revealed the ultrastructural features of ICC-CM and ICC-LM in the rat antrum. They are similar to each other in many respects including the presence of numerous mitochondria, caveolae, formation of gap junctions with each other and with neighboring muscle cells and lack of a continuous basal lamina (Ishikawa et al. 1997; the present study). However, ICC-LM appear to have more well-developed RER than ICC-CM and show different cytoplasmic profiles, depending on the plane of section, of typical ICC characteristics to give a nearly fibroblastic appearance. They also differ from the more muscular type of ICC, which have a continuous basal lamina, such as ICC of the deep muscular plexus of the small intestine (Thuneberg 1982; Rumessen et al. 1992; Zhou and Komuro 1992; Torihashi et al. 1993; Seki and Komuro 1998) and of the submuscular plexus of the colon (Faussone-Pellegrini 1987; Rumessen et al. 1993; Torihashi et al. 1994; Ishikawa and Komuro 1996) in many species. On the other hand, ICC-CM and ICC-LM are distinguished from the fibroblast-like cells observed in the circular muscle layer of the rat stomach (Ishikawa et al. 1997) and mouse small intestine (Horiguchi and Komuro 2000) by the presence of caveolae and large gap junctions connecting with each other.

Since ICC-CM and ICC-LM are closely apposed to the nerve terminals containing many synaptic vesicles in the present study, it is likely that they are involved in the transmission of nerve impulses to the circular and longitudinal muscle cells of the rat antrum as has been suggested for ICC-CM in the mouse fundus and pyloric sphincter (Burns et al. 1996; Ward et al. 1998, 2000). However, because of the generally sparser distribution of nerve fibers in the longitudinal musculature than that in the circular muscle layer (Gabella 1981), ICC-LM seems to be less innervated than ICC-CM in the rat antrum. This view seems to be comparable with the immunohistochemical study of the guinea pig colon showing that ICC-LM run parallel to the longer axis of the muscle cells without accompanying the nerve fibers in the longitudinal muscle layer (Toma et al. 1999).

Regarding neuromuscular junctions in the smooth muscle tissue, Gabella (1995) investigated the rat urinary bladder in detail using ultrastructural serial sections, and he defined less rigid but "soft-patterned" neuromuscular junctions with four parameters: (1) an expanded axon varicosity packed with synaptic vesicles, (2) an exposed axolemma, (3) mostly a 30- to 50-nm gap between the axon and muscle cell membranes, and (4) exclusion of fibrillar elements in the intercellular gap except for a single basal lamina. The electron-dense lining onto the presynaptic axolemma is only rarely observed.

Klemm (1995) observed the longitudinal muscle of the guinea pig ileum and demonstrated that the majority of vesicle-containing nerve fibers of the enteric nervous tertiary plexus formed specialized neuromuscular junctions. They are characterized by: (1) exposed axons separated from muscle cells by intervening clefts of less than 100 nm filled with a single basal lamina, (2) accumulation of synaptic vesicles in the axons toward the area of close contact, and (3) the occasional occurrence (less than 20%) of prejunctional membrane specializations.

The neuromuscular junctions observed in the rat antrum in the present study are characterized by accumulation of synaptic vesicles in the axon varicosities, electron-dense linings on the presynaptic membranes and the disappearance of basal lamina in the narrow gap (less than 20 nm) between the axon varicosities and the muscle cell membranes. These are compatible with the features reported by Gabella (1995) and Klemm (1995).

Therefore, the present study provides ultrastructural evidence for the direct and indirect innervation of the smooth muscle in both the circular and longitudinal layers of the rat antrum. But what is the significance of each

◀ **Fig. 11** Two neuromuscular junctions observed in a single section profile of the circular muscle bundle of the rat antrum. The nerve varicosities (*N*) contain mainly agranular round synaptic vesicles. ×18,000

Fig. 12 Close contact between the circular muscle cell and a nerve terminal (*N*) containing many small flat vesicles (about 35 nm shorter diameter and about 55 nm longer diameter). Note another varicosity containing agranular round vesicles (about 50 nm in diameter). The gap junction between the two processes of the muscles is also seen (*arrow*). ×32,000

Fig. 13 Axon terminal containing mainly small agranular round vesicles (about 50 nm in diameter) on the circular muscle cell. The gap distance between the two membranes measures 10–20 nm and the presynaptic electron-dense lining is indicated by an *arrow*. ×41,000

Fig. 14 An electron micrograph showing close contact between the longitudinal muscle cell and two axon terminals: one containing a mixture of small round agranular vesicles (about 50 nm in diameter) and large granular vesicles (about 110 nm in diameter) and the other containing only large granular vesicles. Electron-dense lining is observed on the axonal membrane of one terminal (*arrow*). ×28,000

type of innervation? How does the direct or indirect innervation contribute to gastric movement, contraction and/or relaxation?

Ward et al. (2000) observed pressure increases as a function of fluid volume and infusion rate in wild-type animals but little basal tone and a minimal increase in pressure with fluid infusion in W/W^v mice which lack ICC-CM. They concluded that ICC-CM play a major role in receiving cholinergic excitatory inputs from the enteric nervous system in the murine fundus. On the other hand, Nakama et al. (1998) reported that the maximum value of the intraluminal pressure of the pylorus did not show a significant difference between the wild-type rats and Ws/Ws rats which lack ICC-CM (Ishikawa et al. 1997) and ICC-LM (R. Mitsui and T. Komuro, unpublished data) in spite of normal motility being impaired. The former indicates that indirect innervation is of essential importance in gastric contraction in the mouse, while the latter suggests that direct innervation may produce a strong enough contraction of the rat stomach without indirect innervation mediated via ICC-CM and ICC-LM. These differences may reflect different innervation patterns in different species.

ICC-CM, which are mainly observed in the septa between the muscle bundles in the circular muscle layer, may function to coordinate contraction or relaxation of muscle bundles, while direct innervation regulates a group of muscle fibers within the bundle. On the other hand, it was reported that ICC-CM of the mouse antrum generate the secondary regenerative component of a slow wave (Dickens et al. 2001), and it was also suggested that septal ICC-CM of the canine antrum transfer pacemaker depolarizations from ICC of the myenteric plexus region to the distant bundles of circular muscle (Horiguchi et al. 2001; Hirst 2001).

ICC-LM may also coordinate muscle movements of longitudinal musculature over a wider span, probably in a way so as to compensate for the lack of large gap junctions between the longitudinal muscle cells. The presence of many ICC-LM in the gastric antrum contrasts with the lack of ICC-LM in the small intestine in the rat (unpublished data). These facts may provide a clue to interpreting the observations that the longitudinal muscles contract concurrently with the circular muscles in the stomach, while they contract at a different phase from the circular muscles in the intestine of dogs (Sarna 1993). This view is consistent with the study of guinea pig colon, of which circular and longitudinal muscle layers, both containing ICC (Burns et al. 1997; Toma et al. 1999), also contract together (Smith and Robertson 1998).

It has been demonstrated hitherto that ICC are involved in nitrergic (Burns et al. 1996; Ward et al. 1998) and cholinergic (Ward et al. 2000) neurotransmission in the mouse stomach. Since different types of nerve varicosities characterized by different appearances of synaptic vesicles are observed in close apposition to both ICC and smooth muscle cells, it is likely that more than one type of functionally defined neuron is involved in both direct and indirect innervation in the rat stomach. Further analysis of the proportional differences of the direct and indirect innervation in each system may be required to adequately account for the muscle movements in the digestive tract.

Acknowledgements The authors would like to thank Dr. Peter Baluk, the Cardiovascular Research Institute, University of California, San Francisco, USA, for reading the manuscript.

References

Burns AJ, Lomax AE, Torihashi S, Sanders KM, Ward SM (1996) Interstitial cells of Cajal mediate inhibitory neurotransmission in the stomach. Proc Natl Acad Sci U S A 93:12008–12013

Burns AJ, Herbert TM, Ward SM, Sanders KM (1997) Interstitial cells of Cajal in the guinea-pig gastrointestinal tract as revealed by c-Kit immunohistochemistry. Cell Tissue Res 290:11–20

Burnstock G (1977) Cholinergic, adrenergic, and purinergic neuromuscular transmission. Fed Proc 36:2434–2438

Dickens EJ, Edwards FR, Hirst GD (2001) Selective knockout of intramuscular interstitial cells reveals their role in the generation of slow waves in mouse stomach. J Physiol 531:827–833

Faussone-Pellegrini MS (1987) Cytodifferentiation of the interstitial cells of Cajal of mouse colonic circular muscle layer. An EM study from fetal to adult life. Acta Anat (Basel) 128:98–109

Gabella G (1981) Structure of muscles and nerves in the gastrointestinal tract. In: Johnson LR (ed) Physiology of the gastrointestinal tract. Raven Press, New York, pp 198–241

Gabella G (1995) The structural relations between nerve fibres and muscle cells in the urinary bladder of the rat. J Neurocytol 24:159–187

Hirst GD (2001) An additional role for ICC in the control of gastrointestinal motility? J Physiol 537:1

Horiguchi K, Komuro T (2000) Ultrastructural observations of fibroblast-like cells forming gap junctions in the W/Wv mouse small intestine. J Auton Nerv Syst 80:142–147

Horiguchi K, Semple GS, Sanders KM, Ward SM (2001) Distribution of pacemaker function through the tunica muscularis of the canine gastric antrum. J Physiol 537:237–250

Ishikawa K, Komuro T (1996) Characterization of the interstitial cells associated with the submuscular plexus of the guinea-pig colon. Anat Embryol (Berl) 194:49–55

Ishikawa K, Komuro T, Hirota S, Kitamura Y (1997) Ultrastructural identification of the c-*kit*-expressing interstitial cells in the rat stomach: a comparison of control and Ws/Ws mutant rats. Cell Tissue Res 289:137–143

Klemm MF (1995) Neuromuscular junctions made by nerve fibres supplying the longitudinal muscle of the guinea-pig ileum. J Auton Nerv Syst 55:155–164

Komuro T (1999) Comparative morphology of interstitial cells of Cajal: ultrastructural characterization. Microsc Res Tech 47:267–285

Komuro T, Seki K, Horiguchi K (1999) Ultrastructural characterization of the interstitial cells of Cajal. Arch Histol Cytol 62:295–316

Llewellyn-Smith IJ, Costa M, Furness JB, Bornstein JC (1993) Structure of the tertiary component of the myenteric plexus in the guinea-pig small intestine. Cell Tissue Res 272:509–516

Nakama A, Hirota S, Okazaki T, Nagano K, Kawano S, Hori M, Kitamura Y (1998) Disturbed pyloric motility in Ws/Ws mutant rats due to deficiency of c-kit-expressing interstitial cells of Cajal. Pathol Int 48:843–849

Richardson KC (1958) Electron microscopic observations on Auerbach's plexus in the rabbit, with special reference to the problem of smooth muscle innervation. Am J Anat 103:99–135

Rumessen JJ, Mikkelsen HB, Thuneberg L (1992) Ultrastructure of interstitial cells of Cajal associated with deep muscular plexus of human small intestine. Gastroenterology 102:56–68

Rumessen JJ, Peters S, Thuneberg L (1993) Light- and electron microscopical studies of interstitial cells of Cajal and muscle cells at the submucosal border of human colon. Lab Invest 68:481-495

Sarna SK (1993) Gastrointestinal longitudinal muscle contractions. Am J Physiol 265:G156–G164

Seki K, Komuro T (1998) Further observations on the gap-junction-rich cells in the deep muscular plexus of the rat small intestine. Anat Embryol (Berl) 197:135–141

Smith TK, Robertson WJ (1998) Synchronous movements of the longitudinal and circular muscle during peristalsis in the isolated guinea-pig distal colon. J Physiol 506:563–577

Thuneberg L (1982) Interstitial cells of Cajal: intestinal pacemaker cells? Adv Anat Embryol Cell Biol 71:1–130

Toma H, Nakamura K, Kuraoka A, Tanaka M, Kawabuchi M (1999) Three-dimensional structures of c-*kit* positive cellular networks in the guinea pig small intestine and colon. Cell Tissue Res 295:425–436

Torihashi S, Kobayashi S, Gerthoffer WT, Sanders KM (1993) Interstitial cells in deep muscular plexus of canine small intestine may be specialized smooth muscle cells. Am J Physiol 265:G638–G645

Torihashi S, Gerthoffer WT, Kobayashi S, Sanders KM (1994) Identification and classification of interstitial cells in the canine proximal colon by ultrastructure and immunocytochemistry. Histochemistry 101:169–183

Torihashi S, Horisawa M, Watanabe Y (1999) c-Kit immunoreactive interstitial cells in the human gastrointestinal tract. J Auton Nerv Syst 75:38–50

Ward SM, Sanders KM (2001) Interstitial cells of Cajal: primary targets of enteric motor innervation. Anat Rec 262:125–135

Ward SM, Morris G, Reese L, Wang XY, Sanders KM (1998) Interstitial cells of Cajal mediate enteric inhibitory neurotransmission in the lower esophageal and pyloric sphincters. Gastroenterology 115:314–329

Ward SM, Beckett EA, Wang X, Baker F, Khoyi M, Sanders KM (2000) Interstitial cells of Cajal mediate cholinergic neurotransmission from enteric motor neurons. J Neurosci 20:1393–1403

Zhou DS, Komuro T (1992) Interstitial cells associated with the deep muscular plexus of the guinea-pig small intestine, with special reference to the interstitial cells of Cajal. Cell Tissue Res 268:205–216

Anat Embryol (2003) 206:453–460
DOI 10.1007/s00429-003-0323-8

ORIGINAL ARTICLE

Retsu Mitsui · Terumasa Komuro

Distribution and Ultrastructure of Interstitial Cells of Cajal in the Gastric Antrum of Wild-type and Ws/Ws rats

Accepted: 4 March 2003 / Published online: 17 April 2003

Abstract Interstitial cells of Cajal (ICC) in the stomach of wild-type and *Ws/Ws* mutant rats that are deficient in *c-kit* were studied by immunohistochemistry and electron microscopy to elucidate their regional specialization in the gastric antrum. Immunohistochemistry for Kit protein demonstrated that in wild-type rats ICC were located at the submucosal border of the circular muscle layer (ICC-SM) in a limited extension of the antrum from the pyloric sphincter towards the corpus, as well as within both the circular (ICC-CM) and longitudinal (ICC-LM) muscle layers and in the myenteric plexus region (ICC-AP). In *c-kit* mutant *Ws/Ws* rats while ICC-CM and ICC-LM were not observed, but unexpectedly, a few ICC-SM and ICC-AP were found. By electron microscopy, ICC-SM and ICC-AP were characterized by abundant mitochondria, many caveolae, a distinct basal lamina and formed gap junctions with other ICC or with smooth muscle cells and make close contacts with nerves. Thus, ICC-SM and ICC-AP of the rat antrum were classified as Type 3 ICC, the type most similar to smooth muscle cells. The functional significance of ICC-SM and their survival in the *c-kit* mutant animals is discussed in reference to the role of the *c-kit*/stem cell factor system for their cellular maturation.

Keywords Kit · Connexin · Immunohistochemistry · Ultrastructure · Stomach

Introduction

Interstitial cells of Cajal (ICC) have been uniformly observed in the region of the myenteric (Auerbach's) plexus (AP) throughout nearly the whole digestive tract, but ICC of other tissue layers showed a characteristic distribution from organ to organ (Komuro et al. 1999). In the small intestine, ICC are associated with the deep muscular plexus (DMP) located between the outer main circular muscle layer and inner thin sublayer (Thuneberg 1982). In the colon, ICC are situated at the submucosal border of the circular muscle layer where the submuscular plexus (SMP) is located (Stach 1972; Ishikawa and Komuro 1996; Komuro 1999). ICC corresponding to those of the DMP or SMP have not been observed in most parts of the stomach. Indeed, the stomach is unique in that ICC have a different distribution in proximal and distal regions of the same organ (Burns et al. 1997; Seki and Komuro 2002). Also, in W/W^v mutant mice which have the major defect in *c-kit*, the ICC of different tissue layers have characteristically different degrees of dependence on *c-kit* (Burns et al. 1996; Ward et al. 1998).

Recent physiological studies focusing on the regional specificity of ICC in the stomach reported a variety of suggested functions of ICC. For example, ICC-AP of the corpus and antrum evoke the initial component of electrical slow waves (Dickens 1999; Ordog 1999), while ICC in the circular muscle layer (ICC-CM) of the same region generate the secondary component of the slow waves (Dickens 2001). Besides, ICC-CM of the fundus mediate neurotransmission to smooth muscle cells (Burns 1996; Ward 2000). The most recent study reported that intracellular recordings from the mouse antrum shows varying electrical potentials due to a differential distribution of ICC along the axis of the greater to the lesser curvature (Hirst et al. 2002). In these studies, the presence of a certain type of ICC is believed to play a key role in their function in the tissue.

ICC at the submucosal border of the stomach (ICC-SM) have been found in the human gastric antrum (Faussone-Pellegrini 1989), in the mouse pylorus (Ward et al. 1998; Seki and Komuro 2002) and in the dog antrum (Horiguchi et al. 2001). However, their ultrastructural features and physiological significance have not yet been elucidated in detail. In the rat stomach, the ultrastructure of ICC has only been described for the ICC-CM (Ishikawa et al. 1997).

R. Mitsui · T. Komuro (✉)
Department of Basic Human Sciences, School of Human Sciences, Waseda University,
Tokorozawa, 359-1192 Saitama, Japan
e-mail: komuro@human.waseda.ac.jp
Fax: +81-42-9484314

Accordingly, the goal of the present study was to demonstrate the distribution and ultrastructure of ICC-SM in wild-type rats and in *Ws/Ws* rats that lack *c-kit* (Niwa et al. 1991). In addition, the ultrastructure of ICC-SM was compared to the ultrastructure of ICC-AP and ICC-CM and the distribution of gap junctions was documented by immunohistochemistry for connexin (Cx) 43 and by electron microscopy. Cx 43 was chosen to represent gap junctions in the rat stomach, since the presence of Cx 43 was demonstrated at the gap junctions between the following pairs of cell types, including ICC and ICC, ICC and smooth muscle cells, and smooth muscle cells and smooth muscle cells in the rat small intestine (Seki and Komuro 2001).

Materials and methods

Homozygous *Ws/Ws* mutant rats and sibling control wild-type rats of both sexes (aged 4-10 weeks) were used in the present study. The rats were anesthetized deeply by ether inhalation. All procedures were performed in accordance with the guidelines for the care and use of laboratory animals of the School of Human Sciences of Waseda University.

Immunohistochemistry

Whole stomachs were removed from the anesthetized rats. After rinsing out the luminal contents of the stomachs with phosphate buffered saline (PBS), parts of the pyloric antrum were cut and immersed in OCT compound and then frozen with liquid nitrogen. Longitudinal sections (10 μm thick) of the antrum were cut with a cryostat, mounted on glass slides, and fixed with acetone for 10 min at room temperature. Specimens were first incubated with Peroxioblock (Zymed) for 45 s to inactivate endogenous peroxidase and then with 4% Block Ace solution (Dainippon Seiyaku) for 20 min at room temperature to reduce non-specific immunoreactivity. The following steps for immunohistochemistry were performed separately for different antibodies as follows:

(1) The specimens were incubated with a rabbit polyclonal antibody against human Kit protein (Santa Cruz Biotechnology) at a dilution of 1:50 for 1 h at room temperature. After washing in PBS, the specimens were further incubated with a peroxidase-conjugated secondary antibody against rabbit IgG (DAKO; K4002) for 30 min at room temperature. The peroxidase reaction was developed in 50 ml 0.1 M Tris-HCl buffer containing 6 mg of 4-chloro-1-naphthol (Sigma) and 8 μl of 30% H_2O_2. After a brief rinse in PBS, the specimens were mounted in Quick-mount and photographed with a Nikon light microscope.
(2) The specimens were incubated with a mouse monoclonal antibody against gap junction protein connexin (Cx) 43 (Chemicon International, MAB3068) at a dilution of 1:100 for 1 h at room temperature. After washing with PBS, the specimens were incubated with a FITC-conjugated secondary antibody against mouse IgG (DAKO) for 1 h at room temperature. These specimens were mounted in Vectashield (Vector) and observed with a Nikon fluorescence microscope.

Electron microscopy

Stomachs were moderately inflated with PBS and then animals were perfused through the left ventricle of the heart with PBS for a prewash and with a fixative (containing 3% glutaraldehyde and 4% paraformaldehyde in 0.1 M phosphate buffer, pH 7.4). The antrum was removed, cut into small pieces and placed in the same fixative for 4 h at 4°C. The specimens were then rinsed in the same buffer, post-fixed in 1% osmium tetroxide in the same buffer for 2 h at 4°C, rinsed in distilled water, block-stained overnight in a saturated solution of aqueous uranyl acetate, dehydrated in a graded series of ethyl alcohols and embedded in Epon epoxy resin. After examination of semithin sections stained with toluidine blue, ultrathin sections were cut using a Reichert ultramicrotome and double-stained with uranyl acetate and lead citrate for observation with a JEOL JEM 1200EX II electron microscope.

Results

Immunohistochemistry

Kit-immunoreactive cells were densely distributed in the pyloric antrum of the wild-type rat stomach. ICC were observed within the circular and longitudinal muscle layers, and in the region of Auerbach's plexus (Fig. 1). ICC-CM tended to be located in the connective tissue space (septa) separating the muscle bundles rather than within the muscle bundles.

At the interface between the submucosal connective tissue and the innermost circular muscle cell layer, Kit-positive cells (ICC-SM) were observed in the limited extension of the antrum from the region adjacent to the pyloric sphincter. The number of ICC-SM gradually decreased through the antrum towards the corpus, and they were not detected in the corpus at all.

To examine the degree of the intercellular coupling in this region, gap junctions were stained immunohistochemically for Cx43 protein. Cx43-immunoreactive deposits were almost homogeneously observed throughout

Fig. 1 A longitudinal section of a wild-type rat antrum stained for Kit immunohistochemistry. Kit-positive cells are found along the interface between the submucosa (*Sb*) and the circular muscle layer (*CM*) to outline its inner margin (*arrows*). Kit-positive cells are densely distributed near the pyloric sphincter (*left side of the figure*) and are sparser in the proximal antrum (*right side*). Kit positive cells are also seen within circular (*CM*) and longitudinal (*LM*) muscle layers, and around the Auerbach's plexus (*). ×130

Fig. 2 A longitudinal section of the wild-type rat antrum stained for Cx43 immunohistochemistry. Strong but intermittent immunoreactive deposits are found in the submucosal border of the circular muscle layer (*arrows*). Dense immunoreactive deposits are almost homogeneously observed in the circular muscle layer (*CM*) except in the inner one fourth part which shows weaker immunoreactivity. Some reactive deposits are also observed in the longitudinal muscle layer (*LM*). ×100

Fig. 3 A high power micrograph showing a part of Fig. 2. Large Cx43 immunoreactive deposits (*arrows*) at the submucosal border of circular muscle layer contrast to the weak activity in the adjacent zone of the circular muscle (*CM*). ×170

Fig. 4 A longitudinal section of the *Ws/Ws* rat antrum stained for Kit immunohistochemistry. Immunoreactive deposits are found along the submucosal border of circular muscle layer (*arrows*) and around Auerbach's plexus (*), but almost no reactive deposits are found in the circular (*CM*) and longitudinal muscle layers. ×90

Fig. 5 A high power micrograph showing a part of Fig. 4. Kit-positive cells are observed at the submucosal border of circular muscle layer as pale nuclei outlined by stained cytoplasmic rims (*arrows*). ×270

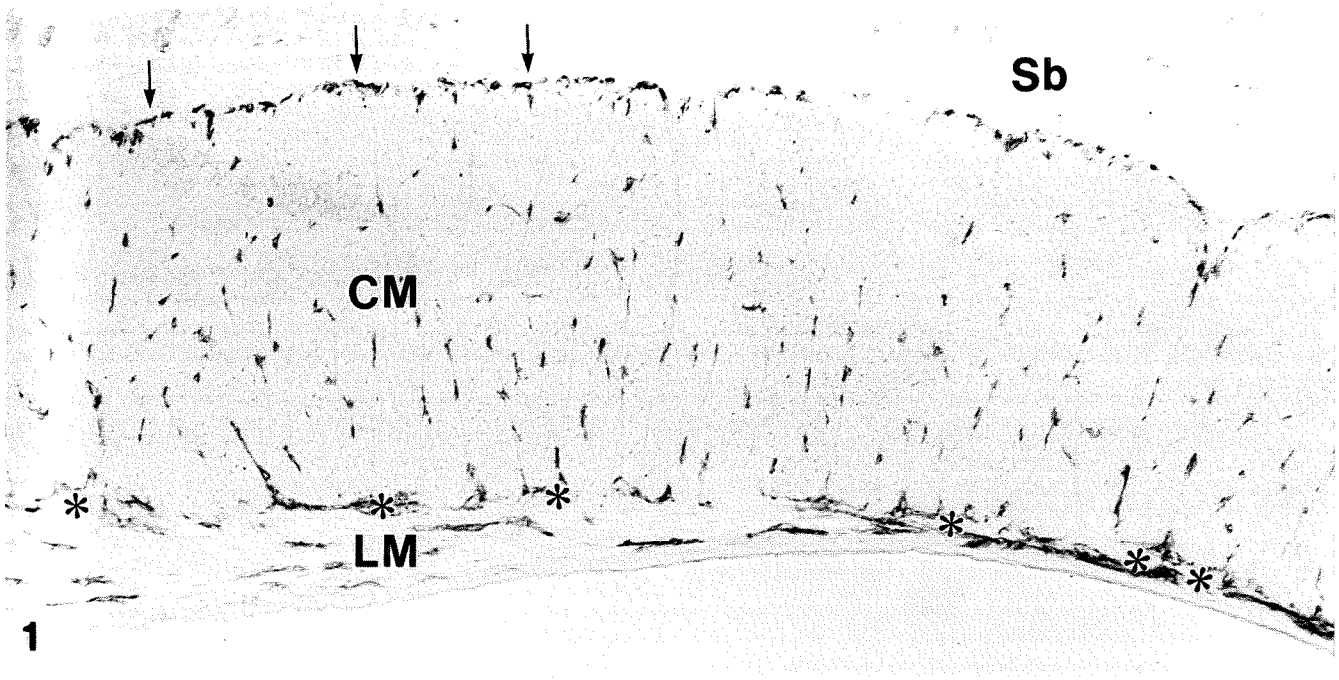
Sb
CM
LM
1

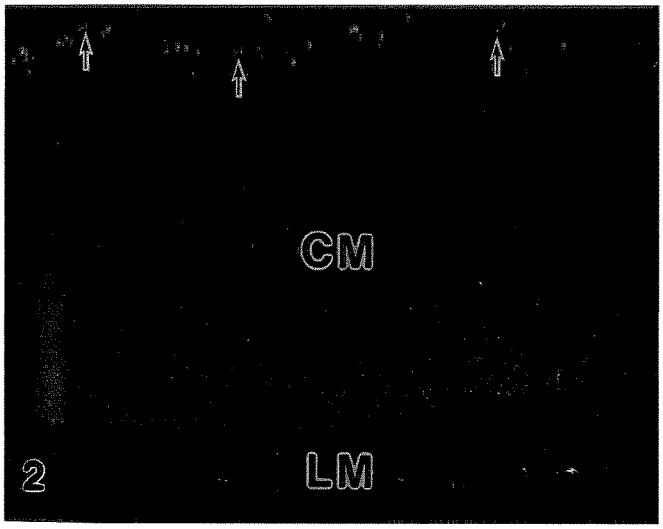
CM
LM
2

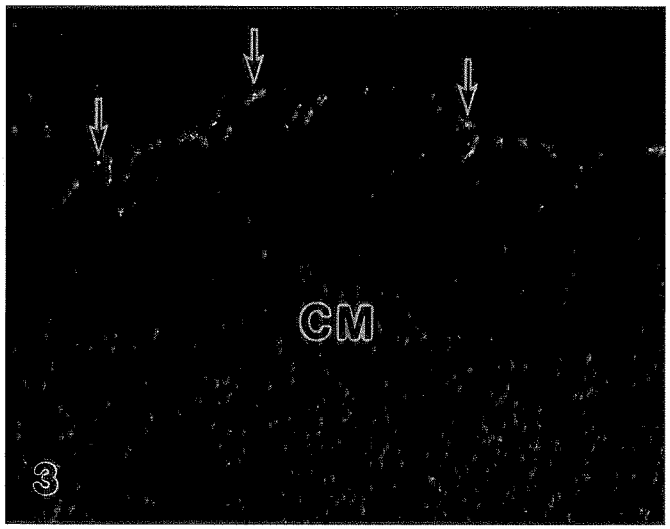
CM
3

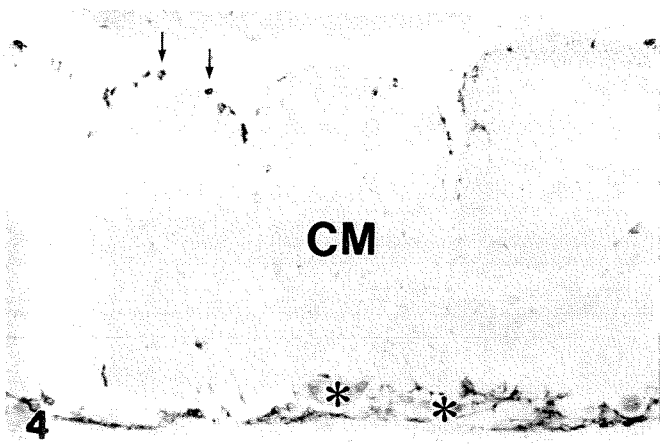
CM
4

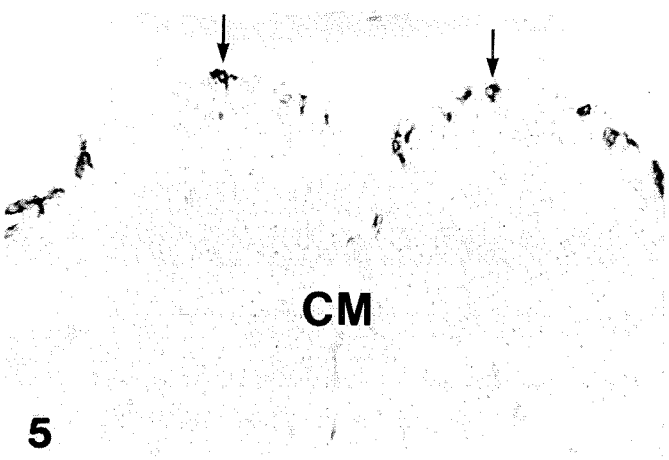
CM
5

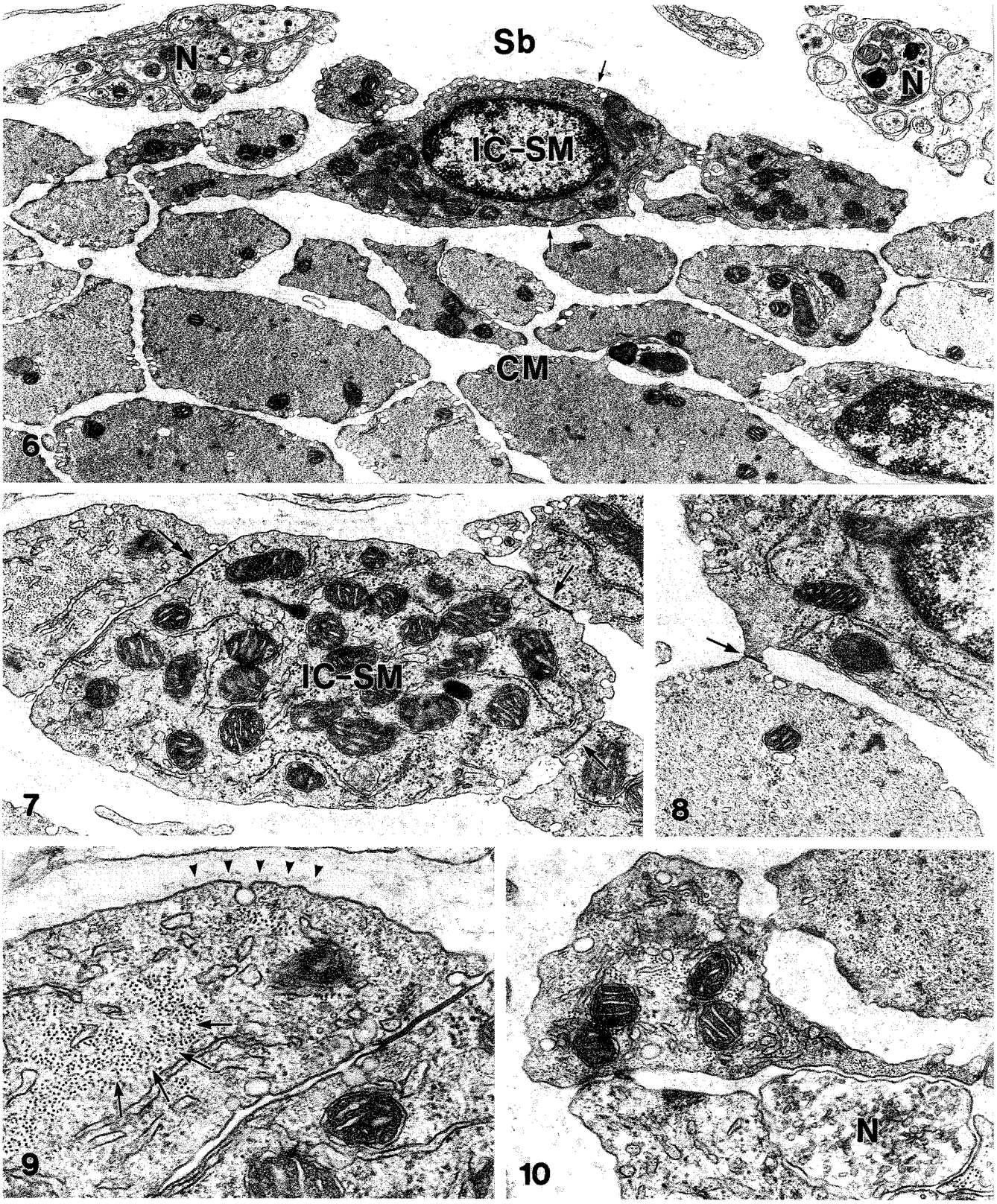

Fig. 6 An electron micrograph showing ICC-SM (*IC-SM*) characterized by many mitochondria and caveolae (*arrows*), located at the interface between the submucosa (*Sb*) and the circular muscle layer (*CM*). Nerve bundles (*N*) are also found in their close vicinity. ×14000

Fig. 7 Cytoplasmic processes of ICC-SM(*IC-SM*) contain many mitochondria and rough endoplasmic reticulum, and form gap junctions with each other (*arrows and double headed arrow*). ×34000

Fig. 8 A gap junction (*arrow*) between ICC-SM and a circular muscle cell. ×25000

Fig. 9 The cytoplasmic process of ICC-SM forming the gap junction indicated by the *double headed arrow* in Fig. 7. Bundles of intermediate filaments (*arrows*), a basal lamina (*arrowheads*) and caveolae are observed. ×53000

Fig. 10 A process of ICC-SM closely associated with a nerve varicosity (*N*) containing many synaptic vesicles. ×41000

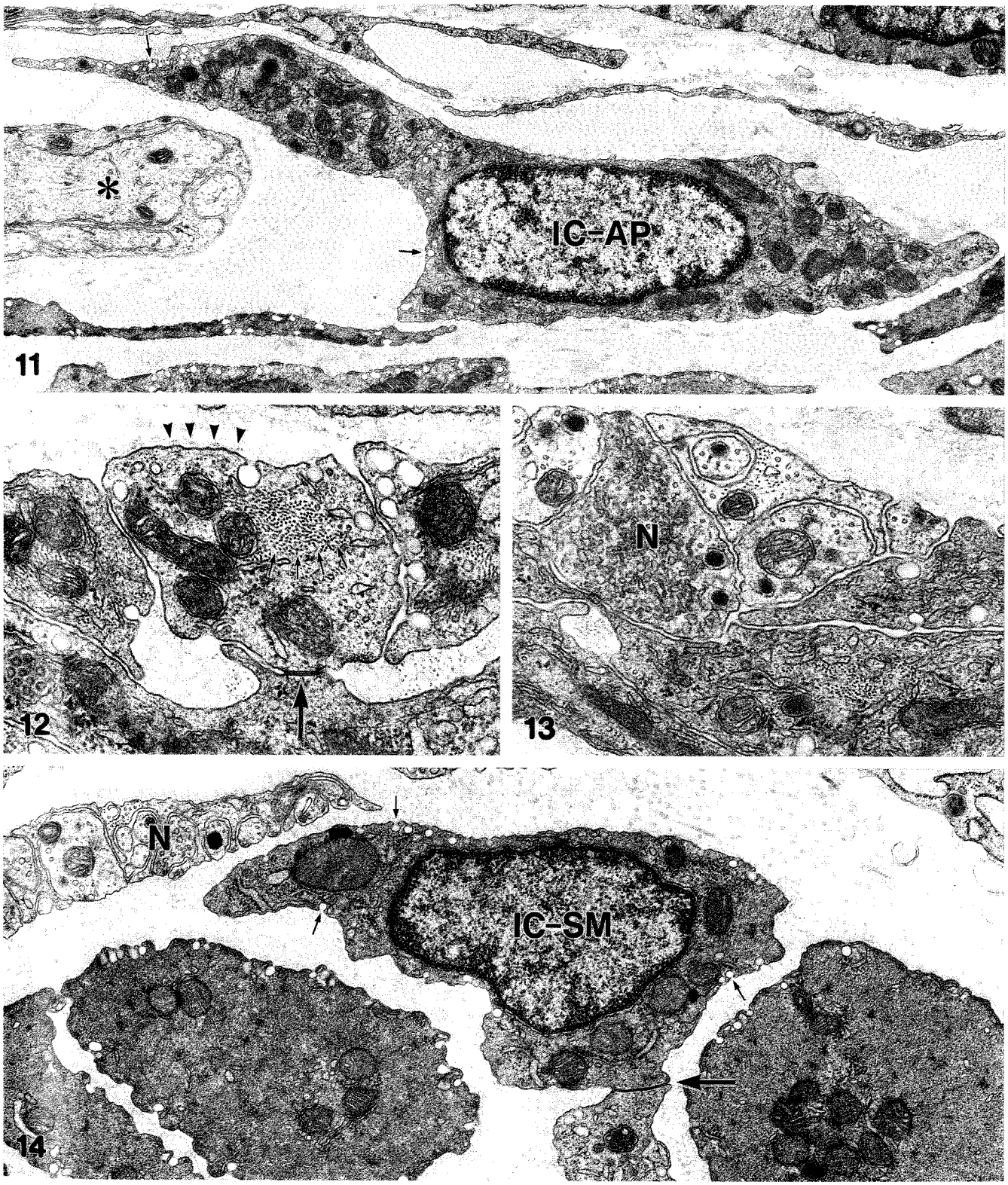

Fig. 11 ICC-AP (IC-AP) containing many mitochondria and rough endoplasmic reticulum located near a ganglion of Auerbach's plexus (*). Many caveolae are observed on the cell membrane (*arrows*). ×16000

Fig. 12 A cytoplasmic process of ICC-AP characterized by abundant intermediate filaments (*small arrows*) and a gap junction formed with another processes of the same type of cell (*large arrow*). A basal lamina is seen around the cell membrane (*arrowheads*). ×42000

Fig. 13 Close contact between the process of ICC-AP and nerve varicosity containing many synaptic vesicles (*N*). ×38000

Fig. 14 ICC-SM (IC-SM) characterized by the presence of caveolae (*small arrows*) and formation of gap junction (*large arrow*) with a neighboring process of ICC-SM in *Ws/Ws* rat. A small nerve bundle (*N*) is seen in its close vicinity. ×24000

the circular muscle layer, except for the inner one fourth part of it, which showed only weak immunoreactivity (Figs. 2, 3). In contrast, large Cx43 immunoreactive deposits were clearly observed along the submucosal border of the circular muscle layer (Fig. 3). Some deposits were also observed in the longitudinal muscle layer.

On the other hand, in the *Ws/Ws* rat antrum, Kit-immunoreactive deposits were almost completely absent within the circular and longitudinal muscle layers (Figs. 4, 5). However, ICC-SM and ICC-AP were observed in the corresponding regions, though they were fewer in number than those of the wild-type rat.

Electron microscopy

At the submucosal border of the circular muscle of the wild-type rat pylorus, ICC-SM were identified as cells containing many mitochondria, rough and smooth endoplasmic reticulum (Figs. 6, 7, 8, 9, 10). They had caveolae and a basal lamina around the cell membrane. They also contain abundant intermediate filaments, in particular in their processes (Fig. 9). They formed gap junctions with each other and with the neighboring muscle cells (Figs. 7, 8, 9). Close contacts between ICC-SM and nerve varicosities containing many synaptic vesicles were also observed (Fig. 10). ICC-AP in the same specimens were characterized by almost exactly the same features as those of ICC-SM (Figs. 11, 12, 13), i.e., the presence of many mitochondria, rough and smooth endoplasmic reticulum, abundant intermediate filaments, caveolae and a basal lamina around the cell membrane. Gap junctions (Fig. 12) and close contacts with nerve varicosities were also seen (Fig. 13). In *Ws/Ws* rats, ICC-SM characterized by the same features as those of wild-type animals were found at the submucosal border of the circular muscle layer (Fig. 14), but ICC-CM were not detected, as previously reported (Ishikawa et al. 1997).

Discussion

The present study clearly demonstrated that ICC-SM are located at the submucosal border of the rat antrum. These cells are only found in this confined area of the whole stomach and therefore they probably have a special significance here. Regarding their functional role, Horiguchi et al. (2001) suggested that ICC-SM of the canine gastric antrum can generate slow waves. This is probably true and potentially of interest because of some similarities between the gastric antrum and colon and because a pacemaker function has been reported for the ICC-SMP of the colon in the dog (Conklin and Du 1990; Serio et al. 1990; Sanders 1996), human (Rae et al. 1998), and the rat (Pluja et al. 2001).

The antrum of the stomach is nearly tubular in shape and has a thick muscular wall. The ingested food in the antrum is still of a rather solid consistency, unlike the liquid chyme of the small intestine, and is probably of similar stiffness as the luminal contents of the colon. Digestive movements to propel the solid contents probably require a thick muscular wall that is provided with common regulating cells including local ICC, namely ICC-SMP or ICC-SM, respectively.

Another observation also suggests a local peculiarity of the ICC in the pyloric region. Patterson et al. (2001) reported that a population of ICC expressing strong immunoreactivity for cholecystkinin A receptors are found in the specific region of the sphincter muscle of the rat pylorus. These authors suggested that these ICC play a role in CCK-induced pyloric sphincter activity and/or in the transpyloric coordination of slow wave activity. There is no evidence to suggest the involvement of ICC-SM to a certain pyloric sphincter activity or transpyloric coordination of muscle movement. However, it is rather likely that ICC-SM cooperate with ICC-DMP of the small intestine, which start to form a continuous cellular network in the closely adjacent tissue layer.

In *Ws/Ws* rats, a decrease in the duration of pyloric contraction (Nakama et al. 1998), and a weaker contractile force of the antrum have been reported (Takayama et al. 2002). At present, it is unknown whether the reduction of ICC-SM contributes to these effects.

On the other hand, since ICC-SM are situated closely to nerve terminals containing many synaptic vesicles and form gap junctions with neighboring smooth muscle cells, they are probably involved in the transmission of nerve impulse to the surrounding muscle cells, as has been suggested for ICC-CM in the stomach of mice (Burns et al. 1996; Ward et al. 1998; 2000) and rats (Ishikawa and Komuro 1998; Mitsui and Komuro 2002). Detection of large Cx43-immunoreactive deposits in the present study suggests that there is a well-developed intercellular electrical coupling between ICC-SM and smooth muscle cells in a particular region of this tissue layer of the rat antrum. In this context, it is another possibility to be examined whether ICC-SM play a role of active propagation of slow waves which was suggested for ICC within the circular muscle layer in the dog stomach (Horiguchi et al. 2001).

One of the most important findings of the present study is that ICC-SM are observed in both wild-type rats and *Ws/Ws* mutant rats, though the cell density is sparser in the latter strain. These cells are ultrastructurally similar to ICC-SM of the dog antrum (Horiguchi et al. 2001) and are classified as Type 3 ICC, the most similar to smooth muscle cells, in respect of the presence of many caveolae and a distinct basal lamina (Komuro et al. 1999).

It should be emphasized that type 3 ICC, the most muscle-like ICC, are observed in both *c-kit* and stem cell factor mutant animals, regardless of the organ or tissue layer concerned. Examples include the ICC-DMP of the *Ws/Ws* rat small intestine (Horiguchi et al. 1995; Horiguchi and Komuro 1998) and ICC-SMP of the *Ws/Ws* rat colon (Ishikawa and Komuro 1998), the ICC-DMP of the small intestine of the W/W^v mouse (Malysz et al. 1996) and Sl/Sl^d mouse (Ward et al. 1995), the ICC-AP of

the *W/W^v* mouse pylorus (Ward et al. 1998), and the ICC-AP of the *Ws/Ws* rat pylorus (present observations).

In contrast to these observations, the least muscle-like Type 1 ICC such as the ICC-AP of the rat small intestine (Horiguchi et al. 1995; Horiguchi and Komuro 1998) and the intermediate Type ICC or ICC-CM of the mouse (Burns et al. 1996) and the rat stomach (Ishikawa et al. 1997; present observations) could not be seen in those *c-kit* mutant animals, *W/W^v* mice and *Ws/Ws* rats, respectively.

In other words, the former evidence suggests that the most muscle-like Type 3 ICC can develop and mature cytologically independent of the *c-kit*/stem cell factor system, or that there is some other compensatory system for their cell maturation. These observations suggest interesting directions for future studies, in the light of reports that ICC and smooth muscle cells originate from the same mesenchymal progenitor cells that co-express both Kit and smooth muscle myosin heavy chain (Kluppel et al. 1998), and that blockade of Kit signaling induces a smooth muscle cell phenotype (Torihashi et al. 1999).

Acknowledgements The authors would like to thank Dr. Peter Baluk of the Cardiovascular Research Institute, University of California, San Francisco, USA for reading the manuscript. This study was supported by a grant from the Ministry of Education and Science of Japan (13670572) and Waseda University Grant for Special Research Project (2001A-601).

References

Burns AJ, Lomax AE, Torihashi S, Sanders KM, Ward SM (1996) Interstitial cells of Cajal mediate inhibitory neurotransmission in the stomach. Proc Natl Acad Sci USA 93: 12008-12013

Burns AJ, Herbert TM, Ward SM, Sanders KM (1997) Interstitial cells of Cajal in the guinea-pig gastrointestinal tract as revealed by c-Kit immunohistochemistry. Cell Tissue Res 290: 11-20

Conklin JL, Du C (1990) Pathways of slow-wave propagation in proximal colon of cats. Am J Physiol 258: 894-903

Dickens EJ, Hirst GD, Tomita T (1999) Identification of rhythmically active cells in guinea-pig stomach. J Physiol 514: 515-531

Dickens EJ, Edwards FR, Hirst GD (2001) Selective knockout of intramuscular interstitial cells reveals their role in the generation of slow waves in mouse stomach. J Physiol 531: 827-833

Faussone-Pellegrini MS, Pantalone D, Cortesini C (1989) An ultrastructural study of the interstitial cells of Cajal of the human stomach. J Submicrosc Cytol Pathol 21: 439-460

Hirst GD, Beckett EA, Sanders KM, Ward SM. (2002) Regional variation in contribution of myenteric and intramuscular interstitial cells of Cajal to generation of slow waves in mouse gastric antrum. J Physiol 540: 1003-1012

Horiguchi K, Komuro T (1998) Ultrastructural characterization of interstitial cells of Cajal in the rat small intestine using control and Ws/Ws mutant rats. Cell Tissue Res 293: 277-284

Horiguchi K, Zhou DS, Seki K, Komuro T, Hirota S, Kitamura Y (1995) Morphological analysis of *c-kit* expressinng cells, with reference to interstitial cells of Cajal. J Smooth Muscle Res 31:303-305

Horiguchi K, Semple GS, Sanders KM, Ward SM. (2001) Distribution of pacemaker function through the tunica muscularis of the canine gastric antrum. J Physiol 537: 237-250

Ishikawa K, Komuro K (1996) Characterization of the interstitial cells associated with the submuscular plexus of the guinea-pig colon. Anat Embryol 194:49-55

Ishikawa K, Komuro T (1998) Ultrastructural characterization of the c-kit-expressing interstitial cells in the rat colon, using Ws/Ws mutant rat. Human Science (In Japanese) 11: 65-72

Ishikawa K, Komuro T, Hirota S, Kitamura Y (1997) Ultrastructural identification of the *c-kit*-expressing interstitial cells in the rat stomach: a comparison of control and Ws/Ws mutant rats. Cell Tissue Res 289:137-143

Kluppel M, Huizinga JD, Malysz J, Bernstein A (1998) Developmental origin and Kit-dependent development of the interstitial cells of cajal in the mammalian small intestine. Dev Dyn 211: 60-71

Komuro T (1999) Comparative morphology of interstitial cells of Cajal: ultrastructural characterization. Microsc Res Tech 47: 267-285

Komuro T, Seki K, Horiguchi K (1999) Ultrastructural characterization of the interstitial cells of Cajal. Arch Histol Cytol 62: 295-316

Malysz J, Thuneberg L, Mikkelsen HB, Huizinga JD (1996) Action potential generation in the small intestine of W mutant mice that lack interstitial cells of Cajal. Am J Physiol 271: G387-399

Mitsui R, Komuro T (2002) Direct and indirect innervation of smooth muscle cells of rat stomach, with special reference to the interstitial cells of Cajal. Cell Tissue Res 309: 219-227

Nakama A, Hirota S, Okazaki T, Nagano K, Kawano S, Hori M, Kitamura Y (1998) Disturbed pyloric motility in Ws/Ws mutant rats due to deficiency of c-kit-expressing interstitial cells of Cajal. Pathol Int 48: 843-849

Niwa Y, Kasugai T, Ohno K, Morimoto M, Yamazaki M, Dohmae K, Nishimune Y, Kondo K, Kitamura Y (1991) Anemia and mast cell depletion in mutant rats that are homozygous at "white spotting (Ws)" locus. Blood 78: 1936-1941

Ordog T, Ward SM, Sanders KM (1999) Interstitial cells of Cajal generate electrical slow waves in the murine stomach. J Physiol 518: 257-269

Patterson LM, Zheng H, Ward SM, Berthoud HR (2001) Immunohistochemical identification of cholecystokinin A receptors on interstitial cells of Cajal, smooth muscle, and enteric neurons in rat pylorus. Cell Tissue Res 305: 11-23

Pluja L, Alberti E, Fernandez E, Mikkelsen HB, Thuneberg L, Jimenez M. (2001) Evidence supporting presence of two pacemakers in rat colon. Am J Physiol 281: G255-266

Rae MG, Fleming N, McGregor DB, Sanders KM, Keef KD (1998) Control of motility patterns in the human colonic circular muscle layer by pacemaker activity. J Physiol 510 : 309-320

Sanders KM (1996) A case for interstitial cells of Cajal as pacemakers and mediators of neurotransmission in the gastrointestinal tract. Gastroenterology 111: 492-515

Seki K, Komuro T (2001) Immunohistochemical demonstration of the gap junction proteins connexin 43 and connexin 45 in the musculature of the rat small intestine. Cell Tissue Res 306:417-422

Seki K, Komuro T (2002) Distribution of interstitial cells of Cajal and gap junction protein, Cx43 in the stomach of wild-type and *W/Wv* mutant mice. Anat Enbryol 206: 57-65

Serio R, Huizinga JD, Barajas-Lopez C, Daniel EE (1990) Interstitial cells of Cajal and slow wave generation in canine colonic circular muscle. J Auton Nerv Syst 30: 141-143

Stach W (1972) The extreme enteric plexus of the large intestine and its relation to the interstitial cells (Cajal). Z Mikrosk Anat Forsch (In German) 85: 245-272

Takayama I, Seto E, Zai H, Ohno S, Tezuka H, Daigo Y, Fujino M (2000) Changes of in vivo gastrointestinal motor pattern in pacemaker-deficient (WsRC-*Ws/Ws*) rats. Dig Dis Sci 45:1901-1906

Thuneberg L (1982) Interstitial cells of Cajal: intestinal pacemaker cells? Adv Anat Embryol Cell Biol 71: 1-130

Torihashi S, Nishi K, Tokutomi Y, Nishi T, Ward S, Sanders KM (1999) Blockade of kit signaling induces transdifferentiation of interstitial cells of Cajal to a smooth muscle phenotype. Gastroenterology 117: 140-8

Ward SM, Burns AJ, Torihashi S, Harney SC, Sanders KM 1995) Impaired development of interstitial cells and intestinal electrical rhythmicity in steel mutants. Am J Physiol 269: C1577-85

Ward SM, Morris G, Reese L, Wang XY, Sanders KM (1998) Interstitial cells of Cajal mediate enteric inhibitory neurotransmission in the lower esophageal and pyloric sphincters. Gastroenterology 115: 314-29

Ward SM, Beckett EA, Wang X, Baker F, Khoyi M, Sanders KM (2000) Interstitial cells of Cajal mediate cholinergic neurotransmission from enteric motor neurons. J Neurosci 20: 1393-403

Anat Embryol (2002) 206:57–65
DOI 10.1007/s00429-002-0279-0

ORIGINAL ARTICLE

Keisuke Seki · Terumasa Komuro

Distribution of interstitial cells of Cajal and gap junction protein, Cx 43 in the stomach of wild-type and *W/W^v* mutant mice

Accepted: 12 September 2002 / Published online: 9 November 2002

Abstract The distribution of different subtypes of interstitial cells of Cajal (ICC) in the tunica muscularis of the stomach of wild-type and *W/W^v* mice was studied by immunohistochemical staining for Kit. Special attention was also given to the distribution of the gap junction protein connexin 43 (Cx 43) immunoreactivity. Kit-immunoreactive cells of the circular and longitudinal muscle layers (ICC-CM and ICC-LM) were densely distributed throughout the cardia, fundus, the squamous epithelial portion of the corpus and the pylorus, but they were decreased in number within the glandular epithelial portion of the corpus. Kit-immunoreactive cells of the myenteric region (ICC-AP) emerged slightly proximal to the squamous-glandular epithelial transition and increased in number towards the pylorus. Kit-positive cells were also observed at the submucosal border of the circular muscle layer (ICC-SM). ICC-CM and ICC-LM were not observed in the stomachs of *W/W^v* mice, but a few ICC-AP were observed in the pylorus. Cx 43 immunoreactive deposits were only sparsely distributed in the circular muscle layers of the cardia, fundus and the squamous epithelial portion of corpus. However, the Cx 43 immunoreactive deposits were densely distributed in the glandular epithelial portion of the corpus that contained fewer ICC-CM. Cx 43 immunoreactive deposits were rare in the circular muscle layer of the pylorus. No Cx 43 immunoreactivity was detected in the longitudinal muscle layer throughout the whole stomach. The distribution of Cx 43 immunoreactivity in the *W/W^v* mouse stomach was almost the same as in wild-type mice. The functional significance of each type of ICC at each region is discussed in reference to regional differences in the distribution of both ICC and Cx 43, and differences between wild-type and *W/W^v* mice.

K. Seki · T. Komuro (✉)
Department of Basic Human Sciences, School of Human Sciences, Waseda University, Tokorozawa, Saitama, 359-1192, Japan
e-mail: komuro@human.waseda.ac.jp
Tel.: +81-42-9484314, Fax: +81-42-9484314

Keywords Immunohistochemistry · c-*kit* · Connexin · Peristalsis · Smooth muscle

Introduction

During the last decade, studies of interstitial cells of Cajal (1911) (ICC) have accumulated evidence that different classes of ICC act either as pacemaker cells of peristaltic movement or as mediators of neural activity to the gastrointestinal musculature (see reviews by Sanders 1996; Ward and Sanders 2001). All ICC share a certain range of common features on the one hand, different subtypes of ICC classified by their anatomical position relative to the tissue layers and levels of the digestive tract, on the other hand, have their own cytological characteristics and different degrees of dependency on the Kit-stem cell factor system for their cytological differentiation (Komuro et al. 1999).

In the stomach, ICC were first reported in the dog corpus (Daniel et al. 1984) and in the human fundus, corpus and pyloric antrum (Faussonne-Pellegrini et al. 1989). More recent studies showed that there are regional differences in the distribution of ICC from the proximal to distal portions of the guinea-pig stomach (Burns et al. 1997) and that ICC in the myenteric region are unexpectedly present in *W/W^v* mice which have mutation on c-*kit* (Burns et al. 1996; Ward et al. 2000). It has also been proved that ICC of the myenteric region act as pacemakers in the guinea-pig and mouse stomach (Dickens et al. 1999; Ördög et al. 1999), as has been reported in many studies of the small intestine (Ward and Sanders 2001). Furthermore, by comparing the antral regions of stomachs of wild-type and *W/W^v* mutant mice, it has been suggested that intramuscular ICC generate the secondary regenerative component of slow waves (Dickens et al. 2001). Similarly, the role of ICC as mediators of neural activity has been analyzed according to the distribution of specific subtypes of ICC (Burns et al. 1996; Ward et al. 1998; 2000; Ördög et al. 1999). Although the presence or absence of a particular

subtype of ICC in a certain region of the stomach was crucial in these studies, the morphological descriptions were limited and did not extend to all subtypes of ICC in the whole stomach. On the other hand, it is known that the electrical properties of the gastric smooth muscles differ from region to region of the stomach (Suzuki 2000).

For these reasons, it seems important to obtain a clear understanding of the precise distribution of ICC in the stomach of experimental animals that are frequently used

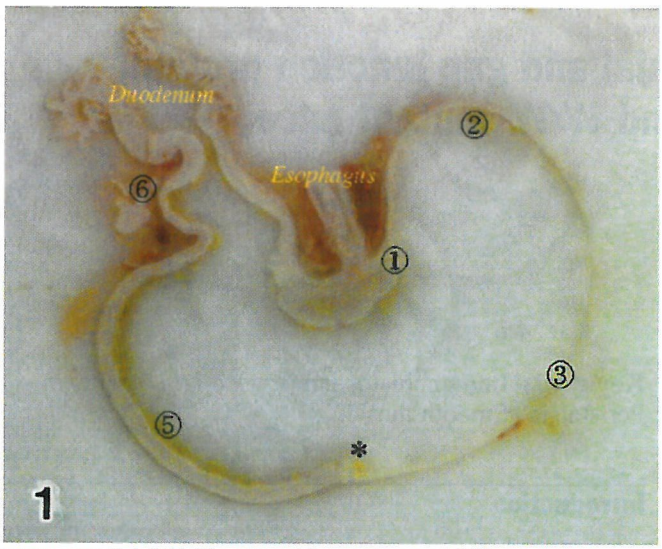

Table 1

	Region	*Thickness of muscle coat*
1	Cardia	600 μm
2	Fundus	170 μm
3	Squamous epithelial portion of the corpus	80 μm
*	Squamous-Glandular Epithelial Junction	70 μm
5	Glandular epithelial portion of the Corpus	30 μm
6	Pylorus	180 μm

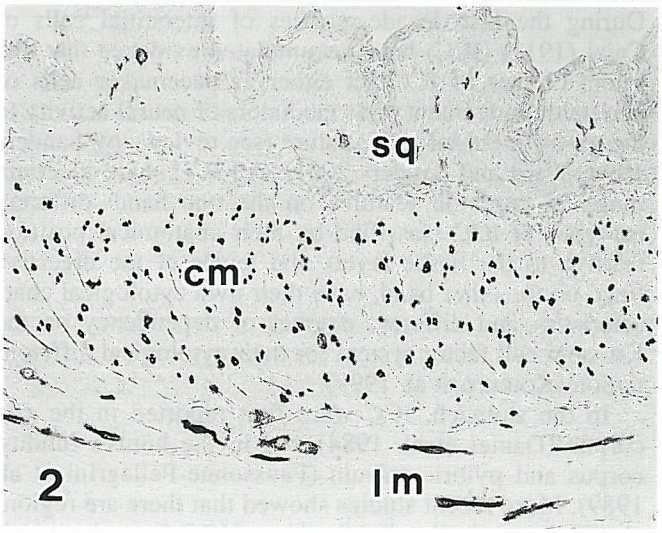

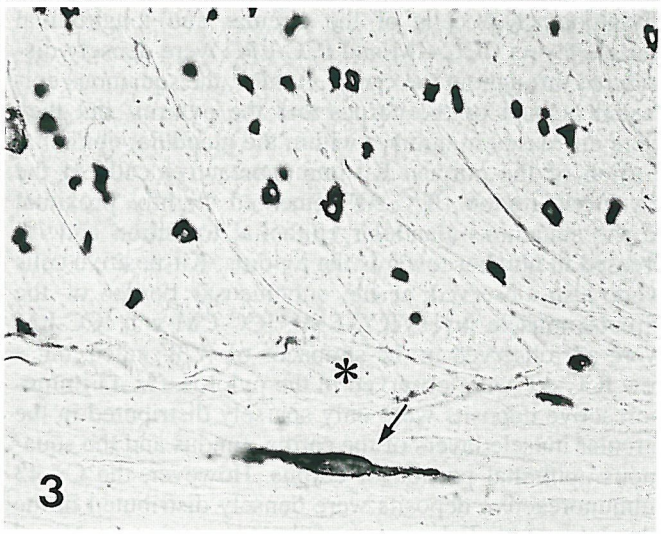

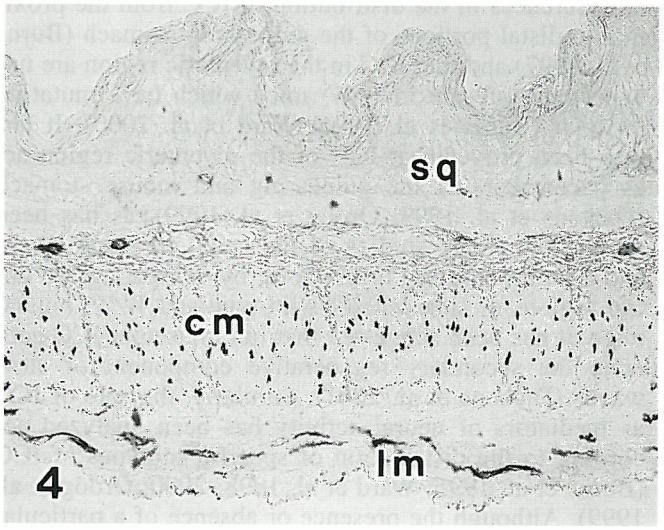

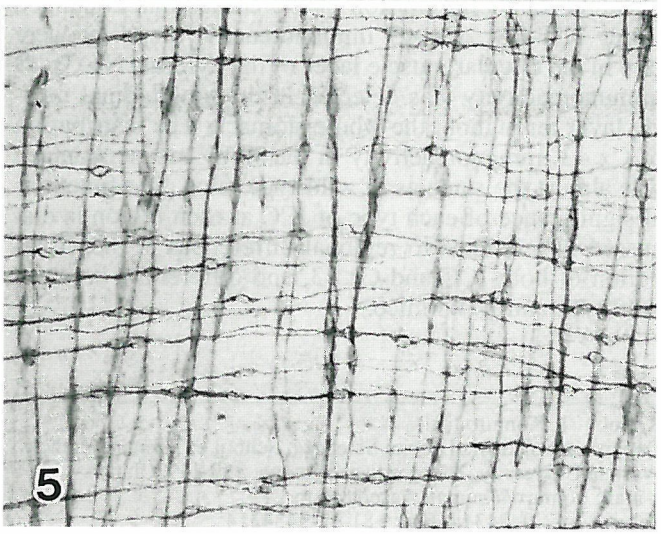

in studies of ICC. The present study was designed to systematically demonstrate the distribution of ICC in all tissue layers of the stomach from the cardiac to pyloric regions in both wild-type and W/W^v mice. In addition, the demonstration of the distribution of the gap junction protein connexin 43 (Cx 43) provides some insights into the degree of the cellular coupling in these muscle layers.

Materials and methods

Animals

Five homozygous WBB6F1-W/W^v and seven +/+ mice (8–10 weeks) of both sexes were purchased from Japan SLC (Shizuoka, Japan). The stomachs were dissected under terminal anesthesia with ether. All procedures were performed in accordance with the guidelines for the care and use of laboratory animals of the School of Human Sciences of Waseda University.

Immunohistochemistry for Kit and Cx 43

Stomachs were briefly rinsed in phosphate-buffered saline (PBS), immersed in OCT compound, and immediately frozen with liquid nitrogen. For immunohistochemistry with sections, longitudinal sections (8–10 μm thick) were cut with a Microm HM 505-E cryostat, mounted on poly-L-lysine coated glass slides, and fixed for 20 min at -20°C with absolute acetone. For immunohistochemistry with whole-mount stretch preparations, the stomach was inflated and fixed with absolute acetone for 40 min at 4°C, and pieces of the cardia, fundus, corpus and antrum were dissected. The mucosa was removed under the dissection microscope, and stretch preparations of the musculature were mounted on glass slides.

The specimens were then first incubated with 4% Block Ace solution (Dainippon Seiyaku, Osaka, Japan) in PBS for 20 min at room temperature to prevent non-specific reaction. Immunohistochemistry was performed as follows: specimens were incubated with a rat monoclonal antibody against Kit (ACK-2; Gibco, no. 3314SA) at a dilution of 1:200. After rinsing in PBS several times, the specimens were incubated with horseradish peroxidase-conjugated secondary antibodies (rabbit anti-rat IgG-HRP, Dako, no. P0450) at a dilution of 1:80. The peroxidase reaction was developed in 50 ml 0.1 M Tris-HCl buffer containing 6 mg of 4-chloro-1-naphthol (Sigma) and 8 μl of 30% H_2O_2. Other sections were incubated with a rabbit polyclonal antibody against Cx 43 (Chemicon International, no. AB1728) at a dilution of 1:100. Peroxidase-conjugated secondary antibodies (Envision+ system for rabbit IgG, Dako, no. K4003) were used, and the peroxidase reaction was performed using the procedure described above. After a brief rinse in PBS, the specimens were mounted in Mount-Quick and photographed with a Nikon light microscope. Control specimens were processed in a similar manner, but the primary incubation solution did not contain ACK-2 or anti-Cx 43.

Results

Localization of ICC

To clarify the portions observed, micrographic montages were made of longitudinal sections passing through the mid-line of the stomachs. The distribution of each subtype of ICC was examined at six key regions (Fig. 1). Those areas were plotted on a cut surface of the frozen specimens indicating the last section cutting through the midpoint of the tubular wall of the esophagus and the pyloric sphincter. The montage examination of whole stomachs demonstrated gradual changes in the density of distribution of some types of ICC and the abrupt appearance or disappearance of other types of ICC along the proximal to distal portions of the stomach. Key regions of the stomach were characterized by differences in the mucosal epithelium and in the thickness of the muscle coat, which ranged from about 30–600 μm in the specimen of Fig. 1 (see also the associated Table 1).

Wild-type mice

Cardia and fundus

Kit-immunoreactive cells were densely distributed throughout the well-developed thick circular muscle layer (ICC-CM) of both cardiac and fundic regions of the mouse stomach (Figs. 2, 3, 4). Kit-positive cells were also observed in the longitudinal muscle layers (ICC-LM) but they were completely lacking from the myenteric region (ICC-AP) between the circular and longitudinal muscle layers. Because of the absence of ICC-AP and the elongated bipolar shape of both ICC-CM and ICC-LM, in whole-mount preparations these ICC were clearly observed arranged perpendicular to each other (Figs. 5, 6 inset).

Squamous epithelial portion of corpus

Although the thickness of the circular musculature gradually decreased from the proximal to distal region, Kit-positive ICC-CM and ICC-LM showed a similarly dense distribution in the squamous epithelial portion of the corpus (Fig. 6) to those in the fundic region. ICC-AP were

◀ **Fig. 1** A section through an entire frozen stomach of the mouse showing the various anatomical regions examined. The thickness of the muscular coat at each portion (*1, 2, 3, *, 5* and *6*) is indicated in the associated Table 1. ×6

Fig. 2 A longitudinal section of the cardia immunostained for Kit. Kit-positive cells are densely distributed in the thick circular muscle layer (*cm*). They are observed as the elongated cells in the longitudinal muscle layer (*lm*). *sq* squamous epithelial layer. ×120

Fig. 3 Higher magnification of the myenteric region of the cardia. Kit-positive cells are not observed around the ganglia (*) or between the two muscle layers. Note bipolar shape of a Kit-positive cell in the longitudinal muscle layer (*arrow*). ×450

Fig. 4 A longitudinal section of the fundus showing rich distribution of Kit-positive cells within both circular (*cm*) and longitudinal (*lm*) muscle layer, but not in the myenteric region. *sq*; squamous epithelial layer. ×150

Fig. 5 A wholemount stretch preparation of the muscle coat of the fundus. Bipolar cells within the circular and longitudinal muscle layers are oriented perpendicularly to each other and are clearly visible because of the lack of Kit-positive cells in the myenteric region. ×180

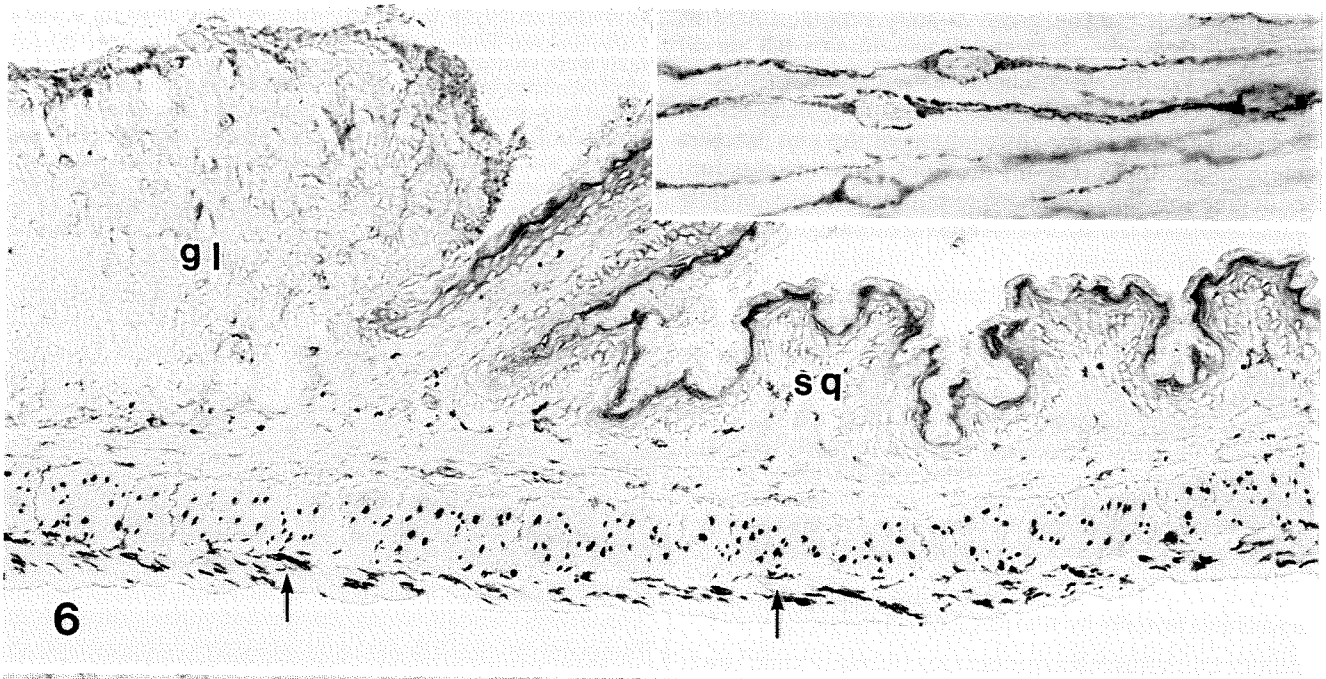
gl
sq
6

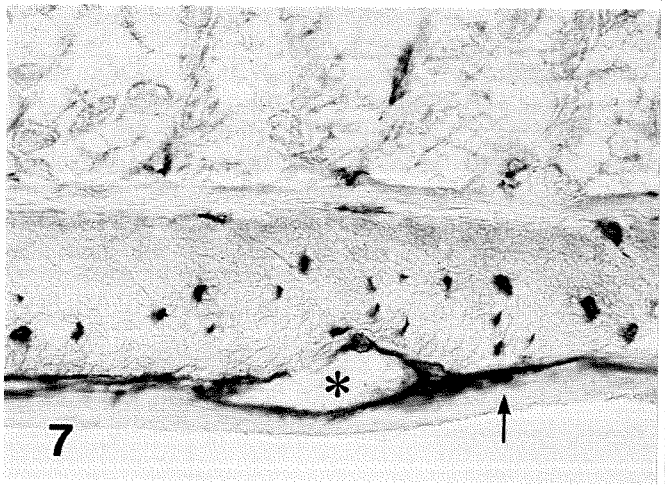
*
7

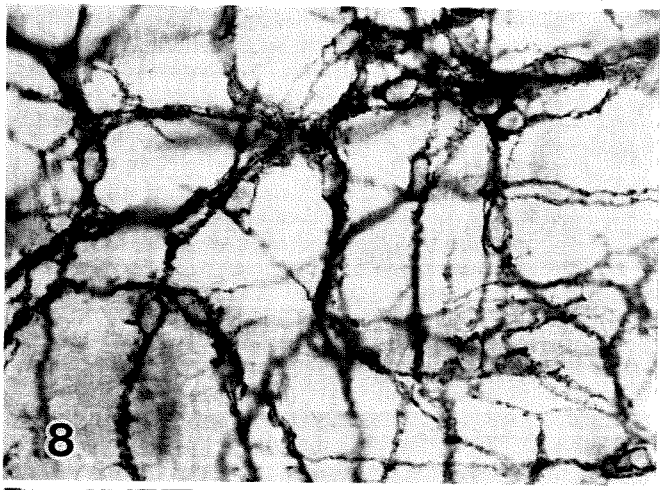
8

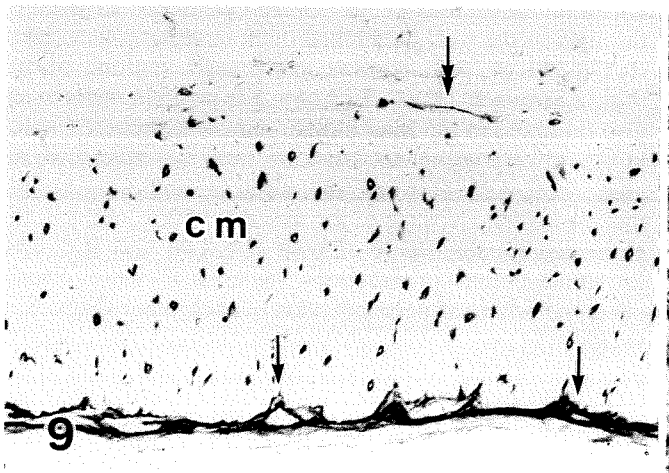
cm
9

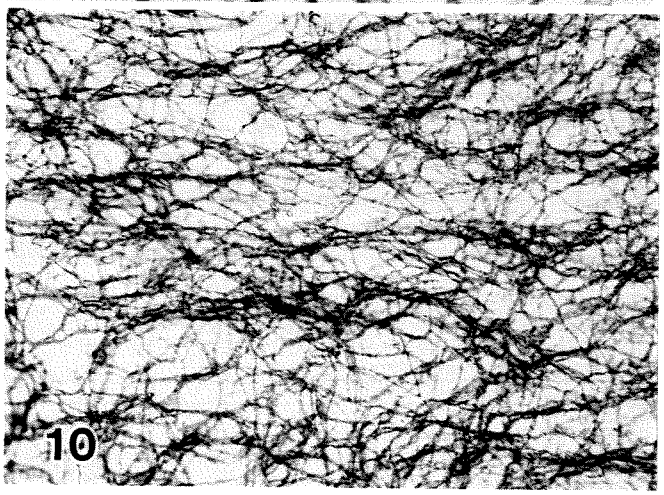
10

not observed in the myenteric region of the squamous epithelial portion of the corpus except in the area adjacent to the glandular corpus.

Glandular epithelial portion of corpus

Away from the squamous-glandular epithelial junction toward the pylorus, the thickness of the muscle coat was reduced to approximately half to one third (Figs. 6, 7). Both ICC-CM and ICC-LM gradually decreased in number and they were rare in the region with a thin muscle coat. On the other hand, ICC-AP were sparse over the squamous-glandular junction but increased in number toward the pylorus. Kit-positive cells surrounded the myenteric ganglia. In whole-mount preparations these ICC-AP showed multipolar shape to form the cellular network (Fig. 8).

Pyloric antrum and pylorus

The circular musculature of the corpus became thicker toward the pylorus and contained many Kit-positive ICC-CM (Fig. 9) but the longitudinal muscle layer was thin and contained only a few ICC-LM. On the other hand, the myenteric region displayed very strong Kit-immunoreactivity in cryosections. In fact, the immunoreactivity was so strong and dense that in low power micrographs of whole-mount specimens the multipolar shape of individual cells was not easily identified in the dense cellular network of ICC-AP (Fig. 10). The most characteristic feature of the musculature in the pylorus was the presence of thick circular muscle bundles of the sphincter and the presence of Kit-positive cells (ICC-SM) at the submucosal border of the circular muscle layer (Fig. 9). Although these ICC-SM were few in number, they were only observed in a confined area directly adjacent to the sphincter. In the sphincter region the distributions of ICC-CM and ICC-LM were similar to those in the antral region, but ICC-AP were usually fewer in number.

W/W^v Mice

No Kit-positive cells were observed in the muscle coats of cardia, fundus and corpus of the stomach of *W/W^v* mice (Figs. 11, 12). However, a few Kit-positive cells (ICC-AP) were observed in the myenteric region of the pyloric portion (Figs. 13, 14) in other words, ICC-CM and ICC-LM were not observed in the stomachs of *W/W^v* mice.

Distribution of Cx 43 immunoreactivity

Wild-type mice

Cardia and fundus

Cx 43 immunoreactivity was very weak and sparsely distributed in the thick circular muscle layers of the cardia and fundus. The rare Cx 43 immunoreactive deposits tended to be located in the connective tissue septa intervening between muscle bundles rather than within the muscle bundles themselves. No immunoreactivity was detected in the myenteric region and in the longitudinal muscle layer (Fig. 15).

Squamous and glandular epithelial portion of corpus

Cx 43 immunoreactivity within the circular muscle layer in the squamous epithelial portion of the corpus was similar to that of the fundus. However, Cx 43 immunoreactivity became dense in the glandular epithelial portion of the corpus that corresponded to the portion described above with only a thin muscle coat and few Kit positive cells (Fig. 16). Those immunoreactive deposits were mainly located within the muscle bundles in this region. The dense distribution of Cx 43 immunoreactivity continued slightly proximal to the pyloric antrum. The myenteric region and the longitudinal muscle layer did not show any substantial immunoreactivity for Cx 43.

Pyloric antrum and pylorus

Cx 43 immunoreactivity was sparsely distributed in the circular muscle layer and was not detected in the longitudinal muscle layer (Fig. 17). However, the immunoreactivity was detected in the space between the two muscle layers and was often observed as if surrounding the myenteric ganglia.

◀ **Fig. 6** The transition from squamous (*sq*) to glandular (*gl*) epithelium of the corpus. Kit-positive cells are evenly distributed in both circular and longitudinal layers throughout adjacent area. A few Kit-positive cells can be observed in the myenteric region (*arrows*). ×170 *Inset*: Bipolar cells observed in a stretch preparation of the fundus. ×480

Fig. 7 The glandular corpus with a thin muscle coat containing a few Kit-positive cells in the circular and longitudinal muscle layers. Note, the presence of Kit-positive cells around the myenteric ganglion (*) and between two muscle layers (*arrow*). ×400

Fig. 8 A wholemount stretch preparation of the muscle coat of the glandular corpus showing a network of Kit-positive multipolar cells at the level of the myenteric plexus. ×400

Fig. 9 A longitudinal section of the pylorus close to the sphincter (*left side*). Dense distribution of the Kit-positive cells in the circular muscle layer (*cm*) and in the myenteric region (*arrows*). Note the presence of a few Kit-positive cells at the border of the submucosa and the circular muscle layer (*double-headed arrow*). ×250

Fig. 10 A wholemount stretch preparation of the pylorus showing a network of multipolar Kit-positive cells at the level of myenteric plexus that is so dense that cell boundaries cannot be accurately distinguished. ×100

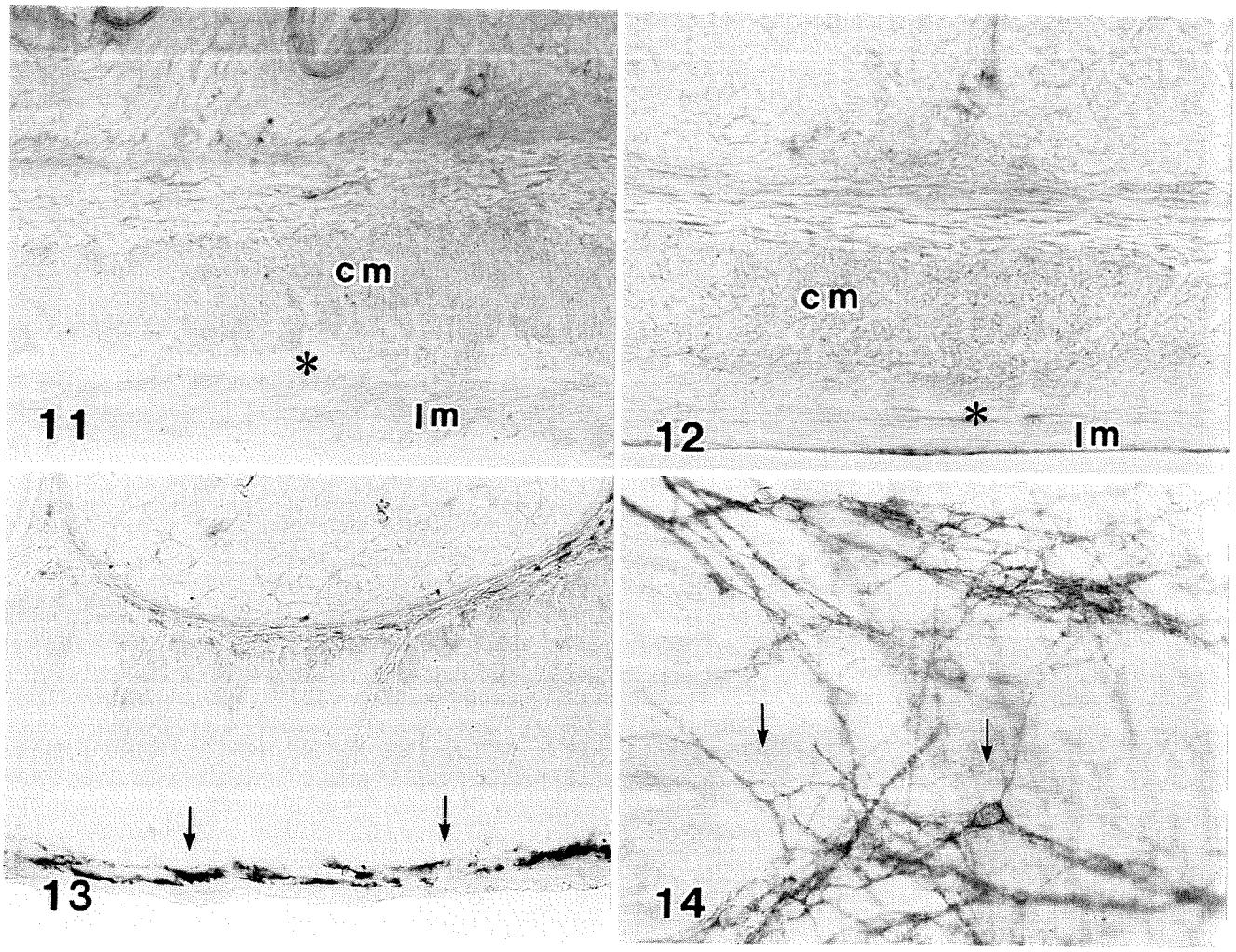

Fig. 11 A longitudinal section of the fundus of *W/W*^{v} mouse stomach showing a lack of Kit-positive cells throughout circular (*cm*) and longitudinal (*lm*) muscle layers and in the myenteric plexus region (*). ×350

Fig. 12 A longitudinal section of the glandular corpus of *W/W*^{v} mouse stomach showing a lack of Kit-positive cells throughout circular (*cm*) and longitudinal (*lm*) muscle layers and in the myenteric plexus region (*). ×500

Fig. 13 A longitudinal section of the pylorus of *W/W*^{v} mouse stomach showing a relatively small number of Kit-positive cells in the myenteric plexus region (*arrows*). ×250

Fig. 14 A wholemount stretch preparation of the pylorus of *W/W*^{v} mouse stomach showing a loose network of multipolar Kit-positive cells at the level of the myenteric plexus (*arrows*). ×400

W/W^{v} *mice*

The distribution of Cx 43 immunoreactivity in the stomach of *W/W*^{v} mice was almost the same as in wild-type mice. One exception was in the pyloric region where Cx 43 immunoreactivity around the myenteric plexus was relatively weak compared to that of wild-type mice. In this region Cx 43 immunoreactive deposits were not observed in the circular muscle layer (Fig. 18).

Discussion

Previous morphological descriptions of ICC focused on specific portions of the mouse stomach, including the fundus and antrum (Burns et al. 1996), pyloric sphincter (Ward et al. 1998)and fundus (Ward et al. 2000). The present study confirmed and extended these reports in great detail. It also becomes clear that the distribution of ICC in the mouse stomach is comparable to the ICC in the fundus, corpus and antrum of the guinea-pig stomach (Burns et al.1997). The comprehensive observations of the whole stomachs of mice clearly revealed that the distribution of each class of ICC changes without regard to the boundary between the squamous and glandular epithelium in the corpus. The distributions of each type of ICC and of the gap junction protein Cx 43 in the whole stomach of the mouse are summarized in Figs. 19 and 20 respectively.

The present study showed that ICC-AP are not found in the cardia and fundus, and only become evident in a certain part of the corpus. The ICC-AP are considered to be essential for the generation of slow wave activity of gastric muscles of the guinea-pig (Dickens et al. 1999) and the mouse (Ördög et al. 1999). Therefore, regular rhythmic peristaltic movements within the mouse stom-

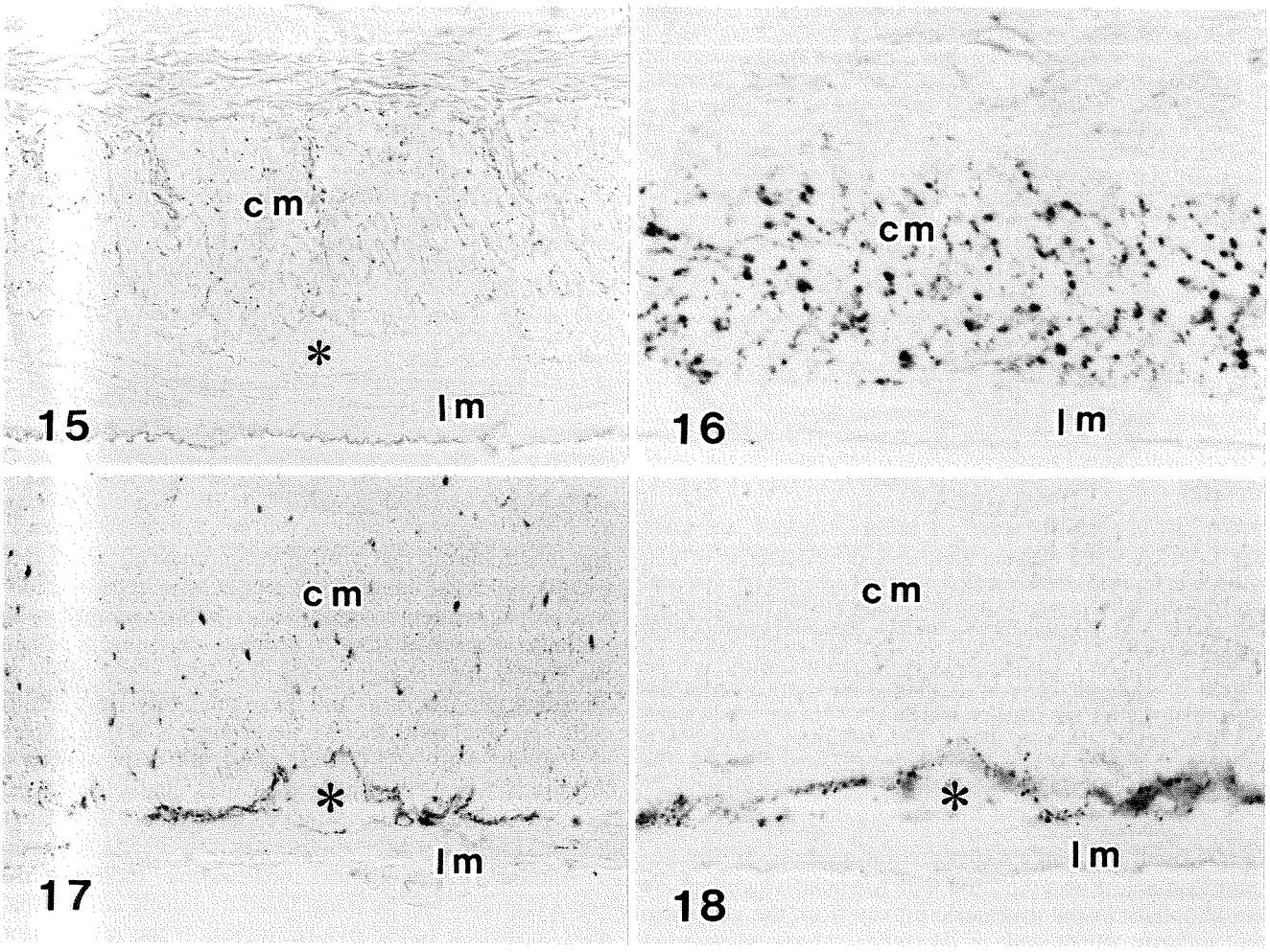

Fig. 15 A longitudinal section of the fundus of wild-type mouse stomach stained for Cx 43 immunoreactivity. Weak reactive deposits are sparsely observed in the circular muscle layer (*cm*), but not in the longitudinal muscle layer (*lm*) and in the myenteric plexus region (*). ×400

Fig. 16 A longitudinal section of the glandular corpus of the wild-type mouse stomach stained for Cx 43 immunoreactivity. The immunoreactive deposits are densely distributed within the circular muscle layer (*cm*). The deposits are not detected in the longitudinal muscle layer (*lm*). ×600

Fig. 17 A longitudinal section of the pylorus of the wild-type mouse stomach stained for Cx 43 immunohistochemistry. The immunoreactive deposits are sparsely distributed within the circular muscle layer (*cm*). They are also observed in the myenteric region as if surrounding the ganglion (*). No immunoreactivity is found in the longitudinal muscle layer (*lm*). ×400

Fig. 18 A longitudinal section of the pylorus of W/W^v mouse stomach stained for Cx 43 immunohistochemistry. The immunoreactive deposits are only observed in the myenteric region (*) but not in the circular (*cm*) and longitudinal muscle layers (*lm*). ×450

ach probably start from the region where ICC-AP first start to form a proper cellular network. The portion slightly proximal to the pyloric sphincter that showed the strongest Kit immunoreactivity in the present observation may represent the most active site for generating rhythmic slow waves. Dickens et al. 1999) also observed that the region with the highest density of ICC-AP usually occurred as a region located some 4 mm from the gastro-duodenal junction in the mouse stomach. Cx 43 immunoreactivity found in the myenteric region of only the pyloric area seems to indicate the presence of abundant gap junctions formed over the dense cellular network composed of a large number of ICC-AP.

The presence of ICC-SM along the submucosal surface of the circular muscle layer was first noticed in the antrum of the human stomach (Faussone-Pellegrini et al. 1989) and then described as occasional observations within the pyloric sphincter of the mouse stomach (Ward et al. 1998). Their occurrence in the pyloric region was also confirmed by the present study. ICC-SM were recently reported in the corresponding location of the dog antrum and were suggested to have a pacemaker function (Horiguchi et al. 2001). Similar types of cells have also been observed in a confined area of the rat pyloric region (R. Mitsui and T. Komuro, unpublished data). An important question for future studies may be why only a limited area of the pylorus contains ICC-SM on the submucosal surface of the circular muscle layer.

A further interesting question is to what extent are the cytological and physiological features of ICC similar be-

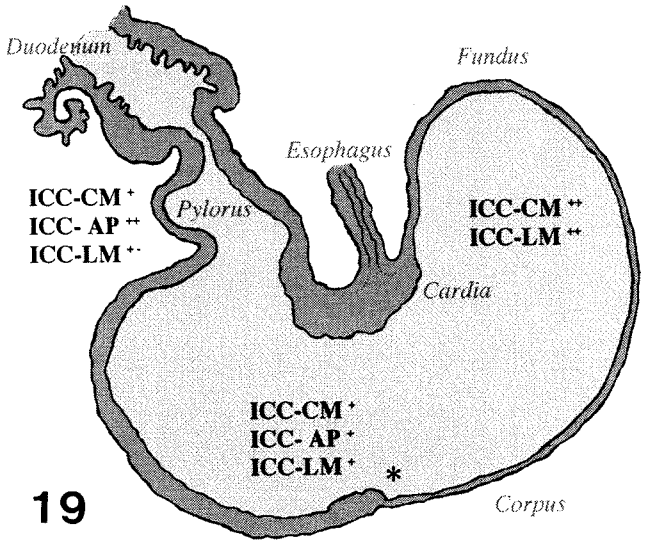

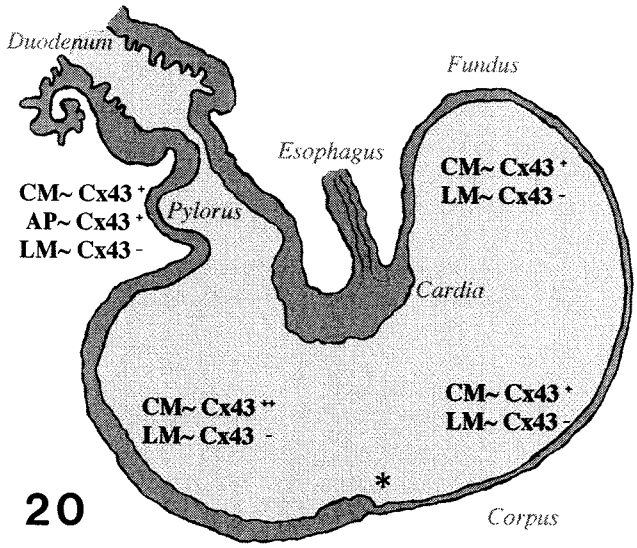

Fig. 19 A schematic diagram illustrating the distribution of subtypes of ICC in the whole stomach of a wild-type mouse. The density of distribution is represented by abundant (++), moderate (+), and sparse (+ –). The squamous-glandular epithelial junction is indicated by (*)

Fig. 20 A schematic diagram illustrating the distribution of immunoreactivity for gap junction protein Cx 43 in the whole stomach of a normal wild-type mouse. The density of distribution is represented by abundant (++), moderate (+), and none (–). The squamous-glandular epithelial junction is indicated by (*)

tween small and large experimental animals. In the human stomach it was reported that Kit-positive cells were not abundant in the myenteric plexus from the corpus to the pylorus (Torihashi et al.1999). These apparently inconsistent observations may be clarified by a better understanding of the question whether homologous ICC of different tissue layers or different regions of the digestive tract retain common functional roles in a variety of species.

One of the most important findings of the present study is the reciprocal distribution of ICC-CM and Cx 43 immunoreactivity. The regions with a thick circular muscle layer in the cardia and fundus had a very dense distribution of ICC-CM but only weak Cx 43 immunoreactivity, while the thin muscle portion of the corpus was characterized by a sparse distribution of ICC-CM but a dense distribution of Cx 43 immunoreactivity. Cx 43 immunoreactivity found in the connective tissue septa in the cardia and fundus appear to represent gap junctions to form the network of ICC-CM. On the other hand, in the latter case, most of Cx 43 immunoreactivity probably represents gap junctions between muscle cells, because it does not show a substantial difference between wild-type mice and W/W^v mice that lack ICC-CM.

Recent studies provide experimental support for the intercalation hypothesis for ICC (Cajal 1911; Thuneberg 1982) for both inhibitory and excitatory neurotransmission (Burns et al. 1996; Ward et al. 1998, 2000). Thus, the present observations suggest that muscle cells of the cardia and fundus are not well coupled to each other by gap junctions and that instead these relatively small electrically syncytial units and/or single muscle cells receive and propagate nerve signals via a well-developed cellular network of ICC-CM. In contrast, the muscle cells of the corpus are frequently coupled with each other via abundant gap junctions and these relatively large electrically syncytial units receive nerve signals at much sparser contacts with ICC-CM. In short, different regions of the stomach appear to have their own characteristic patterns of contractile units under the influence of a single ICC-CM or ICC-LM.

Another morphological observation indicates that nerve impulses can be transmitted to muscle cells by parallel pathways. In the pyloric region of the rat stomach, muscle cells are both directly and indirectly innervated via ICC (Mitsui and Komuro 2001, 2002). The question arises what is the physiological meaning of the large variety of pathways for transmission of nerve impulses to the gastric muscle. Does the intercalation of ICC between the nerves and muscle cells simply substitute for neuromuscular junctions and compensate for the lack of gap junctions between the muscle cells? In this respect, it is unlikely that ICC-CM and ICC-LM act as simple mediators of neural activity. Instead, the different degrees of intercalation of ICC in different regions may have their own special significance. The ICC-CM may have additional functions, such as the augmentation of pacemaker depolarizing waves generated by ICC-AP, as suggested by Dickens et al. 2001). Thus the different types of innervation and impulse propagation which are peculiar to each region of the stomach may explain the different regional electrical and contractile properties of the gastric muscle (Suzuki 2000).

Acknowledgements The authors would like to thank Dr. Peter Baluk of the Cardiovascular Research Institute, University of California, San Francisco, USA, for reading the manuscript. This study was supported by grants from the Ministry of Education and Science of Japan (13670572, 13770721), Waseda University Grant for Special Research Project (2001A-601), and by a grant from the Japanese Clinical Study Group of Esophagocardiac Regions (2000).

References

Burns AJ, Lomax AEJ, Torihashi S, Sanders KM, Ward SM (1996) Interstitial cells of Cajal mediate inhibitory neurotransmission in the stomach. Proc Natl Acad Sci USA 93: 12008–12013

Burns AJ, Herbert TM, Ward SM, Sanders KM (1997) Interstitial cells of Cajal in the guinea-pig gastrointestinal tract as revealed by c-Kit immunohistochemistry. Cell Tissue Res 290:11–20

Cajal SR (1911) Histologie du système nerveux de I'homme et des vertébrés, vol 2. Maloine, Paris

Daniel EE, Sakai Y, Fox JET, Posey-Daniel V (1984) Structural basis for function of circular muscle of canine corpus. Can J Physiol Pharmacol 62:1304–1314

Dickens EJ, Hirst GDS, Tomita T (1999) Identification of rhythmically active cells in guinea-pig stomach. J Physiol 514:515–531

Dickens EJ, Edwards FR, Hirst GDS (2001) Selective knockout of intramuscular interstitial cells reveals their role in the generation of slow waves in mouse stomach. J Physiol 531:827–833

Faussone-Pellegrini MS, Pantalone D, Cortesini C (1989) An ultrastructural study of the interstitial cells of Cajal of the human stomach. J Submicrosc Cytol Pathol 21:439–460

Horiguchi K, Semple GSA, Sanders KM, Ward SM (2001) Distribution of pacemaker function through the tunica muscularis of the canine gastric antrum. J Physiol 537:237–250

Komuro T, Seki K, Horiguchi K (1999) Ultrastructural characterization of the interstitial cells of Cajal. Arch Histol Cytol 62:295–316

Mitsui R, Komuro T (2001) Ultrastructural and immunohistochemical study of the interstitial cells of Cajal in the rat pylorus. Acta Anatomica Nipponica 76:63

Mitsui R, Komuro T (2002) Direct and indirect innervation of smooth muscle cells of rat stomach, with special reference to interstitial cells of Cajal. Cell Tissue Res 309:219–227

Ördög T, Ward SM, Sanders KM (1999) Interstitial cells of Cajal generate electrical slow waves in the murine stomach. J Physiol 518:257–269

Sanders KM (1996) A case for interstitial cells of Cajal as pacemakers and mediators of neurotransmission in the gastrointestinal tract. Gastroenterology 111:492–515

Suzuki H. (2000) Cellular mechanisms of myogenic activity in gastric smooth muscle. Jpn J Physiol 50:289–301

Thuneberg L. (1982): Interstitial cells of Cajal: intestinal pacemaker cells? Adv Anat Embryol Cell Biol 71:1–130

Torihashi S, Horisawa M, Watanabe Y (1999) c-Kit immunoreactive interstitial cells in the human gastrointestinal tract. J Auton Nerv Syst 75:38–50

Ward SM, Sanders KM (2001) Interstitial cells of Cajal: primary targets of enteric motor innervation. Anat Rec 262:125–135

Ward SM, Morris G, Reese L, Wang XY, Sanders KM (1998) Interstitial cells of Cajal mediate enteric inhibitory neurotransmission in the lower esophageal and pyloric sphincters. Gastroenterology 115:314–329

Ward SM, Beckett EA, Wang X, Baker F, Khoyi M, Sanders KM (2000) Interstitial cells of Cajal mediate cholinergic neurotransmission from enteric motor neurons. J Neurosci 20:1393–1403

Morphological features of Interstitial Cells of Cajal

Terumasa Komuro
School of Human Sciences, Waseda University,
Mikajima 2-579-15, Tokorozawa, Saitama, Japan 359-1192

Abstract

This review deals with the distribution, overall shape and ultrastructural features of the interstitial cells of Cajal (ICC) in the digestive tract in mice, rats and guinea-pigs as obtained by the author's research group, and compares these observations with reports in the literature of ICC in different species and in humans. ICC show some morphological heterogeneity depending on their species, tissue and anatomical location. They share certain common features such that they comprise a distinct cell type of mesenchymal origin. Their common features are the presence of numerous mitochondria and abundant intermediate filaments, formation of gap junctions with other ICC and with smooth muscle cells, and c-Kit immunoreactivity. In addition, depending on their region and species, ICC can show certain fibroblast-like features such as well-developed rough endoplasmic reticulum and Golgi apparatus, or on the other hand, a certain degree of myoid features including a basal lamina, caveolae, subsurface cisterns and dense bodies. Those are classified as the least muscle-like Type 1 ICC, intermediate Type 2 ICC, and the most muscle-like Type 3 ICC. This review also briefly describes recent advances in understanding the possible functions of ICC which suggest that they have a pacemaker role in peristaltic movement, and are mediators of nerve impulses from nerves to muscles and stretch mechanoreceptors.

Introduction

In 1982, Thuneberg proposed that interstitial cells of Cajal (ICC) might act as pacemaker cells and as an impulse conduction system in the gut musculature in a way analogous to the pacemaker cells in the heart (74). This novel and surprising hypothesis effectively revived modern research into ICC, and was a significant advance over the almost century of purely histological debate about them, which had continued ever since Cajal described "cellules interstitielles" associated with the terminal arborization of autonomic nerves stained with methylene blue and Golgi methods (Fig. 1)(6,7).

Since that time, an accumulation of evidence from morphological and physiological studies has made it clear that ICC are a distinct mesenchymal cell type (44,93) that has a pacemaker function and act as neuromediators in the tunica muscularis of the gastrointestinal tract (see reviews 30,42,43,68,75,84).

The presence of ICC has been reported in a wide variety of species, including the frog (56), lizard (36), turkey (58) and many mammals including bat, rabbit, opposum, hedgehog, pig, horse, conventional experimental animals such as the mouse, rat, guinea-pig and dog, and also in the monkey and human (see review 43). ICC have also been reported in the tissues beyond the gastrointestinal tract: the gall bladder (53), renal pelvis (37), urinary bladder (47), vas deference (5) and prostate gland (14).

In the human, ICC have been found throughout the digestive tract from the esophagus (16,81) to the inner sphincter region of the anus (21). It has been suggested that ICC are implicated in many diseases, including gastrointestinal stromal tumors, Hirschsprung's disease, diabetes mellitus, chronic idiopathic constipation etc (see section entitled '*ICC in Humans*').

A clear understanding of the cytological features of ICC seems an essential basis for further studies of their etiological, clinical and therapeutic aspects. The goal of this review is therefore to elucidate the specific distribution of each subclass of ICC in the gastrointestinal tract and to describe the morphological features of ICC that make it possible to distinguish them from other types of cells.

Morphological identification of ICC

After a long period of debate in which even the existence of interstitial cells of

Cajal as a distinct cell type was questioned, a key breakthrough in ICC research was the discovery of the important role of c-Kit in their cellular maturation. Abnormal development of ICC was demonstrated in studies in which c-Kit receptors were blocked experimentally (45,80) or in animals with genetic defects in c-Kit production (29,85).

The gap between the old histological descriptions and more recent findings was bridged by various techniques, including immunohistochemical studies of the expression of c-Kit and vimentin, ultrastructural observations, and the zinc iodide-osmium tetroxide (ZIO) staining method that shares properties with methylene blue staining, (41,42). Cells of the guinea-pig small intestine that stain for c-Kit and vimentin immunoreactivity (Figs. 2, 3) show almost the same characteristics as ICC illustrated by Cajal with methylene blue staining (Fig. 1). Such results establish the usefulness of c-Kit immunostaining for specific identification of ICC at the light microscopic level.

Cell shape and arrangement of ICC

The cell shape and arrangement of ICC appear to be determined by several factors; the presence or absence of local nerve plexuses, their close (or loose) relationships to those plexus, the orientation of the smooth muscle layer in which they lodged, and frequency of connections between ICC themselves. Immunostaining for c-Kit of the whole-mount stretch preparations proves to be very useful for visualizing the overall structures of ICC.

ICC around the myenteric (Auerbach's) plexus (AP) are generally multipolar cells with long slender processes with smooth and rather straight contours. Even though the ICC-AP are distributed around the myenteric plexus, the ICC form their own dense network with many connections with the same type of cells fairly independent of the nerve plexus (Fig. 4),. Three to five primary processes branch repeatedly to form secondary, tertiary and further branches (Fig. 2). One of the most distinct features of this cell type is the formation of a triangular knot at every branching point of the processes. Such features are well illustrated by immunohistochemistry for vimentin (Fig. 3).

ICC of the deep muscular plexus (DMP) of the small intestine can take a variety of forms depending on the sites of their associated nerve bundles, because they typically form close relationships with a characteristic network of DMP. At straight portions of

the nerves, they show slim spindle shapes with long bipolar processes, while at the intersections the cells project three to five processes along the nerve bundles (Fig. 5) (42).

ICC of the circular (CM) and longitudinal (LM) muscle layers are mainly bipolar cells along the axis of surrounding smooth muscle cells (Figs. 6,7). The secondary and tertiary processes are generally not well developed. The perpendicular arrangement of elongated bipolar shape of ICC-CM and ICC-LM to each other is clearly observed in whole-mount preparations of the mouse gastric fundus because of the absence of ICC-AP in this region (Fig. 7).

Distribution of ICC revealed by c-Kit immunohistochemistry

This review will focus on description of ICC in the stomach, small intestine and colon. However, the existence of ICC has been well documented in the esophagus, including the striated muscle portion in the guinea-pig (4) and the mouse (67), and the portion of the smooth musculature or the lower esophageal sphincter in the opposum (10), human (16,81), dog (1) and mouse (87).

Stomach

ICC are uniformly found around the myenteric plexus throughout nearly the entire digestive tract, but ICC of other gastrointestinal tissue layers show a characteristic organ-specific distribution (43). In this respect, the stomach is unique in that ICC have a different distribution in proximal and distal regions of the same organ (4,70). ICC-CM and ICC-LM are densely distributed throughout the well-developed thick circular and longitudinal muscle layers of the cardia, fundus and the most part of the squamous epithelial portion of the corpus in the mouse stomach respectively (Fig. 8). However, ICC-AP are completely lacking from the myenteric region between the circular and longitudinal muscle layers (Fig. 9). ICC-AP emerge in the area adjacent to the glandular corpus and become well-developed in the distal region of the corpus with a thin muscle coat, while both ICC-CM and ICC-LM decrease in number in this area (Fig. 10).

The circular musculature of the pylorus is thick and contains many ICC-CM (Fig. 11), but the longitudinal muscle layer is thin and contains only a few ICC-LM. In contrast, ICC-AP have a very dense distribution. Another characteristic feature of the pylorus is

the presence of c-Kit-positive cells (ICC-SM) at the submucosal border of the circular muscle layer (Fig. 11), though these ICC-SM are few in number and are only located in a confined area directly adjacent to the sphincter. A denser and wider distribution of ICC-SM is observed in the rat pylorus (49).

Small Intestine

c-Kit-immunoreactive ICC are localized in two regions; the myenteric plexus and DMP that extends two-dimensionally in a plane between the inner thin (1-3 cells thick) and outer thick sublayers of the circular muscle in the mouse, rat and guinea-pig small intestine (Fig. 12). ICC-DMP are closely associated with the plexus of nerve bundles running parallel to the smooth muscle cells of the circular layer and transverse interconnecting nerve bundles (40,63,95). Very few ICC-CM are found within the thick main sublayer of the circular muscle. c-Kit immunoreactivity is absent in the longitudinal muscle layer.

Colon

ICC are found in the myenteric region, as in the stomach and small intestine, and also at the interface between the submucosa and the circular muscle layer where submuscular plexus is located (ICC-SMP) (Fig. 13). Sparse c-Kit immunoreactivity is observed in the circular muscle layer. Those deposits are often located in the connective tissue septa, apparently outlining muscle bundles. A few c-Kit positive cells are found in the longitudinal muscle layer.

Ultrastructural features of ICC

One of the first pieces of ultrastructural evidence that ICC are a unique type of cell was obtained in the dog intestine, where ICC were designated as "hybrid cells" (11). As the name suggests, these ICC were interpreted as having a mixture of features typical of other types of cells such as fibroblasts, smooth muscle cells or Schwann cells such as a basal lamina, caveolae, subsurface cisterns and gap junctions. Because of these features, certain populations of ICC were considered by many investigators as modified or specialized smooth muscle cells (8,15,42,62,68,74,76,78,91). However,

ICC do not contain the well-organized contractile apparatus characteristic of muscle cells, even in those cases where myosin filaments and dense bodies have been reported (78,79). Some ICC have a similar appearance to fibroblasts and lack clear muscle-like features. However, such ICC can be distinguished from fibroblast-like cells by a combination of features including numerous mitochondria, abundant intermediate filaments, a different electron density of the cytoplasm and large gap junctions.

As described above, ICC of different tissue layers or different levels of the digestive tract or different species show a certain range of morphological heterogeneity. Thus, the different classes of ICC in different anatomical locations will be described separately.

Stomach

At the submucosal border of the circular muscle of the rat pylorus, ICC-SM are identified as cells containing many mitochondria, Golgi apparatus, rough (RER) and smooth (SER) endoplasmic reticulum (Fig. 14)(49). They have caveolae and a basal lamina around the cell membrane. They also contain abundant intermediate filaments, in particular in their processes (Fig. 15). They form gap junctions with each other and with the neighboring muscle cells (Figs. 14, 15). Close contacts between ICC-SM and nerve varicosities containing many synaptic vesicles are also present (Fig. 16).

ICC-CM within the circular muscle layer of the pylorus and corpus of the rat stomach are characterized by similar features to those of ICC-SM described above, in respects of cell organelles and their relationships with the same type of cells, smooth muscle cells and nerve terminals (Fig. 17)(34,48). But their cytoplasm is usually more electron-dense than that of smooth muscle cells and a basal lamina cannot be clearly identified around the cell membrane. Cells with the same features are also observed in the mouse and guinea-pig pylorus (39) and in the mouse fundus (unpublished data). ICC-LM with nearly same features as those of ICC-CM are found in the longitudinal muscle layer of the rat pylorus (48).

ICC-AP of the rat and mouse are characterized by almost the same features as those of ICC-SM of the rat, i.e. large gap junctions, many mitochondria, abundant intermediate filaments (Figs. 18-20), numerous caveolae and a distinct basal lamina (Fig.

21). Thus, ICC-AP are easily distinguished by these features from fibroblast-like cells, which have a less electron-dense cytoplasm containing well-developed RER with dilated cisterns (Fig. 18). Close contacts between ICC-AP and nerve terminals are also observed in the mouse stomach (Fig. 22).

Small intestine

ICC-DMP of the mouse and rat small intestine are observed as elongated cells of which cytoplasm is usually less electron-dense than that of the neighboring smooth muscle cells (Fig. 23). A basal lamina and numerous caveolae are observed along the cell membrane (Fig. 23 inset). Well-developed Golgi apparatus and RER are mainly located in the perinuclear region, while many mitochondria are observed throughout the cytoplasm. Cytoskeletal elements such as microtubules, microfilaments and intermediate filaments are abundant in the cytoplasmic processes. Subsurface cisterns of smooth endoplasmic reticulum have been found immediately beneath the cell membranes (40,69). The most conspicuous feature of ICC-DMP is the frequent occurrence of large gap junctions that interconnect the same type of cells with each other and also with smooth muscle cells. Their gap junctions with muscle cells are mainly formed with those of the outer subdivision, but some gap junctions with the muscle cells of inner sublayer are also observed (40). Their close contacts with nerve varicosities containing accumulations of synaptic vesicles have been well documented (25,40,69).

ICC-AP of the rat small intestine have a less-electron dense cytoplasm, numerous mitochondria, and large gap junctions which mainly connect with each other at the ends of thin processes (Fig. 24 and inset). Golgi apparatus and both SER and RER are also seen in the cytoplasm. However, cisterns of RER are rarely dilated, in contrast to fibroblast-like cells which often have this form of RER (Fig. 25). Intermediate filaments are abundant in the cytoplasmic processes. A few caveolae can be seen, but a basal lamina is not observed. ICC-AP of the mouse small intestine are very similar in many respects to ICC-AP of the rat small intestine (43). Three-dimensional relationships of ICC-AP to the myenteric plexus and smooth muscle cells are visualized by scanning electron microscopy (38).

Here, it is worth noting that fibroblast-like cells are found wherever ICC are found (39,43). They are characterized by typical ultrastructural features of fibroblasts (Fig. 25), and by the formation of small gap junctions with smooth muscle cells and close contacts with nerve terminals.

Colon

ICC-SMP of the rat colon are observed at the interface between the submucosa and the circular muscle layer (Fig. 26). They are ultrastructurally similar to ICC-SM of the stomach and ICC-DMP of the small intestine, and thus are clearly distinguished from fibroblasts (32).

ICC-CM of the rat colon are characterized by an electron-dense cytoplasm, caveolae and many mitochondria, similar to those in the stomach. Their differences from fibroblast-like cells are clearly seen in a micrograph showing both types of cells in one frame (Fig. 27). Similar types of cells have been observed in the guinea-pig colon (39).

ICC-AP of the rat colon are similar to those of the rat pylorus, but they differ from those of the small intestine. They are characterized by moderate to electron-dense cytoplasm (43). However, a basal lamina is not clearly defined, unlike ICC-AP of the mouse pylorus. Gap-junctions are observed between processes of the same type of cells.

Dependency of ICC on the c-kit /SCF system

In spite of the widely accepted notion that ICC express c-Kit and that their cell maturation depends on signaling between the c-Kit receptor and its ligand stem cell factor (SCF), there are many reports indicating survival of a certain population of ICC in the absence of a normal Kit/SCF signaling pathway. They were observed in both *c-kit* and stem cell factor mutant animals, regardless of the organ or tissue layer concerned. Those are ICC-AP in the pylorus of *W/Wv* mouse (Fig. 28) (70,87), and ICC-AP and ICC-SM in the pylorus of *Ws/Ws* rat (Fig. 29) (49). Other examples include the ICC-DMP of the *Ws/Ws* rat small intestine (Fig. 30) (25,26), the ICC-DMP of the small intestine of the *Sl/Sld* mouse (86) and *W/Wv* mouse (46) and ICC-SMP of the *Ws/Ws* rat colon (Fig. 31) (33).

It should be emphasized that these ICC share common ultrastructural features and are classified into Type 3 ICC, the most similar to smooth muscle cells, in respect of the presence of many caveolae and a distinct basal lamina (43). In contrast to these observations, the least muscle-like Type 1 ICC such as the ICC-AP of the rat small intestine (25,26) and the intermediate Type 2 ICC or ICC-CM of the mouse (3) and the rat stomach (34) could not be seen in those *c-kit* mutant animals, i.e. in *W/Wv* mice and *Ws/Ws* rats, respectively. The former evidence suggests that the most muscle-like Type 3 ICC can develop and mature cytologically independent of the *c-kit*/stem cell factor system, or that some other system that compensates in their cell maturation.

ICC in the human

Distribution

By c-Kit immunostaining, ICC were observed in the tunica muscularis from the lower esophagus to the sigmoid colon, wherever the muscle was composed of smooth muscle cells (81). An immunohistochemical study of c-Kit staining reported that the myenteric region of the transverse colon had a greater density of ICC in comparison to the ascending or descending colon and rectum (22). Few ICC were observed within the internal anal sphincter by immunohistochemistry (21). Wester et al. reported that c-Kit-immunoreactive ICC were visualized from 13 weeks of gestation onwards in association with the myenteric plexus and formed a cellular layer around the plexus from about 17-18 weeks of gestation (90).

Ultrastructural features in normal human tissues

ICC of the human digestive organs were described in detail in a series of studies by Rumessen and his colleagues (62, 64-66). ICC-AP of the small intestine resemble modified smooth muscle and have an incomplete basal lamina, conspicuous caveolae, dense bodies, abundant intermediate filaments and well developed SER (62). However, thick myosin filaments were not observed.

ICC-DMP of the small intestine are sandwiched between a thin inner layer (1~5 cells thick) and a very thick outer layer (150~200 cells thick) of circular muscle, and more closely resemble smooth muscle cells, in comparison with ICC from conventional

experimental animals, with a continuous basal lamina and subsurface cisterns, in addition with the features of ICC-AP. However, they were distinguished from the smooth muscle cells in the presence of well-developed RER, many mitochondria and the absence of thick myosin filaments (64).

Two types of ICC-CM were observed in the circular muscle layer of the small intestine. One type was found in the septa and in the outer third of the circular lamellae corresponding to the morphology of ICC-AP, and the other type in the inner third of the circular lamellae corresponding to ICC-DMP (65). Close contacts between nerve terminals and ICC-AP, ICC-DMP and ICC-CM were often observed, but their gap junctions with the same type of cells or smooth muscle cells were only observed in ICC-DMP.

In the colon, ICC were observed at the submucosal border of the circular muscle, within the circular muscle and in the main septa in all regions of colon including the ascending, transverse and sigmoid colon, (66). They are characterized by the features similar to ICC-DMP of the human small intestine just described above. Mitochondria and RER are abundant. However, close contacts to nerves and gap junctions to other ICC or smooth muscle cells are rare.

Pathological features in specimens from patients

The distribution of ICC was studied by c-Kit immunohistochemistry to shed light on the cause of intestinal dysmotility in patients with Hirschsprung's disease. Some authors reported a reduction in the number and impairment of the cellular network in the aganglionic segments, (51,60,82,92), while others claimed an unchanged distribution (28).

In a study examining the relationship between the development of the enteric nervous system and ICC of the human small intestine, Huizinga et al. reported the presence of abundant ICC-AP, in contrast to the absence of ICC-DMP and ICC-CM in a full term infant who presented with intestinal pseudo-obstruction and showed no enteric nerves and ganglia(31). The lower esophageal sphincter from the patients with esophageal achalasia was reported to show almost the same distribution of ICC as control specimens (89).

In infantile hypertrophic pyloric stenosis, c-Kit-immunoreactive ICC were absent or greatly reduced in number in most tissues, including around the myenteric plexus and the circular and longitudinal muscle layers, but they were observed at the submucosal border of the inner circular muscle layer (82). Porcher et al. reported that tissues from patients with Crohn's disease showed a significant reduction of ICC-DMP and ICC-AP in the small intestine, in addition to an almost complete abolition of ICC-CM and ICC-LM (55).

A reduction in the number of ICC was also reported in specimens from patients with a myopathic form of chronic idiopathic intestinal pseudo-obstruction (35), from patients with pseudo-obstruction and megaduodenum (2) and from patients with diabetes mellitus (50). In a case of the patients with chronic idiopathic constipation, a marked reduction of number of ICC-SMP, ICC-CM and ICC-LM was observed in the colon, while ICC-AP in these specimens showed no significant deference from those of controls (94). Ultrastructural alterations were reported in the ICC-SMP of the colon from the patients with ulcerative colitis (61).

Functional role of ICC

Pacemaker function

Soon after the proposal of the pacemaker hypothesis (74), physiological studies started to provide evidence for a pacemaker function of ICC-AP or for their generation of slow waves (23,72,73). After the discovery that the c-Kit receptor is essential for the normal development of ICC (45,80), further strong evidence for such a function came from the demonstration of the loss of pacemaker activity of the mice with a genetic defect in c-*kit* (29,85). Eventually, direct evidence of the pacemaker activity or slow wave was recorded from ICC-AP in the stomach of the mouse (52) and the guinea-pig (12,59). A pacemaker function was also reported for the ICC-SMP of the colon in the dog (9,68,71), human (57), and the rat (54). Recently, Horiguchi et al. suggested that ICC-SM of the canine gastric antrum have the ability to generate slow waves (27).

In addition, it was shown that ICC-CM of the mouse antrum generate the secondary regenerative component of slow waves (13) and that septal ICC-CM of the canine antrum transfer pacemaker depolarizations from ICC-AP to the distant bundles

of circular muscle (24,27).

Neuromediators

Several morphological studies in the last decade revealed that certain types of ICC are closely apposed to nerve terminals and form numerous gap junctions with neighboring smooth muscle cells at different levels of the gastrointestinal tract in many species (see reviews 39,43). These studies suggested that ICC are mediators between the nerves and muscles. In particular, every report indicated that ICC-DMP have a rich innervation and frequent contacts with smooth muscle cells via gap junctions. Intimate relationships between ICC-DMP and nitrergic neurons were observed in the guinea-pig small intestine (77,83). Therefore, it is quite possible that a certain type of ICC can act as an accessory route for neuromuscular transmission, as originally suggested by Cajal (7). Indeed, recent physiological studies showed that ICC-CM had a functional significance in both inhibitory (3,87) and excitatory (88) neurotransmission in the mouse stomach.

A significant function of gap junctions in ICC-DMP is suggested by evidence that the percentage of the total cell area occupied by gap junctions is 1.3% in rats (69) and 4% in guinea-pigs (95). The latter values are about 20 times greater than the corresponding percentage area (0.2%) occupied by gap junctions on smooth muscle cells of the guinea-pig intestine (20). The presence of highly developed gap junctions seem to be consistent with the notion that the well organized network of ICC-DMP acts as an impulse-conducting system analogous to that in the heart.

Since ICC-LM are also closely apposed to the nerve terminals containing many synaptic vesicles in the rat gastric antrum (48), it is likely that they are also involved in transmission of nerve impulse to the longitudinal muscle cells. Thus, those ICC-CM and ICC-LM are considered to be primary targets of enteric motor innervation and play an important role in enteric neurotransmission (84).

Mechanoreceptors

The DMP region between the inner and outer sublayers of the circular musculature was suggested as being suitably located to act as a mechanical stretch

receptor (19) and the significance of ICC-DMP for this role was repeatedly suggested by ultrastructural studies (11,63,64). An array of intramuscular vagal nerves innervating smooth muscles and ICC-CM or ICC-LM is believed to be an intramuscular mechanoreceptor (17). This formation loses its normal structure in the forestomach of *steel* mutant mice, which lack the ligand for the c-Kit receptor, probably because of lack of ICC-CM or ICC-LM (18). These mice showed decreased meal size and increased meal frequency and thus the alterations of these feeding behavior was assumed to be affected by loss of mechanoreceptor containing ICC. Additionally, a role of spindle proprioreceptors has been suggested for ICC in the striated muscle portion of the mouse esophagus (67).

Conclusions

The foregoing descriptions make it clear that different types of ICC can express a wide range of phenotypes, ranging from those most similar to smooth muscle cells, to those with the least muscle-like features, and those expressing an intermediate character. ICC can be classified into three types and can distinguished from fibroblast-like cells or smooth muscle cells on the basis of the features summarized in Table 1. Their heterogeneity may reflect their physiological roles and the microenvironment that they live in, including the effects of mechanical force, type of nerve supply, spatial relationships with muscle cells, the feeding habits of the animal, gastrointestinal movement patterns, etc.

In spite of their heterogeneity in ultrastructure and dependency on the c-Kit/SCF system for cell maturation, ICC share a common embryological origin from mesenchymal cells (44,93). ICC are specific and differ from fibroblast-like cells and smooth muscle cells expressing c-Kit receptors on their cell surface in normal adult animals. Thus, ICC are best regarded as a structurally and functionally distinct family of cells adapted to specialized functions such as pacemaking, intercellular communication with each other, mediation of nerve impulses and possibly as mechanoreceptors.

Acknowledgments

The author wishes to thank Dr. Peter Baluk, Cardiovascular Research Institute, University of California, San Francisco, USA for reading the manuscript.

References

1. Berezin I, Daniel, E.E., and Huizinga, J.D. Ultrastructure of interstitial cells of Cajal in the canine distal esophagus. Can J Physiol Pharmacol. 72, 1049-59 (1994).

2. Boeckxstaens, G.E., Rumessen, J.J., Wit, L., Tytgat, G.N., and Vanderwinden, J.M. Abnormal distribution of the interstitial cells of Cajal in an adult patient with pseudo-obstruction and megaduodenum. Am. J. Gastroenterol. 97, 2120-2126 (2002).

3. Burns, A.J., Herbert, T.M., Ward, S.M., and Sanders, K.M. Interstitial cells of Cajal in the guinea-pig gastrointestinal tract as revealed by c-Kit immunohistochemistry. Cell. Tissue. Res. 290, 11-20 (1997).

4. Burns, A.J., Lomax, A.E., Torihashi,S., Sanders, K.M., and Ward, S.M. Interstitial cells of Cajal mediate inhibitory neurotransmission in the stomach. Proc. Natl. Acad. Sci. U. S. A. 93, 12008-12013 (1996).

5. Burton, L.D., Housley, G.D., Salih, S.G., Jarlebark, L., Christie, D.L., and Greenwood, D. P2X2 receptor expression by interstitial cells of Cajal in vas deferens implicated in semen emission. Auton. Neurosci. 84,147-161 (2000).

6. Cajal, S.R. Sur les ganglions et plexus nerveux de l'intestin. Compt. Rend. Soc. Biol. Paris 45, 217-223(1893).

7. Cajal, S.R. Histologie du systeme nerveux de l'homme et des vertebres. Tome 2 Paris Maloine (1911).

8. Christensen, J. A commentary on the morphological identification of interstitial cells of Cajal in the gut. J. Auton. Nerv. Syst. 37, 75-88 (1992).

9. Conklin, J.L., and Du, C. Pathways of slow-wave propagation in proximal colon of cats. Am J Physiol 258, 894-903(1990).

10. Daniel, E.E. and Posey-Daniel, V. Neuromuscular structures in opossum esophagus: role of interstitial cells of Cajal. Am. J. Physiol. 246, G305-315 (1984).

11. Duchon, G., Henderson, R., and Daniel, E.E. Circular muscle layers in the small intestine. In Daniel E.E. (eds) Proc. 4th Int. Symp. gastrointest. Motil. Banff, Alberta, Canada, Mitchell Press, Vancouver, pp 635-646 (1974).

12. Dickens, E.J., Edwards, F.R., and Hirst, G.D. Selective knockout of intramuscular interstitial cells reveals their role in the generation of slow waves in mouse stomach. J Physiol 531, 827-33 (2001).

13. Dickens, E.J., Hirst, G.D. and Tomita, T. Identification of rhythmically active cells in guinea-pig stomach. J. Physiol. 514, 515-31 (1999).

14. Exintaris, B., Klemm, M.F., and Lang, R.J. Spontaneous slow wave and contractile activity of the guinea pig prostate. J. Urol.168, 315-322 (2002).

15. Faussone-Pellegrini, M.S. Histogenesis, structure and relationships of interstitial cells of Cajal (ICC): from morphology to functional interpretation. Eur. J. Morphol. 30, 37-148 (1992).

16. Faussone-Pellegrini, MS., and Cortesini, C. Ultrastructural features and localization of the interstitial cells of Cajal in the smooth muscle coat of human esophagus. J. Submicrosc. Cytol.Patol.,17, 187-197 (1985)

17. Fox, E.A., Phillips, R.J., Martinson, F.A., Baronowsky, E.A., and Powley, T.L. Vagal afferent innervation of smooth muscle in the stomach and duodenum of the mouse Morphology and topography. J. Comp. Neurol. 428, 558-576 (2000).

18. Fox, E.A., Phillips, R.J., Byerly, M.S., Baronowsky, E.A., Chi, M.M., and Powley, T.L. Selective loss of vagal intramuscular mechanoreceptors in mice mutant for steel factor , the c-Kit receptor ligand. Anat. Embryol. 205, 325-342 (2002).

19. Gabella, G. Special muscle cells and their innervation in the mammalian small intestine. Cell Tissue Res.153, 63-77 (1974).

20. Gabella, G., and Blundell, D. Nexuses between the smooth muscle cells of the guinea-pig ileum. J. Cell Biol. 82, 239-247 (1979).

21. Hagger, R., Gharaie, S., Finlayson, C., and Kumar, D. Regional and transmural density of interstitial cells of Cajal in human colon and rectum. Am. J. Physiol. G1309-1316 (1998a).

22. Haggar, R., Gharaie, S., Finlayson, C., and Kumar, D. Distribution of the interstitial of Cajal in the human anorectum. J. Auton. Nerv. Syst. 73,75-79 (1998b).

23. Hara, Y., Kubota, M., and Szurszewski, J.H. Electrophysiology of smooth muscle of the small intestine of some mammals. J. Physiol. 372, 501-520 (1986).

24. Hirst, G.D. An additional role for ICC in the control of gastrointestinal motility? J. Physiol. 537, 1 (2001).

25. Horiguchi, K., and Komuro, T. Ultrastructural characterization of interstitial cells of Cajal in the rat small intestine using control and Ws/Ws mutant rats. Cell Tissue Res. 293, 277-284 (1998).

26. Horiguchi, K., Zhou, D.S., Seki, K., Komuro, T., Hirota, S., and Kitamura,Y. Morphological analysis of *c-kit* expressing cells, with reference to interstitial cells of Cajal. J Smooth Muscle Res 31, 303-305 (1995).

27. Horiguchi, K., Semple, G.S., Sanders, K.M., and Ward, S.M. Distribution of

pacemaker function through the tunica muscularis of the canine gastric antrum. J. Physiol. 537, 237-250 (2001).

28. Horisawa, M., Watanabe,Y., and Torihashi, S. Distribution of c-kit immunopositive cells in normal human colon and in Hirschsprung's disease. J. Pediatr. Surg. 33, 1209-1214 (1998).

29. Huizinga, J.D., Thuneberg, L., Kluppel, M., Malysz, J., Mikkelsen, H.B., and Bernstein, A. W/kit gene required for interstitial cells of Cajal and for intestinal pacemaker activity. Nature 373, 341-349 (1995).

30. Huizinga, J.D., Thuneberg, L., Vanderwinden, J.M., and Rumessen, J.J. Interstitial cells of Cajal as targets for pharmacological intervention in gastrointestinal motor disorders. TIPS. 18, 393-403 (1997).

31. Hunzinga, J.D., Berezin, I., Sircar, K., Hewlett, B., Donnelly, G., Bercik, P., Ross, C., Algoufi, T., and Jacobson, K. Development of interstitial cells of Cajal in a full-term infant without an enteric nervous system. Gastroenterology.120, 561-567 (2001).

32. Ishikawa, K., and Komuro, T. Characterization of the interstitial cells associated with the submuscular plexus of the guinea-pig colon. Anat. Embryol. 194, 49-55 (1996).

33. Ishikawa, K., and Komuro, T. Ultrastructural characterization of the c-kit-expressing interstitial cells in the rat colon. Using Ws/Ws mutant rat (in Japanese). J. Human. Sci. 11, 65-72 (1998).

34. Ishikawa, K., Komuro, T., Hirota, S., and Kitamura, Y. Ultrastructural identification of the c-*kit*-expressing interstitial cells in the rat stomach a comparison of control and Ws/Ws mutant rats. Cell Tissue Res. 289, 137-143(1997).

35. Isozaki, K., Hirota, S., Miyagawa, J., Taniguchi, M., Shinomura,Y., and Matsuzawa,Y. Deficiency of c-*kit*+cells in patients with a myopathic form of chronic idiopathic intestinal pseudo-obstruction. Am. J .Gastroenterol. 92, 332-334 (1997).

36. Junquera, C., Martinez-Ciriano, C., Castiella, T., Serrano, P., Aisa,J., Calvo, E., and Lahoz, M. Enteric plexus and intersititial cells of Cajal interrelationship in the stomach of *Podarcis hispanica* (Reptilia). An ultrastructural study. Histol. Histopathol, 16, 869-881(2001).

37. Klemm, M.F, Exintaris, B, and Lang, R.J., Identification of the cells underlying pacemaker activity in the guinea-pig upper urinary tract. J. Physiol. 519, 867-884 (1999).

38. Komuro, T. Three-dimensional observation of the fibroblast-like cells associated with the rat myenteric plexus, with special reference to the interstitial cells of Cajal.

Cell Tissue Res. 255, 343-351 (1989).

39. Komuro, T. Comparative morphology of interstitial cells of Cajal ultrastructural characterization. Microsc. Res. Tech. 47, 267-85 (1999).

40. Komuro, T., and Seki, K. Fine structural study of interstitial cells associated with deep muscular plexus of the rat small intestine, with special reference to the intestinal pacemaker cells. Cell Tissue Res. 282, 129-134 (1995).

41. Komuro, T., and Zhou, D.S. Anti-c-*kit* protein immunoreactive cells corresponding to the interstitial cells of Cajal in the guinea-pig small intestine. J. Auton. Nerv. Syst. 61 169-174 (1996).

42. Komuro, T., Tokui, K., and Zhou, D.S. Identification of the interstitial cells of Cajal. Histol. Histopathol. 11, 769-786 (1996).

43. Komuro, T, Seki, K., and Horiguchi, K. Ultrastructural characterization of the interstitial cells of Cajal. Arch. Histol .Cytol. 62, 295-316 (1999).

44. Lecoin, L., Gabella, G., and Dourain, N.L. Origin of the c-*kit*-positive interstitial cells in the avian bowel. Development 122, 725-733(1996).

45. Maeda, H., Yamagata, A., Nishikawa, S., Yoshinaga, K., Kobayashi, S., Nishi,K., and Nishikawa, S. Requirement of c-*kit* for development of intestinal pacemaker system. Development 116, 369-375 (1992).

46. Malysz, J., Thuneberg, L., Mikkelsen, H.B., and Huizinga, J.D. Action potential generation in the small intestine of W mutant mice that lack interstitial cells of Cajal. Am. J. Physiol. 271, G387-399 (1996).

47. McCloskey, K.D., and Gurney, M. KIT positive cells in the guinea pig bladder. J. Urol. 168, 832-836 (2002).

48. Mitsui, R., and Komuro, T. Direct and indirect innervation of smooth muscle cells of rat stomach, with special reference to the interstitial cells of Cajal. Cell Tissue Res. 309, 219-27 (2002).

49. Mitsui, R and Komuro, T. Distribution and ultrastructure of interstitial cells of Cajal in the gastric antrum of wild-type and Ws/Ws rats. Anat. Embryol. In press (2003).

50. Nakahara, M., Isozaki, K., Hirota, S., Vanderwinden, J. M., Takakura, R., Kinoshita, K., Miyagawa, J., Chen, H., Miyazaki, Y., Kiyohara, T., Shinomura, Y., and Matsuzawa, Y. Colonic dysmotility in diabetes mellitus Deficiency of KIT-positive cells in the colon of patients with diabetes mellitus. J. Gastroenterol. Hepatol. 17, 666-670 (2002).

51. Nemeth, L., Yoneda, A., Kader, M., Devaney, D., and Puri, P. Three-dimensional morphology of gut innervation in total intestinal aganglionosis whole-mount preparations . J. Ped. Surg. 36, 291-295 (2001).

52. Ördög, T., Ward, S.M., and Sanders, K.M. Interstitial cells of Cajal generate electrical slow waves in the murine stomach. J. Physiol. 518, 257-269 (1999).

53. Ortiz-Hidalgo, C., deLeon, Bojorge B., and Albores-Saavedra, J. Stromal tumor of the gallbladder with phenotype of interstitial cells of Cajal: a previously unrecognized neoplasm. Am. J. Surg. Pathol. 24, 1420-1423 (2000).

54. Pluja, L., Alberti, E., Fernandez, E., Mikkelsen, H.B., Thuneberg, L., and Jimenez, M. Evidence supporting presence of two pacemakers in rat colon. Am. J. Physiol. 281, G255-266 (2001).

55. Porcher, C., Baldo, M., Henry, M., Orsoni, P., Jule,Y., and Ward, S.M. Deficiency of interstitial cells of Cajal in the small intestine of patients with Crohn's disease. Am. J. Gastroenterol. 97, 118-125 (2002).

56. Prosser, C.L. Rhythmic electrical and mechanical activity in stomach of toad and frog. Am. J. Physiol, 269, G386-395 (1995).

57. Rae, M.G., Fleming, N., McGregor, D.B., Sanders, K.M., Keef, K.D. Control of motility patterns in the human colonic circular muscle layer by pacemaker activity. J. Physiol. 510, 309-320 (1998).

58. Reynhout, J.K., and Duke, G.E. Identification of interstitial cells of Cajal in the digestive tract of turkeys (Meleagris gallopavo). J. Exp. Zool. 283 426-440 (1999).

59. Rich, A., Hanani, M., Ermilov, L.G., Malysz, J., Belzer, V., Szurszewski, H., and Farrugia, G. Pysiological study of interstitial cells of Cajal identified by vital staining. Neurogastroenterol. Mot. 14, 189-196 (2002).

60. Rolle, U., Piotrowska, A.P., Nemeth, L., and Puri, P. Altered ditsribution of interstitial cells of Cajal in Hirschsprungs disease. Arch. Pathol. Lab. Med. 126, 928-933 (2002).

61. Rumessen, J. J. Ultrastructual of Interstitial cells of Cajal at the colonic Submusuclar border in patients with ulcerative colitis. Gastroenterology 111,1447-1455 (1996)

62. Rumessen, J.J., and Thuneberg, L. Interstitial cells of Cajal in human small intestine. Ultrastructural identification and organization between the main smooth muscle layers. Gastroenterology 100, 1417-1431 (1991).

63. Rumessen, J.J., Thuneberg, L., and Mikkelsen, H.B. Plexus muscularis profundus and associated interstitial cells. II. Ultrastructural studies of mouse small intestine.

Anat. Record. 203 129-146 (1982).

64. Rumessen, J.J., Mikkelsen, H.B., and Thuneberg, L. Ultrastructure of interstitial cells of Cajal associated with deep muscular plexus of human small intestine. Gastroenterology 102, 56-68 (1992).

65. Rumessen, J.J., Mikkelsen, H.B., Qvortrupand, K., and Thuneberg, L. Ultrastructure of interstitial cells of Cajal in circular muscle of human small intestine. Gastroenterology 104, 343-350 (1993a).

66. Rumessen, J.J., Peters, S., and Thuneberg, L. Light and electron microscopical studies of interstitial cells of Cajal and muscle cells at the submucosal border of human colon. Lab. Invest. 68, 481-495 (1993b).

67. Rumessen, J. J., Exaerde, A. K., Migonon, S., Bernex, F., Timmerman, J. P., Schiffmann, S.N., Pantheir,J.J., and Vanderwinden, J.M. Interstitial cells of Cajal in the striated musculature of the mouse esophagus. Cell. Tissue. Res. 306, 1-14 (2001).

68. Sanders, K.M. A case for interstitial cells of Cajal as pacemakers and mediators of neurotransmission in the gastrointestinal tract. Gastroenterology 111, 492-515 (1996).

69. Seki, K., and Komuro, T. Further observation of the gap junction-rich cells in the deep muscular plexus of the rat small intestine. Anat. Embryol., 197, 135-141 (1998).

70. Seki, K., and Komuro, T. Distribution of interstitial cells of Cajal and gap junction protein, Cx 43 in the stomach of wild-type and W/Wv mutant mice. Anat. Embryol. 206, 57-65 (2002).

71. Serio, R., Huizinga, J.D., Barajas-Lopez, C., and Daniel, E.E . Interstitial cells of Cajal and slow wave generation in canine colonic circular muscle. J. Auton. Nerv. Syst. 30 Suppl S141-143 (1990).

72. Smith, T.K. Spontaneous junction potential and slow waves in the circular muscle of isolated segments of guinea-pig ileum. J. Auton. Nerv. Syst. 27, 147-154 (1989).

73. Suzuki, N., Prosser, C.L., and Dahms, V. Boundary cells between longitudinal and circular layers essential for electrical slow waves in cat intestine. Am. J. Physiol. 250, G287-294 (1986).

74. Thuneberg, L. Interstitial cells of Cajal: Intestinal pacemaker cells? Adv. Anat. Embryol. cell Biol. 71, 1-130 (1982).

75. Thuneberg, L. Interstitial cells of Cajal In Wood J.D. (ed) Handbook of physiology. The gastrointestinal system, Vol 1. Am. Physiol. Soc., Bethesda Maryland, pp 349-386 (1989).

76. Thuneberg, L. One hundred years of interstitial cells of Cajal. Microscop. Res. Tech. 47, 223-238 (1999).

77. Toma, H., Nakamura, K. Kuraoka, A., Tankana, M., and Kawaguti, M. Three-dimentional structures of c-Kit-positive cellular networks in the guinea pig small and colon. Cell Tissue.Res. 295, 425-436 (1999).

78. Torihashi, S., Kobayashi, S., Gerthoffer, W.T., and Sanders, K.M. Interstitial cells in deep muscular plexus of canine small intestine may be specialized smooth muscle cells. Am. J. Physiol. 265, G638-G645 (1993).

79. Torihashi, S., Gerthoffer, W.T., Kobayashi, S., and Sanders, K.M. Identification and classification of interstitial cells in the canine proximal colon by ultrastructure and immunocytochemistry. Histochemistry 101, 169-183 (1994).

80. Torihashi, S., Ward, SM., Nishikawa, S., Nishi, K., Kobayashi, S., and Sanders, K. c-kit-Dependent development of interstitial cells and electrical activity in the murine gastrointestinal tract. Cell Tissue Res., 280, 97-111 (1995).

81. Torihashi, S, Horisawa M., and Watanabe Y., c-Kit immunoreactive interstitial cells in the human gastrointestinal tract. J. Auton. Nerv. Syst. 75, 38-50 (1999).

82. Vanderwinden, J.M., Rumessen, J.J., Liu, H., Descamps, M.H., De Laet, M.H., and Vanderhaeghen, J.J. Interstitial cells of Cajal in human colon and in Hirschsprung's disease. Gastroenterology 111, 901-910 (1996).

83. Wang, X.Y., Sanders, K.M., and Ward, S.M. Intimate relationship between interstitial cells of Cajal and enteric nerves in the guinea-pig small intestine. Cell Tissue Res. 295, 247-256 (1999).

84. Ward, S.M., and Sanders, K.M. Interstitial cells of Cajal primary targets of enteric motor innervation. Anat. Rec. 262, 125-135 (2001).

85. Ward, S.M., Burns, A.J., Torihashi, S., and Sanders, K.M. Mutation of the proto-oncogene c-*kit* blocks development of interstitial cells and electrical rhythmicity in murine intestine. J. Physiol. (London) 480, 91-97 (1994) .

86. Ward, S.M., Burns, A.J., Torihashi, S., Harney, S.C and Sanders, K.M. Impaired development of interstitial cells and intestinal electrical rhythmicity in steel mutants. Am. J. Physiol. 269, C1577-1585 (1995).

87. Ward, S.M., Morris, G., Reese, L. Wang, X.Y., and Sanders, K.M. Interstitial cells of Cajal mediate enteric inhibitory neurotransmission in the lower esophageal and pyloric sphincters. Gastroenterology 115, 314-329 (1998).

88. Ward, S.M, Beckett, E.A., Wang, X., Baker, F., Khoyi, M., and Sanders, K.M. Interstitial cells of Cajal mediate cholinergic neurotransmission from enteric motor neurons. J.Neurosci. 20, 1393-403 (2000).

89. Watanebe, Y., Ando, H., Seo, T., Katsuno, S., Marui, Y., Ono, Y., and Torihashi, S. Attenuated nitrergic Inhibitory neurotransmission to interstitial cells of Cajal in the lower esophageal sphincter with esophageal achalasia in children. Pediatrics International. 44, 145-148 (2002).

90. Wester T., Eriksson. L., Olsson Y. and Olsen L. Interstitial cells of Cajal in the human fetal small bowel as shown by c-kit immunohistochemistry. Gut 44, 65-71 (1999)

91. Yamamoto, M. Electron microscopic studies on the innervation of the smooth muscle and the interstitial cell of Cajal in the small intestine of the mouse and bat. Arch. Histol. Jan. 40, 171-201 (1977).

92. Yamataka, A., Kato, Y., Tibboel, D., Murata, Y., Sueyoshi, N., Fujimoto, T., Nishiye, H., and Miyano, T. A lack of intestinal pacemaker (c-*kit*) in aganglionic bowel of patients with Hirschsprung's disease. J. Pediatr. Surg. 30, 441-444 (1995).

93. Young, H.M., Ciampoli, D., Southwell, B.R., and Newgreen, D.F. Origin of interstitial cells of Cajal in the mouse intestine. Dev. Biol. 180, 97-107 (1996) .

94. Yu, C.S., Kim, H.C., Chung,D.H., Kim, H.J., Kang, G.H., and Kim, J.C. Evaluation of myenteric ganglion cells and interstitial cells of Cajal in patients with chronic idiopathic constipation. Int. J.Colorectal Dis. 17, 253-258 (2002).

95. Zhou, D.S., and Komuro,T. Interstitial cells associated with the deep muscular plexus of the guinea-pig small intestine, with special reference to the interstitial cells of Cajal. Cell Tissue Res. 268, 205-216 (1992).

Figuer legends

Fig. 1. A drawing by Cajal of ICC-AP in the rabbit intestine stained with methylene blue. Reproduced from Cajal, 1911 (Fig. 572). Note the close similarity in shape of the cells (*) to the cells in Figs. 2, 3.

Fig. 2. ICC-AP (*) in the guinea-pig small intestine, demonstrated by c-Kit-immunostaining (purple). The nerve plexus is stained brown by the cholinesterase reaction (arrow). x 520. (Figs. 2, 3; reproduced from Komuro and Zhou, 1996 with permission of the publisher).

Fig. 3. ICC-AP (*) in the guinea-pig small intestine, demonstrated by vimentin-immunostaining (purple). The nerve plexus is stained brown by the cholinesterase reaction (arrow). x 480.

Fig. 4. A confocal laser micrograph showing an extensive cellular network of ICC-AP (green fluorescence of Alexa 488) over the myenteric plexus (red fluorescence of TRITC) in the guinea-pig small intestine. Note, the two networks show totally independent pattern from each other. x 110. (Courtesy of Dr. Horiguchi, Waseda University).

Fig. 5. ICC-DMP in the guinea-pig small intestine demonstrated by c-Kit immunostaining. Their cell bodies are often observed in pairs where parallel nerve bundles branch and anastomose. x 340.

Fig. 6. Bipolar shape of ICC-CM in the guinea-pig small intestine demonstrated by c-Kit-immunostaining. x 340.

Fig. 7. A wholemount stretch preparation of the muscle coat of the mouse fundus. Bipolar cells within the circular and longitudinal layers are oriented perpendicularly to each other and are clearly visible because of the lack of c-Kit-positive cells in the myenteric region. x 200. (Courtesy of Dr. Seki, Yamaguchi University).

Fig. 8. A longitudinal section of the fundus of the mouse stomach. c-Kit-positive cells are densely distributed in the thick circular (cm) and longitudinal muscle layers (lm). se; squamous epithelial layer. x 120. (Figs. 8-11; reproduced from Seki and Komuro, 2002 with permission of the publisher).

Fig. 9. A part of the myenteric region of the cardia. c-Kit-positive cells are not observed around the ganglia (*) or between the two muscle layers. Note bipolar shape of a c-Kit-positive cell in the longitudinal muscle layer (arrow). x 360.

Fig. 10. The glandular corpus with a thin muscle coat containing a few c-Kit-positive cells in the circular and longitudinal muscle layers. Note, the presence of c-Kit-positive cells around the myenteric ganglion (*) and between two muscle layers (arrow). x 320.

Fig. 11. A longitudinal section of the pylorus close to the sphincter (left side). Dense distribution of the c-Kit-positive cells in the circular muscle layer (cm) and in the myenteric region (arrow). Note the presence of a few c-Kit-positive cells at the border of the submucosa and the circular muscle layer (double headed arrow). x 160.

Fig. 12. A longitudinal section of the guinea-pig small intestine demonstrated by c-Kit-immunostaining. Dense reaction deposits are localized in the DMP region (arrows) and around the myenteric ganglion (*). x 100. (Figs. 12, 13; reproduced from Seki et al., 1998 with permission of the publisher).

Fig. 13. A longitudinal section of the guinea-pig colon demonstrated by c-Kit-immunostaining. Reaction deposits are distributed in the SMP region (arrow), around a myenteric ganglion (*) and within the circular muscle layer (cm). A few immunoreactive deposits are found in the longitudinal muscle layer. x 80.

Fig. 14. An electron micrograph showing ICC-SM (IC) characterized by many

mitochondria and caveolae, located at the interface between the submucosa (sb) and the circular muscle layer (cm). A gap junction is present between their processes (arrow). x 7500. (Courtesy of Dr. Mitsui, Waseda University).

Fig. 15. The cytoplasmic process of ICC-SM forming a gap junction indicated by the arrow in Fig. 14. Bundles of intermediate filaments (arrows), a basal lamina (arrowheads) and caveolae are observed. x 42,000. (Figs. 15, 16; reproduced from Mitsui and Komuro, 2003 with permission of the publisher).

Fig. 16. A process of ICC-SM closely associated with a nerve varicosity (N) containing many synaptic vesicles. x 32,000

Fig. 17. ICC-CM in the rat stomach characterized by electron-dense cytoplasm, caveolae (arrows), a gap junction with a smooth muscle cell (double headed arrow) and a close contact with nerve terminal (N). x 16,000. (Reproduced from Ishikawa et al., 1997 with permission of the publisher).

Fig. 18. An electron micrograph showing ICC-AP (IC) and a fibroblast-like cell (FL) located beside a nerve bundle (N) in the space between the circular and longitudinal muscle layers of the mouse pylorus. Note a large gap junction of the ICC-AP (arrow) and the well-developed RER in the fibroblast-like cell, and the difference in electron-density of the cytoplasm in these cells. x 6400. (Figs. 18, 19, 22; reproduced from Komuro et al., 1999 with permission of the publisher).

Fig. 19. A bundle of intermediate filaments in the cytoplasmic process of ICC-AP in the mouse pylorus. The arrow indicates a gap junction between thin processes. x 25,000.

Fig. 20. A cross section of bundles of intermediate filaments in the cytoplasmic process of ICC-CM of the mouse stomach. x 24,000. (Figs. 20, 21; Courtesy of Dr. Horiguchi, Waseda University)

Fig. 21. A cytoplasmic process of ICC-AP of the mouse stomach showing a continuous basal lamina (arrows) and caveolae. x 40,000.

Fig. 22. Close contact between the nerve terminals and ICC-AP of the mouse stomach. x 18,000.

Fig. 23. ICC-DMP in the mouse small intestine. Note, their gap junctions with the same type of cell (arrow) and with a smooth muscle cell (double headed arrow). x 10,000. (Courtesy of Dr. Horiguchi, Waseda University) Inset: A cytoplasmic process of ICC-DMP of the rat showing a continuous basal lamina and caveolae along the cell membrane. x 42,000.

Fig. 24. ICC-AP of the rat intestine characterized by many mitochondria and less electron-dense cytoplasm. x 8000. Inset: A gap junction between slender cytoplasmic processes of ICC-AP. Note there is no basal lamina. x 44,000. (Figs. 24, 25; reproduced from Horiguchi and Komuro 1998 with permission of the publisher).

Fig. 25. Fibroblast-like cell in the myenteric region of Ws/Ws rat, which is characterized by well-developed RER. It forms small gap junctions with muscle cells of both circular (arrowhead) and longitudinal layers (arrow). x 8000. Inset: Higher magnification of the gap junctions indicated by the arrow. x 42,000

Fig. 26. ICC-SMP of the rat colon located at the submucosal border of the circular muscle layer. It contains many mitochondria and forms a gap junction with the same type of cell at the tip of the cytoplasmic process (arrow). x 7200. Inset: A part of ICC-SM showing a continuous basal lamina and caveolae. x 42,000. (Reproduced from Ishikawa and Komuro, 1998 with permission of the publisher).

Fig. 27. ICC-CM (IC) and fibroblast-like cell (FL) of the rat colon. ICC-CM is

characterized by an electron-dense cytoplasm and caveolae (arrows), while the fibroblast-like cell is characterized by less electron-dense cytoplasm and a well developed RER. x 12,000. (Coutesy of Dr. Ishikawa, Waseda University).

Fig. 28. A longitudinal section of the pylorus of *W/W^v* mouse stomach showing the presence of c-Kit-positive cells in the region of the myenteric plexus (arrows). x 200 (Reproduced from Seki and Komuro, 2002 with permission of the publisher).

Fig. 29. A longitudinal section of the *Ws/Ws* rat pylorus stained for c-Kit immunohistochemistry. Immunoreactive deposits are found along the submucosal border of circular muscle layer (arrowheads) and around the myenteric plexus (arrows). x 80. (Reproduced from Mitsui and Komuro, 2003 with permission of the publisher).

Fig. 30. ICC-DMP found in the Ws/Ws rat small intestine characterized by many mitochondria, caveolae and gap junction with a process of muscle cell. x 22,000. (Courtesy of Dr. Horiguchi, Waseda University)

Fig. 31. ICC-SMP of Ws/Ws rat colon. x 10,000. Inset: The gap junction indicated by an arrow in Fig. 31. x 40,000. (Courtesy of Dr. Ishikawa, Waseda University).

Cell Type	c-Kit	BL	CV	GJ	IF	MIT	NC	RER	Examples (references)
Type 1 Least muscle-like ICC	++	-	+-	++	++	++	++	+	**ICC-AP** in rat (25, 38) and guinea-pig (41) small intestine.
Type 2 Intermediate type ICC	++	+-	++	++	++	++	++	+	**ICC-CM** in rat stomach (34)and rat colon (33), and guinea-pig stomach (39). **ICC-AP** in mouse small intestine (74).
Type 3 Most muscle-like ICC	++	++	++	++	++	++	++	+	**ICC-SM** in dog (27)and rat (49)pylorus. **ICC-DMP** in mouse (74), rat (69), guinea-pig (95), dog (78) and human (62) small intestine. **ICC-SMP** in rat (33), guinea-pig(32) and dog (1) colon. **ICC-AP** in mouse pylorus (39).
Smooth Muscle	-	++	++	++		++	+	+	
FL Fibroblast- Like cell	-	-	-	+	+	+	+	++	**FL-AP** in rat small intestine (25, 38). **FL-DMP** in rat small intestine (25, 40). **FL-CM** in rat stomach(34) and colon (33).

c-Kit : immunoreactivity for c-Kit staining BL : basal lamina CV : caveolae GJ : gap junction
IF : intermediate filaments MIT : mitochondria NC: close nerve contact RER : rough endoplasmic reticulum

Table I

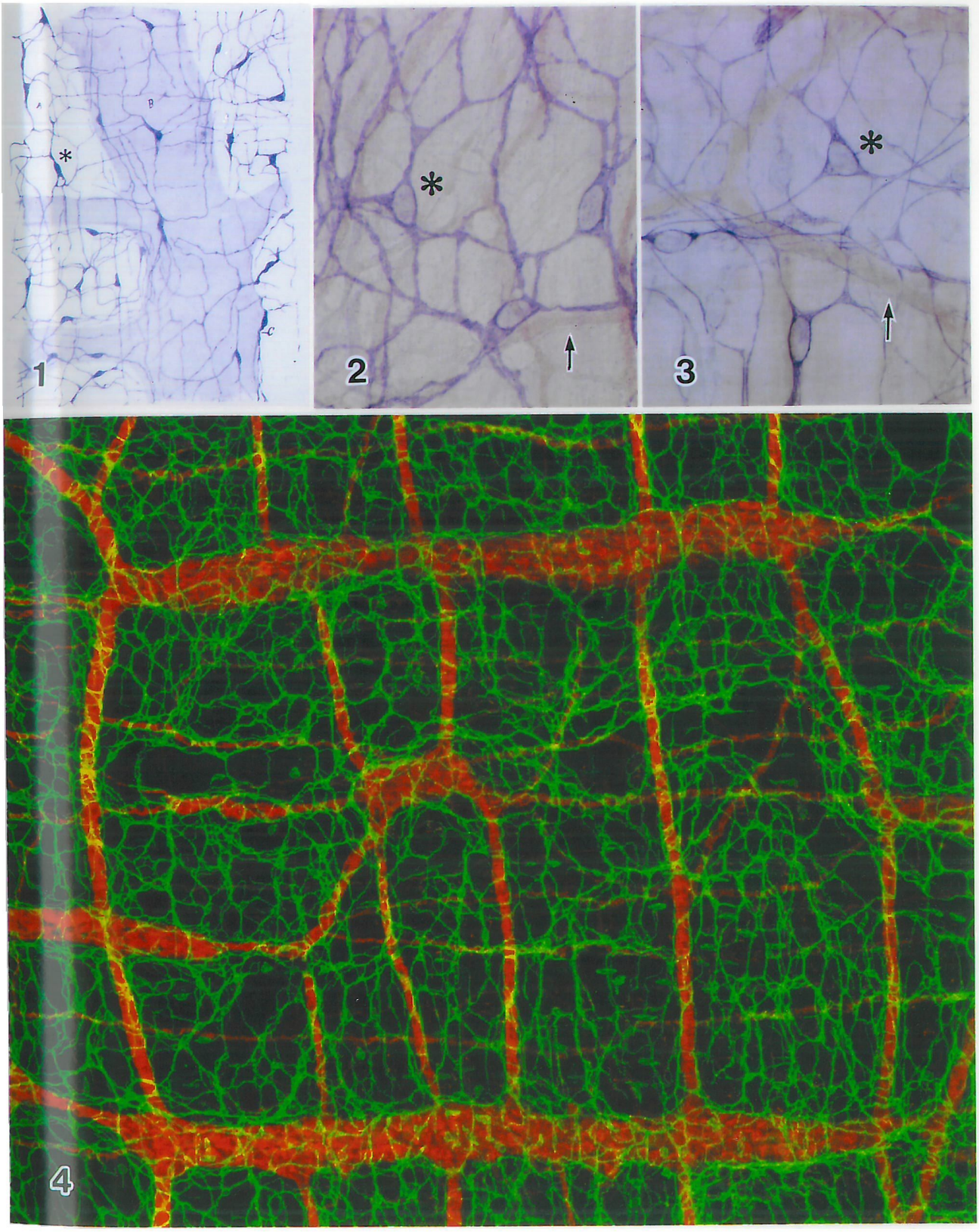
1
2
3
4

5

6

7

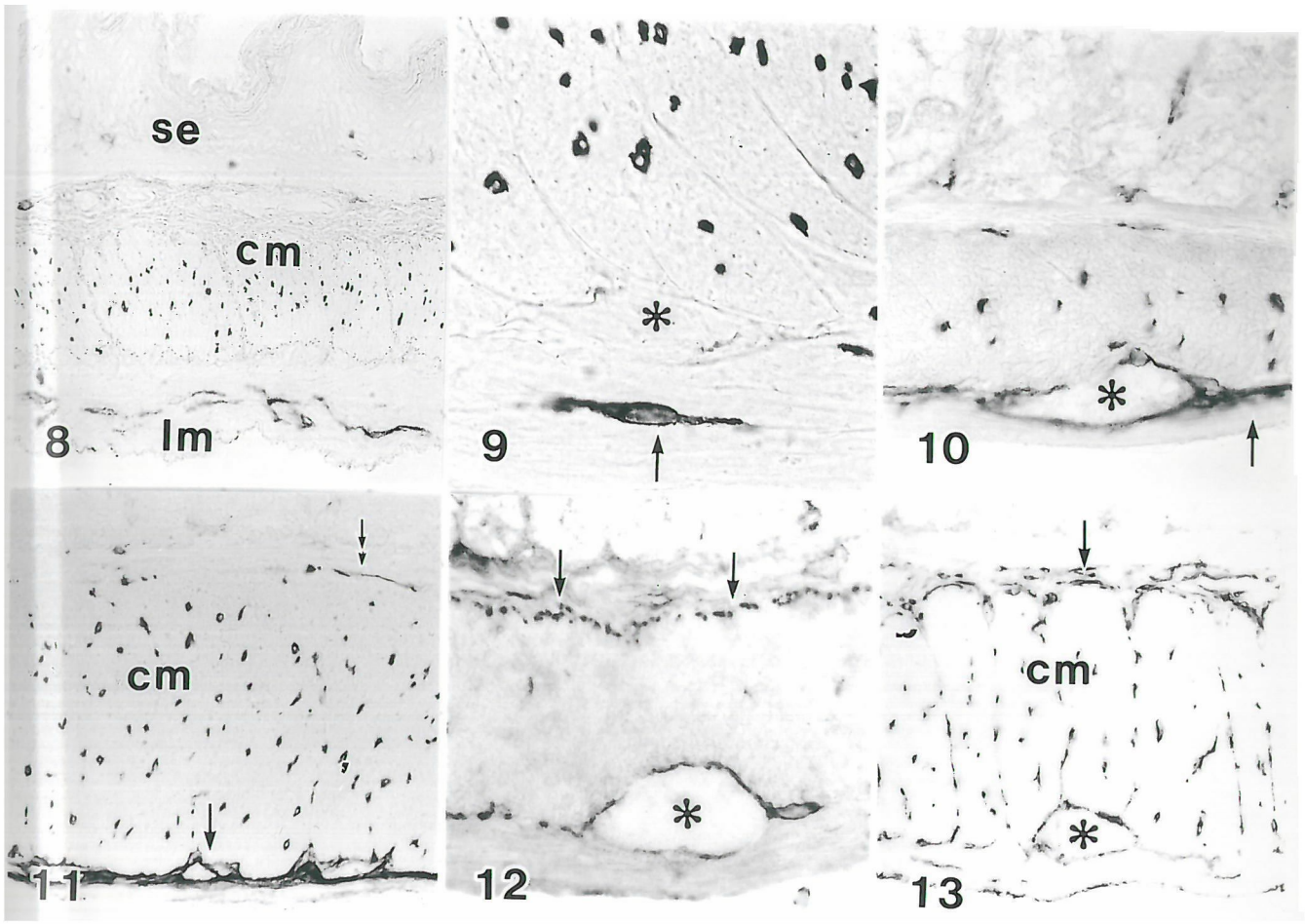
se
cm
lm
8
*
9
*
10
cm
11
*
12
cm
*
13

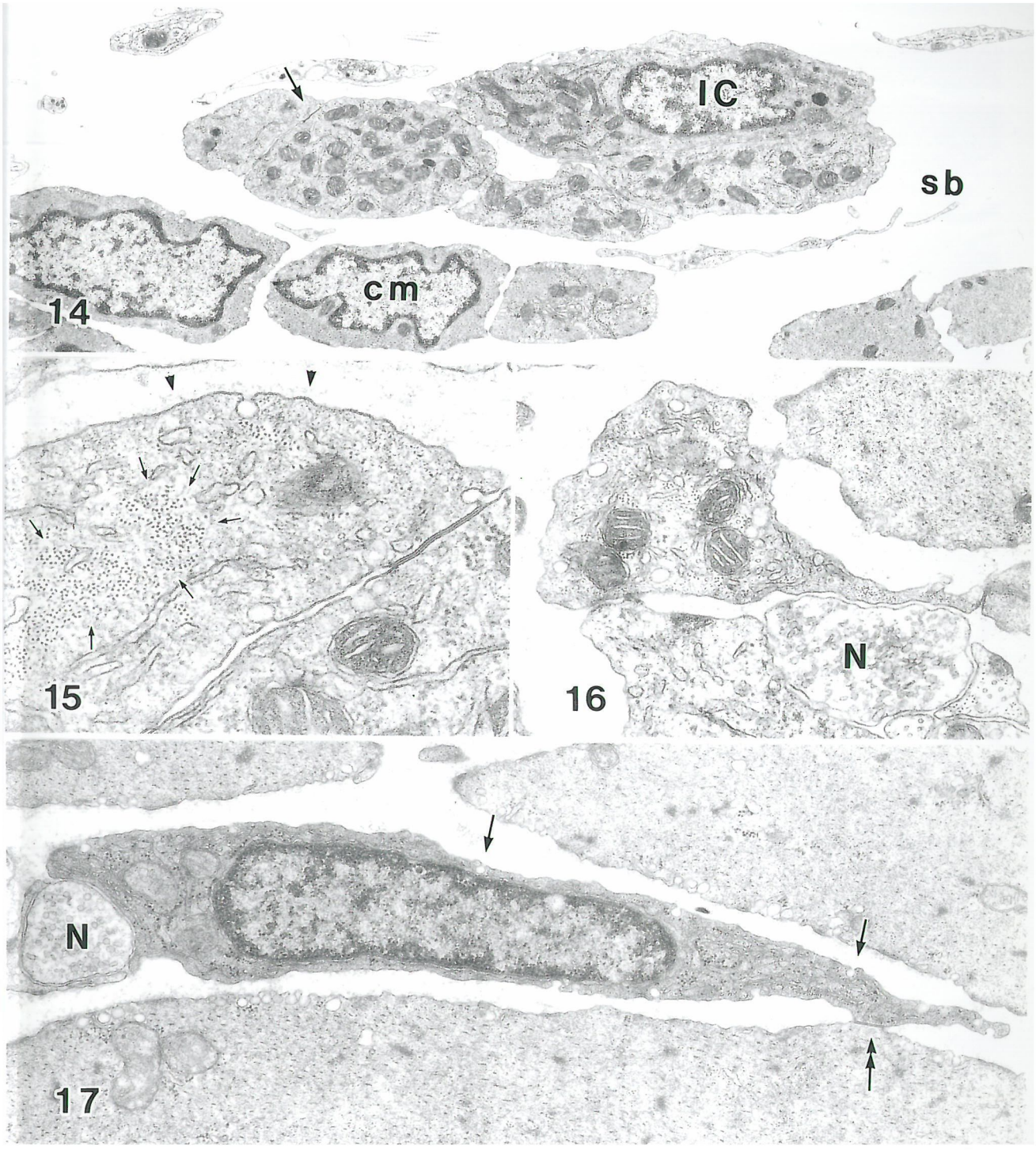
IC
sb
cm
14
15
16
N
N
17

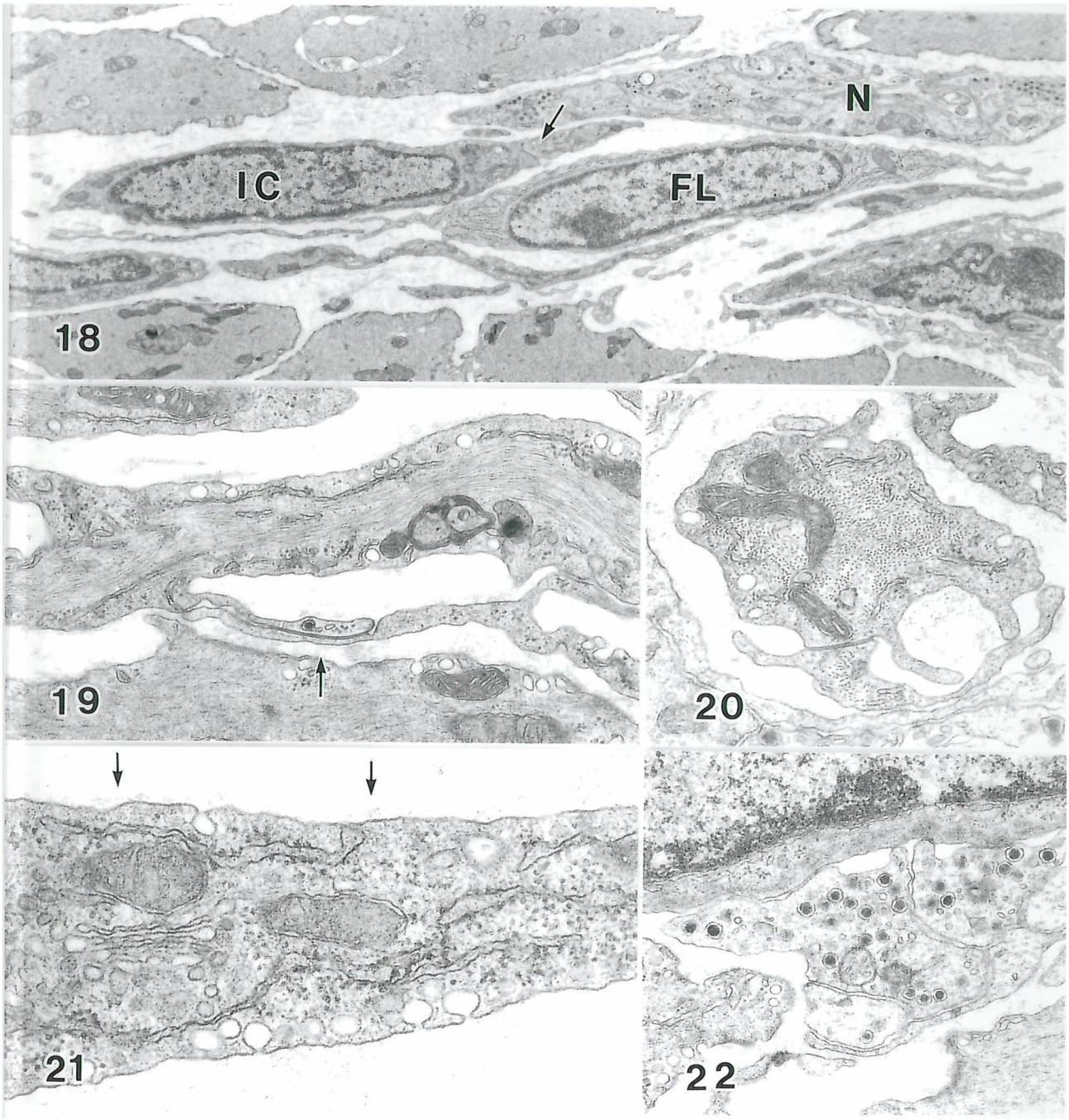
N
IC
FL
18
19
20
21
22

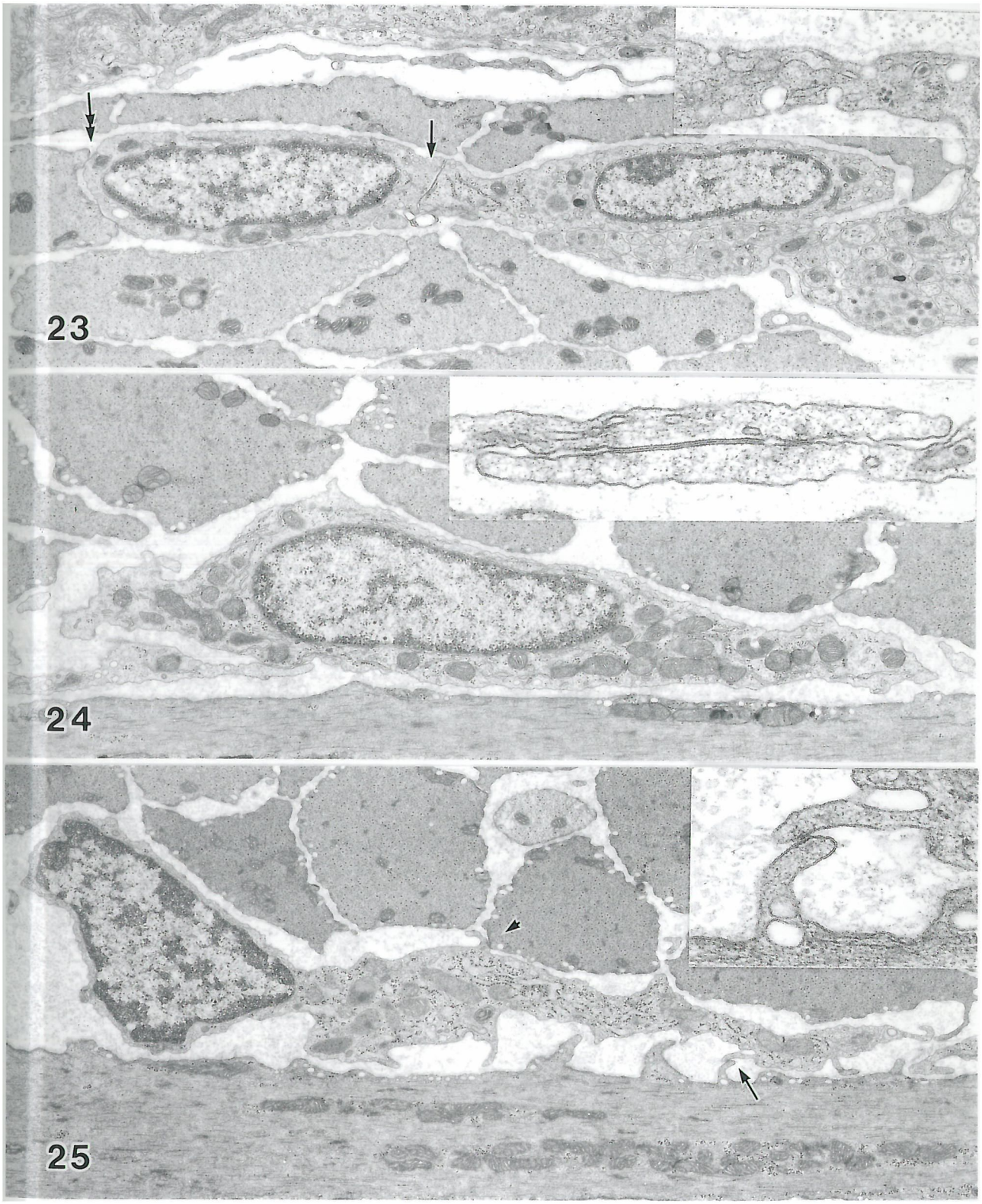
23
24
25

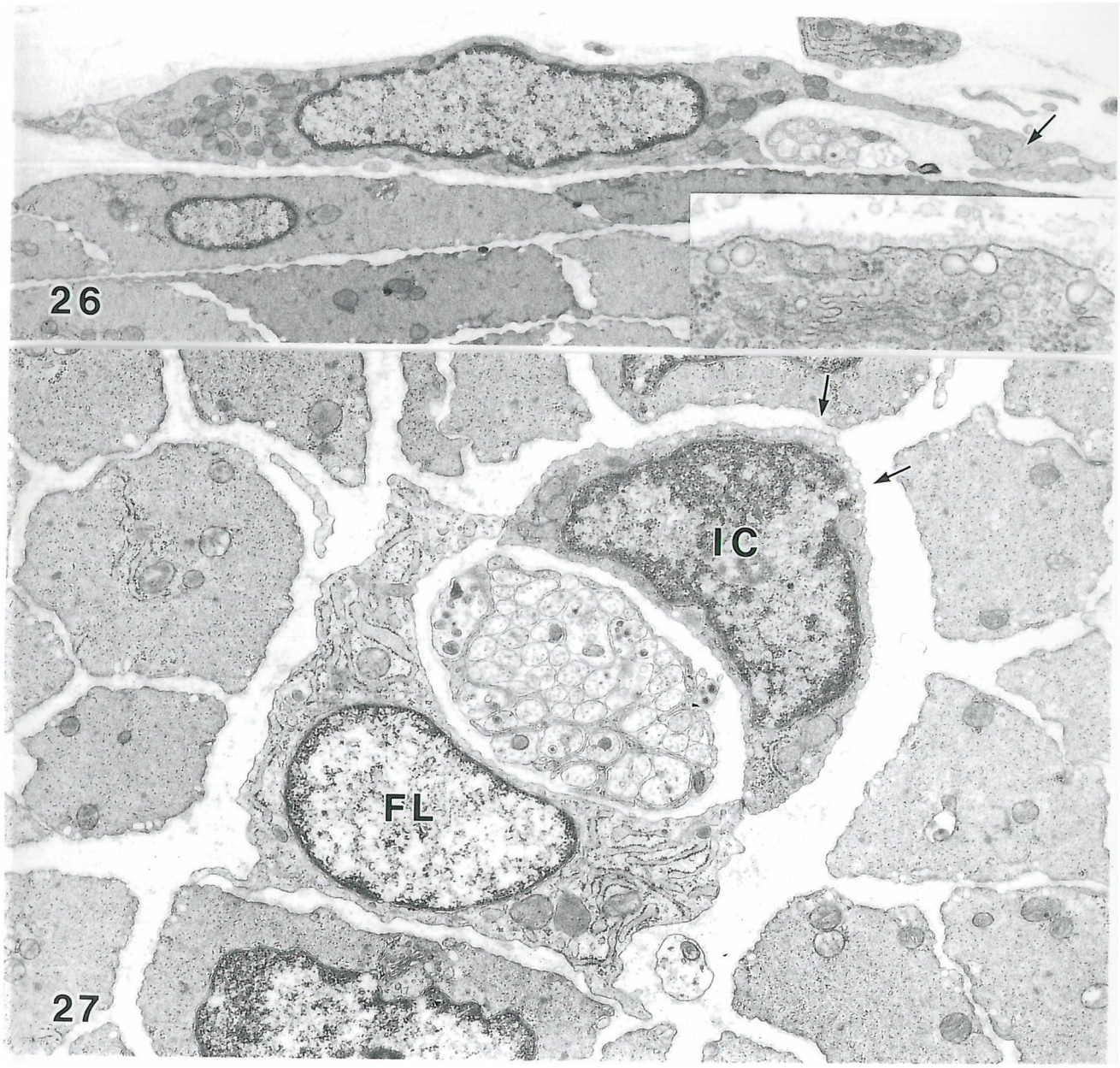
26
IC
FL
27

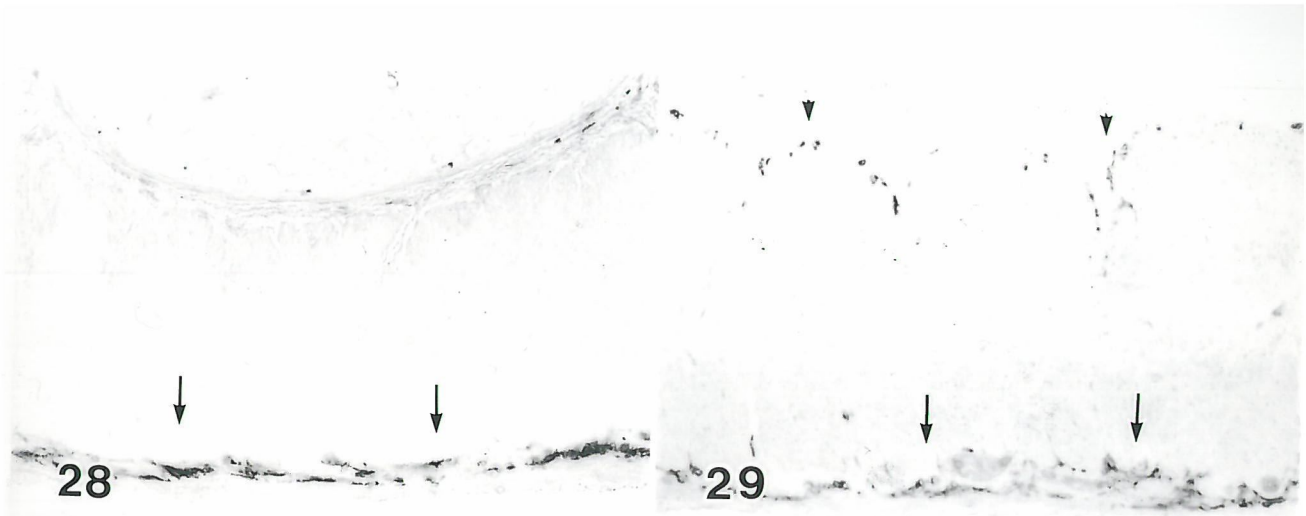
28
29


30


31